WIDE FIELD FIBER-FED OPTICAL MULTI-OBJECT SPECTROMETER

WFMOS

STUDY SUMMARY

JANUARY 30, 2009

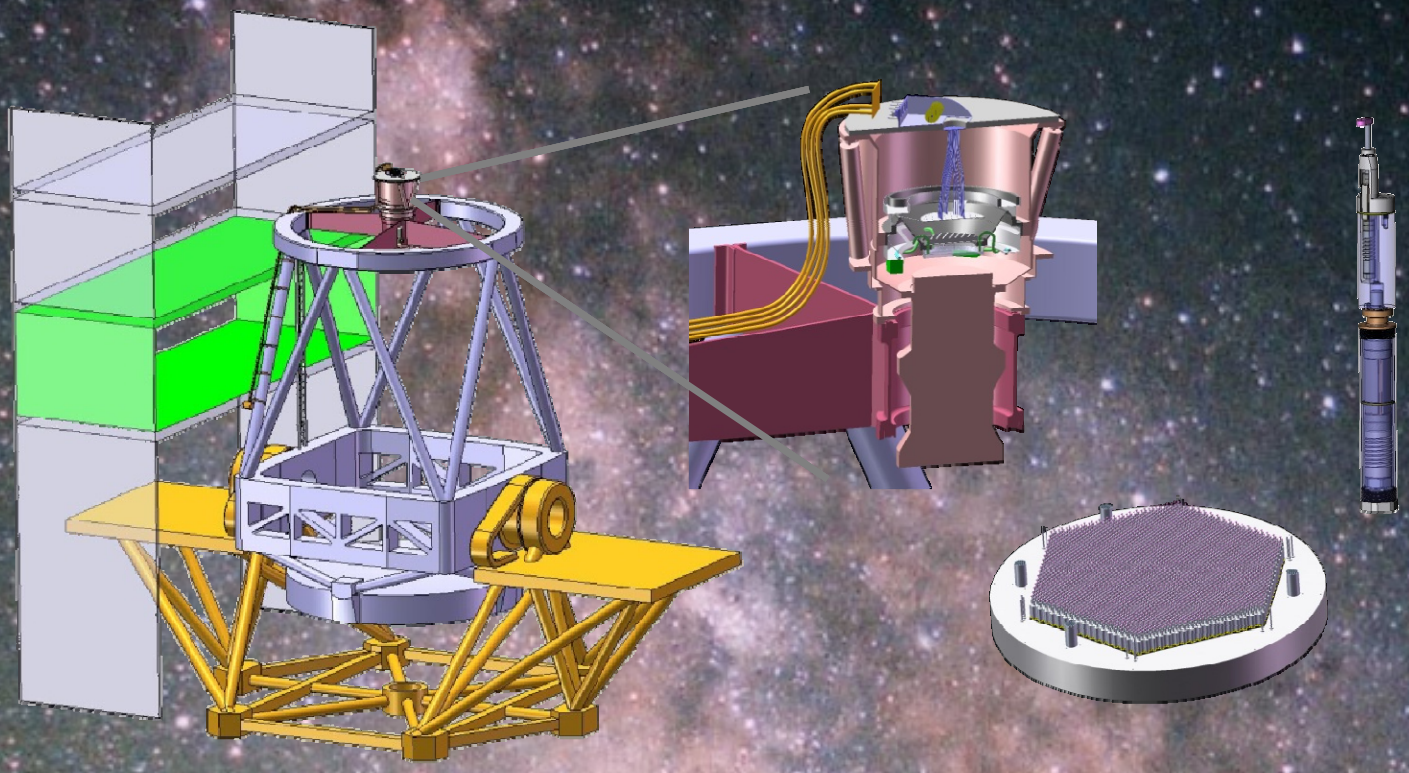

LNA LABORATÓRIO NACIONAL DE ASTROFÍSICA

PENNSTATE

UK Astronomy Technology Centre

CALTECH

IoA UNIVERSITY OF CAMBRIDGE

UCL

JPL

Wide Field Fiber-Fed Optical Multi-Object Spectrometer (WFMOS)

SCIENCE

WFMOS is the premier tool for addressing the nature of dark energy and the assembly history of galaxies such as M31 and our Milky Way.

WFMOS will:

- Provide a constraint on the dark energy equation of state, *w*, to 3%
- Measure the growth rate of density fluctuations, f_g, to 1.5% at 0.7<*z*<1.6 and 7% at 2.5<*z*<3.3
- Measure the mass, extent, and substructure of the Milky Way dark matter halo
- Conduct kinematic measurements of dwarf spheroid candidates
- Measure the extent, substructure, and kinematics of Milky Way stellar populations
- Explore the fossil record of chemical evolution of stellar populations in the Milky Way

Dark Energy	Low Redshift	High Redshift
Redshift Range	$0.7 \le z \le 1.6$	$2.5 \le z \le 3.3$
Number of galaxies	> 4,000,000	> 100,000
Spectral Range	6300–9700 Å	4200 – 6500 Å
Spectral Resolution	3500	1500
Magnitude Limit	$R_{AB} < 23.0$	$R_{AB} < 25$

Galactic Archaeology	Low Res	High Res
Number of Stars	3×10^6	1×10^6
Spectral Range	8150–8850 Å 4800–5500 Å	4800–6800 Å
Spectral Resolution	5000	20,000
Sensitivity Limit	V=20, S:N10-15/Å	V=17 S:N 150 / Å

INSTRUMENT

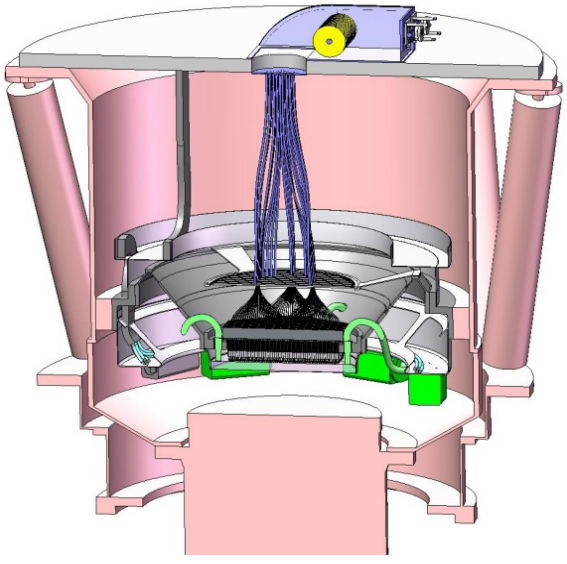

Prime Focus Instrument

The instrument survey efficiency is maximized with highly accurate positioners, fast reconfiguration time, broad spectral range, and high quantum efficiency.

Rigid Fiber Positioners that reconfigure in ~40 sec with 5 µm translational accuracy and no tilt

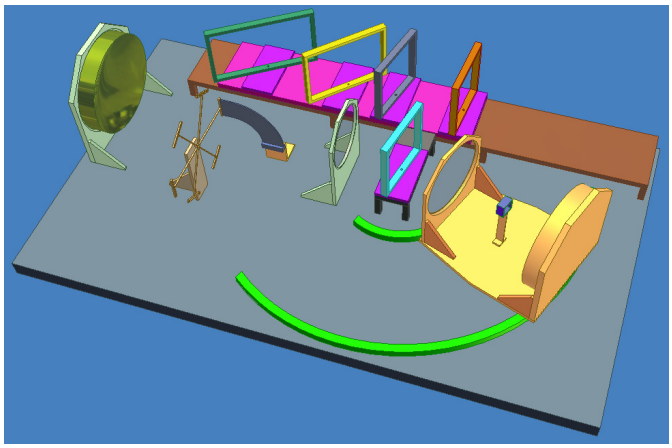

One of three identical Schmidt Spectrographs offering flexible spectral resolution and wavelength coverage

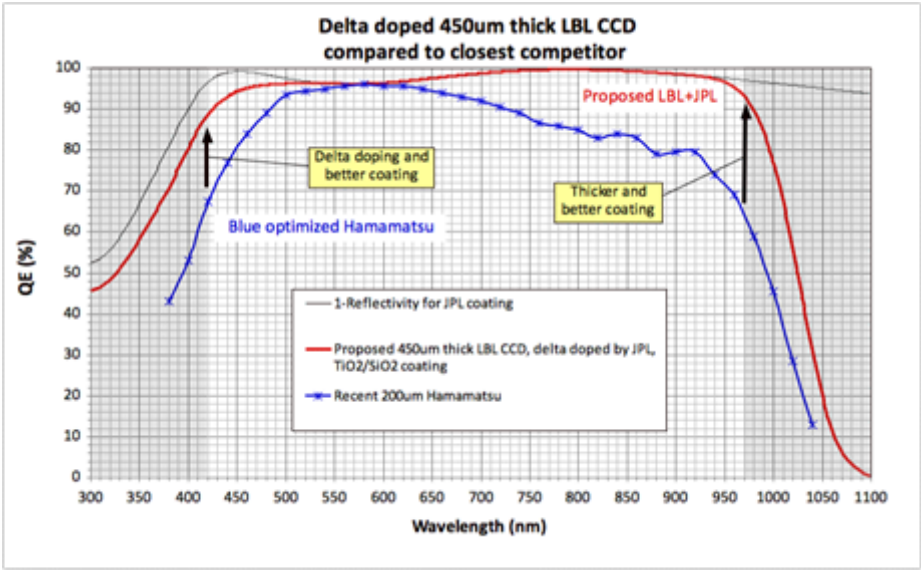

Detectors with high quantum efficiency in the blue and red range

Each of the 3 Spectrographs	
Collimator f-ratio	f/2.12
Camera f-ratio	f/1.07
Minimum beam size	~300 mm diameter
Fiber pitch at slit	230 µm, center-center
Projected fiber size at detector	54 µm diameter
SRE* width at detector	54.0 µm
Projected fiber pitch	116.25 µm
** SRE – Spectral Resolution Element*	

Detectors	
Detectors / spectrograph	2
Detector format	93 mm x 46.5 mm 5760 x 2880 pixels
Pixel size	16 µm
Red optimization	450 µm thick fully depleted p-channel
Blue optimization	Delta-doped
AR coating	custom dual layer TiO2/SiO2

MANAGEMENT

Development of this ground breaking instrument with an international team is accomplished with a management strategy developed from a history of delivering complex science instruments.

Partner	Responsibility	Cost $K
JPL	Mgmnt, Sys Eng., Positioner, PFI, A&G, I&T	27,237
Cambridge	Spectrograph	10,383
PSU	Positioner Software	563
Caltech	Detector System	2,578
LNA	Fiber System	3,550
UK-ATC	System Software, Data Reduction	4,355
UCL	Metrology System	1,639
Subaru Elements		8,000
Baseline Total		**58,305**
Reserves		10,222
Total w/ Reserves		**68,527**

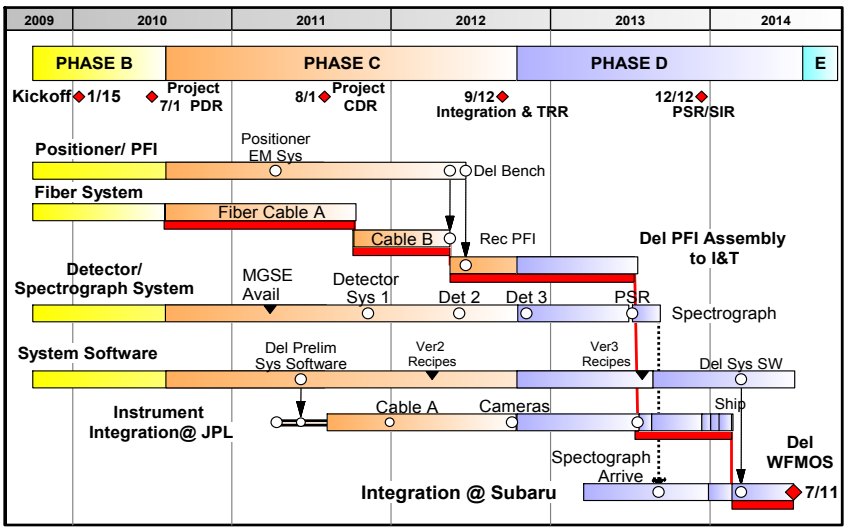

Contributors to the WFMOS Study:

Richard Ellis, *Principal Investigator, Caltech*

Mary White, *Project Manager, JPL*

Robin Bruno, *Proposal Manager, JPL*

Michael Seiffert, *Project Scientist, JPL*

Stuart Lynn, *IfA, Univ. of Edinburgh*

Peder Norberg, *IfA*, *Univ. of Edinburgh*

John Peacock, *IfA*, *Univ. of Edinburgh*

Fergus Simpson, *IfA, Univ. of Edinburgh*

Masahiro Takada, *IPMU, University of Tokyo*

Masami Ouchi, *Carnegie Observatories*

Thomas Kitching, *Univ. of Oxford*

Filipe Abdalla, *Univ. College London*

Ofer Lehav, *Univ. College London*

Ignacio Ferreras, *MSSL—Univ College London*
Laerte Sodre, Sau Paulo

Scott Chapman, *Inst. of Astronomy, Univ. of Cambridge*

Mike Irwin, *Inst. of Astronomy, Univ. of Cambridge*

Geraint Lewis, *School of Physics, Univ. of Sydney*

Rodrigo Ibata, *Observatoire de Strasbourg*

Vanessa Hill, *Observatoire de Paris*

Alan McConnachie, *Dept. of Physics and Astronomy, Univ. of Victoria*

Kim Venn, *Dept. of Physics and Astronomy, Univ. of Victoria*

Mark Wilkinson, *Dept. of Physics & Astronomy, University of Leicester*

Nobuo Arimoto, *National Astronomical Observatory of Japan*

Amina Helmi, *Kapteyn Astronomical Institute, Univ. of Groningen*

Chris Evans, *UK Astronomy Technology Centre, Royal Observatory, Edinburgh*

Beatriz Barbuy, *Universidade de Sao Paulo, IAG*

Luciana Pompeia, *IP&D, Universidade do Vale do Paraiba*

Dante Minniti, *Dept. of Astronomy, Pontificia Universidad Catolica*

Rich Dekany, *Caltech*

Anna Moore, *Caltech*

Roger Smith, *Caltech*

Steven Beard, *UK Astronomy Technology Centre*

Ian Bryson, *UK Astronomy Technology Centre*

Andy Vick, *UK Astronomy Technology Centre*

Peter Doel, *Univ. College London*

Dave King, *Univ. of Cambridge*

Ian Parry, *Univ. of Cambridge*

Dave Braun, *JPL*

Charles Fisher, *JPL*

Amanda Frieze, *JPL*

Larry Hovland, *JPL*

Muthu Jeganathan, *JPL*

Joel Kaluzny, *JPL*

Roger Lee, *JPL*

Norman Page, *JPL*

Lewis Roberts, *JPL*

S. Tere Smith, *JPL*

Ron Steinkraus, *JPL*

Karl Reichard, *Penn State University*

Antonio Cesar de Oliveira, *LNA, Brazil*

Ligia Souza de Oliveira, *LNA, Brazil*

Table of Contents

Table of Figures

Table of Tables

Executive Summary

The Wide Field Fiber-Fed Optical Multi-Object Spectrometer (WFMOS) will become the premier tool for addressing two dominant themes in contemporary astrophysics: the nature of the dark energy (DE) responsible for the cosmic acceleration and the assembly history of galaxies such as M31 and our Milky Way. Coordinated galaxy surveys delivering spectroscopic redshifts for over 4 million galaxies will use baryonic acoustic oscillations and redshift-space distortions to bring a major advance in our understanding of dark energy; the potential for the first breakthrough in this area is high. Equally ambitious Galactic Archaeology (GA) stellar surveys will provide kinematic and chemical abundance data in order to identify and study the history and nature of galactic sub-components and their relation to dark matter halos surrounding galaxies.

This proposal is the outcome of our detailed WFMOS concept study. We have revisited and rebalanced the scope and design of the DE and GA surveys compared to the earlier Feasibility Study. We have optimized the instrument for survey efficiency and flexibility. Our survey design is complementary to the HyperSuprimeCam imaging survey, which will utilize weak gravitational lensing to constrain the growth of structure. With input from Japanese colleagues, we have also examined a broader range of science applications ensuring our design is compatible with their requirements.

In designing WFMOS, we have placed the greatest emphasis on survey efficiency and positioner reliability. Our prime-focus fiber positioning system comprises 2,400 actuated elements that fill a hexagonally-shaped 1.3 degree field of view. Piezo-electric motors rapidly translate rigidly-mounted fiber optic tips without any tilting over 9.5 mm overlapping patrol regions, minimizing exposure overheads. Acquisition/guide and metrology cameras ensure accurate placement and tracking with reference to a fixed set of fiducial fibers. High-throughput fiber connectors convey signals to 3 identical spectrographs on the third floor of the Subaru Observatory. Each spectrograph is of a fast Schmidt design and permits a variety of moveable gratings offering flexibility in spectral resolution and wavelength coverage. Thick deep-depletion silicon CCDs provide enhanced red sensitivity for our proposed surveys.

Our team brings unique strengths to this ambitious project. The lead organization, JPL, is world-recognized in the delivery of complex astrophysical facilities; it offers impressive technical depth in its engineering and management expertise. The Caltech-based PI has over two decades of experience managing observatories and instrumentation at the 4–10 m class telescope scale. Our design team is drawn from a selection of institutes and individuals with excellent records in the design and delivery of innovative facility class instruments. Via the Thirty Meter Telescope project, Caltech and JPL have established strategically-important links with the Subaru community, which ensure this proposal has strong institutional support. The science team comprises highly productive world leaders in observational cosmology and galactic structure, each with valuable experience in survey design and implementation. Excellent relations have been established with Japanese astronomers involved in faint object spectroscopy and the HyperSuprimeCam project.

Our cost for WFMOS is $58.3 M in real year dollars plus 20% reserves on the instrument for a total cost of $68.5 M. (These reserves are not applied to the Subaru provided elements and are separate from the Gemini contingency.) This proposal focuses on accurate cost estimates, a clear rationale for the level of reserves, and early identification of potential risks. The management approach in delivering a complex instrument at cost with an international partnership draws on practices developed over JPL's history in the development and build of science instruments.

This Study Summary encapsulates the results of our WFMOS concept study. We summarize the development of our science objectives and requirements, present the instrument design features, trades and performance estimates, and discuss the implementation plan and management and cost details for the construction phase.

1.0 Introduction

The Wide Field Fiber-Fed Optical Multi-Object Spectrometer (WFMOS) is a fiber-fed spectrograph designed to be mounted at the prime focus of the Subaru telescope. It has two primary science objectives: 1) investigations of dark energy via baryonic acoustic oscillations and redshift-space distortions, and 2) the determination of the assembly history of the Milky Way and nearby galaxies through the study of stellar dynamics and chemical abundances (Galactic Archaeology). Such an instrument also has tremendous potential for discoveries over a much broader area of astronomy including studies of galaxy formation and large scale structure.

The WFMOS instrument is designed to allow simultaneous spectral investigations of 2,400 objects within a 1.3-degree field of view provided by the optical system of the Subaru Telescope. The combination of a large primary aperture (8.2 m) and a rapidly reconfigurable multiplex system provides the capability to survey up to 100,000 objects in a single clear night. WFMOS will use the Subaru primary mirror to focus light onto a focal plane incorporating 2,400 optical fibers. These fibers relay light to three remotely located spectrographs (800 fibers per spectrograph), which simultaneously record 2,400 spectra on arrays of CCD detectors. Data are processed and archived for further study and analysis by the WFMOS Data Reduction System.

The WFMOS instrument, described in Section 3, is comprised of the major elements shown in Figure 1.0-1, which serves as a useful introductory guide.

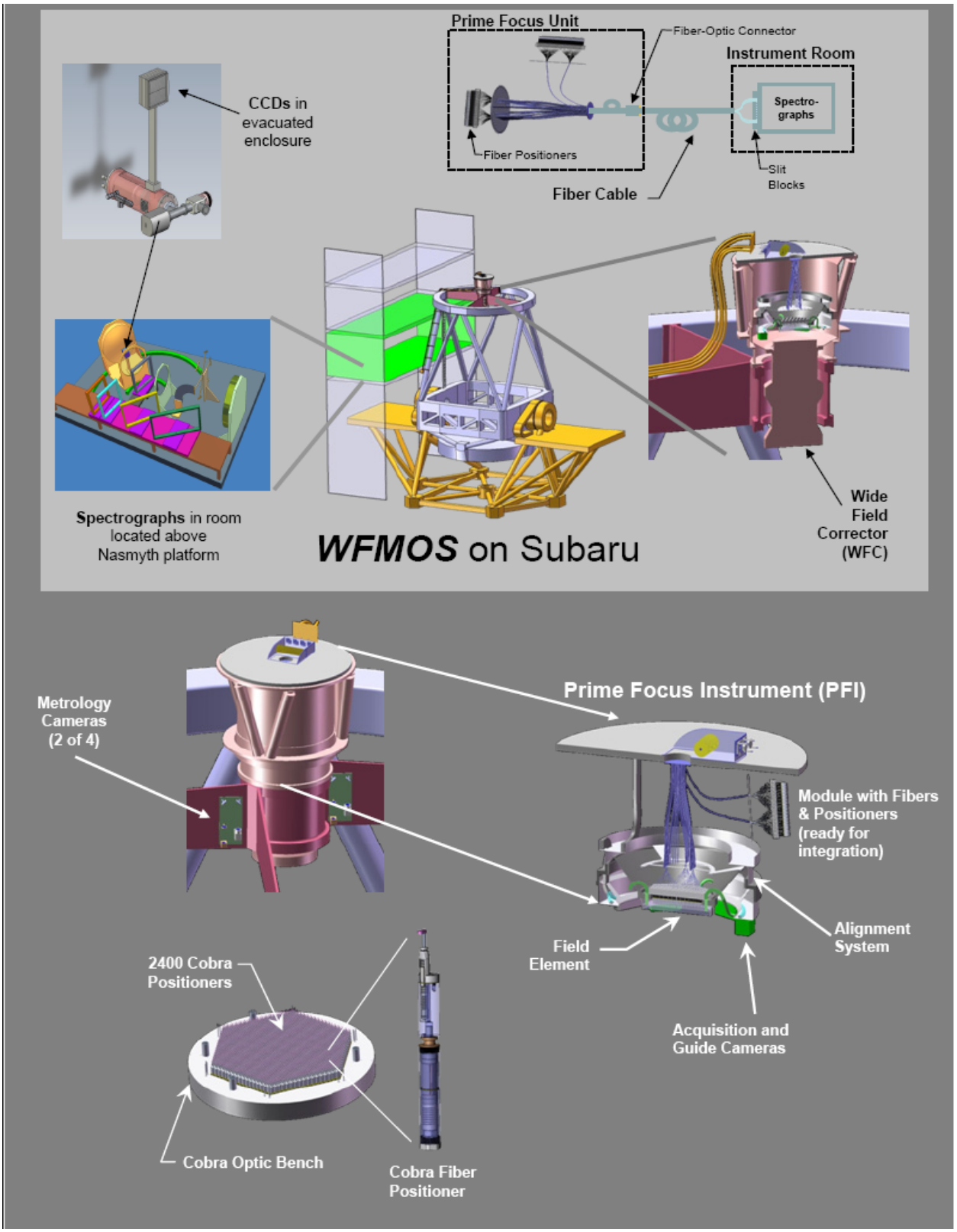

Figure 1.0-1: WFMOS Instrument System Elements

1.1 Proposal Organization

The **Study Summary** summarizes the concept study and includes an overview of the scientific motivation and survey strategy (Section 2), an instrument overview (Sections 3–5), operations description (Section 6), and the management and system engineering approach including total cost (Section 7). The **Management and Cost Volume** provides project organization, cost and schedule estimates, management techniques, and contract structure. The **Detailed Technical Design** document is a detailed description of the instrument that supplements the instrument description in the Study Summary. The **Operation Concept and Design Document** presents detailed scientific context, science requirements, and operational mode and the Level 1 requirements. The **Functional/Performance Requirements Document** lists the instrument Level 2 and Level 3 requirements.

Figure 1.1-1 shows an outline of the document tree with the current document shaded in blue.

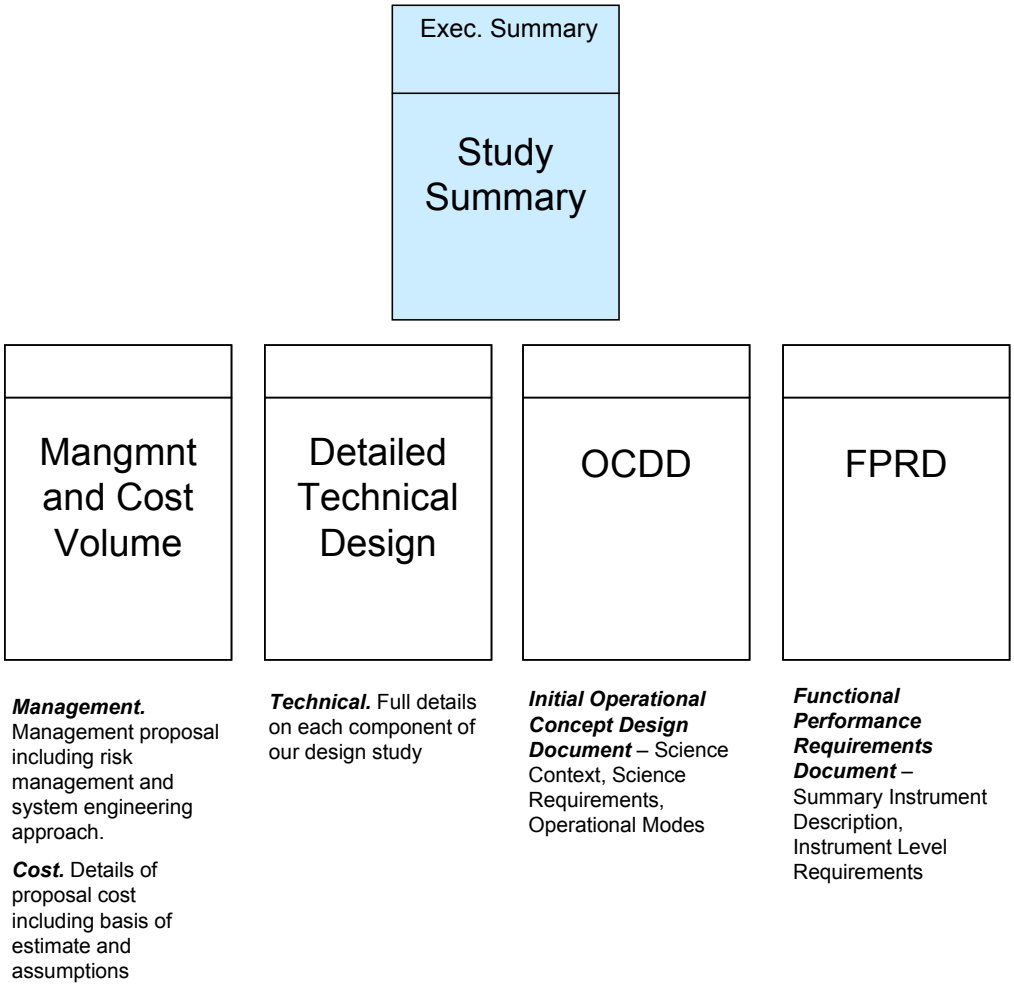

Figure 1.1-1: Organization of submittal. Our concept study is summarized in the *Study Summary* (this document). Separate volumes include: *Management and Cost Volume*, *Detailed Technical Design*, the *Operational Concept Design Document*, and the *Functional Performance Requirements Document*.

2.0 Scientific Case and Requirements

2.1 Context

We can trace the motivation for an ambitious wide field, multi-fiber spectrograph such as WFMOS to the early days of Gemini when the scientific promise of an f/6 Cassegrain focus on Gemini-South was being enthusiastically promoted by various members of the UK, US, and Canadian communities. The f/6 secondary and its associated wide field corrector were eventually eliminated for financial reasons. However, the huge impact of galaxy surveys conducted using multiplexed spectrographs on wide field 2.5–4 m telescopes such as SDSS and the AAT later resurrected the need for an equivalent facility on an 8-m aperture telescope. The discovery of dark energy in the late 1990s and the recognition that baryonic acoustic oscillations provide a valuable tracer of the cosmic expansion, independently of supernovae, has given the issue further impetus. The aim of this proposal is to make the strongest possible case for proceeding with the construction of WFMOS, in collaboration with our Japanese colleagues.

Our starting point in this study was the valuable Feasibility Study (FS) conducted by a consortium led by the Anglo-Australian Observatory. Gemini, Subaru, and the Gemini Board concluded such a facility should be installed at the prime focus of the Subaru telescope where it could share the optics destined for the (then proposed, now funded) HyperSuprime Camera (HSC). The FS study proposed a range of ambitious surveys motivated by questions in both dark energy and Galactic science. These questions, in turn, followed discussions by the Gemini community at the Aspen meeting in June 2003.

We have revised the science strategy proposed in the FS and, as a consequence, significantly improved the design of the instrument. Recognizing that HSC is now funded, we have put considerable emphasis on harnessing the synergy between these two wide-field instruments. We have also reassessed the role that WFMOS should play in dark energy studies. When the FS was published, WFMOS was a rare example of a facility semi-dedicated to probing dark energy. Today, there are a number of potential probes using various methods with at least three (AAT WiggleZ, SDSS-3 BOSS and the Hobby Ebberley HETDEX) proposing a major spectroscopic effort using baryonic acoustic oscillations. In the future there is optimism for one or two space missions dedicated to studying dark energy. Likewise, experience and progress with Keck's DEIMOS spectrograph and the ESO VLT's FLAMES spectrograph has significantly shaped our thinking of the optimum parameters for Galactic science.

One thing has not changed since the FS. Subaru remains the unique platform for an instrument like WFMOS. Investigations by others have shown that such an ambitious wide field spectrograph could not be accommodated at Keck or the VLT. Short of building a dedicated wide-field telescope, WFMOS on Subaru is the only route to achieving the science goals discussed in this proposal.

The unique capabilities of the Subaru prime focus raise the important question of the attitude of the Japanese community to WFMOS. Through active discussions and Japanese membership of both WFMOS teams, this question has been brought into sharp focus over the past few years, culminating in two major conferences—*Panoramic Views of Galaxy Formation and Evolution* (Hayama, December 2007) and *Cosmology Near and Far—Science with WFMOS* (Kona, May 2008). Recognizing the unique synergy between HSC and WFMOS on their national telescope, the Japanese community views WFMOS as a general resource whose scientific impact should extend well beyond that envisaged by the Aspen process or the FS. To address this, we co-opted a group of 5 Japanese extragalactic astronomers enthusiastic about using WFMOS for programs

not considered by the FS. We demonstrate in this proposal how our instrument, designed for dark energy and Galactic surveys, is compliant with their needs.

The following sections summarize a more comprehensive discussion of the science goals, instrument requirements and proposed survey strategies contained in the Operational Concept Design Document (OCDD), to which the reader is referred.

2.2 Dark Energy and Modified Gravity

2.2.1 The Challenge of Cosmic Acceleration

The most radical development in observational cosmology in the late 20th century was the discovery that the cosmic expansion has not decelerated as expected from the gravitational material it contains, but is now accelerating. The most direct evidence emerged from studies of distant SNe Ia used as standard candles. Additionally, by combining the now well-studied fluctuations in the microwave background with measures of large scale structure, we can confirm independently that dark energy dominates the energy density of the Universe today.

To the extent that existing data can constrain the cosmic acceleration, it is consistent with that expected for a non-zero cosmological constant Λ. However, adopting this explanation postpones solving the mystery, as no physical explanation can yet be found by physicists for such a small value of the vacuum energy. The term 'dark energy' was coined to encapsulate our ignorance of the detailed physics being probed.

2.2.2 A Dark Energy Strategy

Dark energy can differ from a cosmological constant in being a dynamical phenomenon. To test this we need to measure its equation of state through the parameter $w = P / \rho c^2$ where P is the negative pressure and ρ its energy density. In principle w can also evolve: e.g., as a function of the scale factor a, viz. $w(a) = w_0 + w_a (1 - a)$. To constrain both the value of w (= -1 for a cosmological constant) and to determine whether it evolves, requires precise measures of the distance - redshift $D(z)$ relation in the large scale distribution of galaxies as a 'standard ruler.' High precision is required: to measure w to 5% accuracy requires measuring the inferred distance D to 1%.

An obvious strategy discussed widely in the community is to first undertake a concerted attempt to reject or otherwise constrain the cosmological constant (i.e., is w = -1.00?) leaving until later the more challenging question of whether w evolves with cosmic time. A complication with measures based on the distance–redshift relation is that the bulk of the sensitivity to w arises not at the redshift at which the large-scale structure is being measured but, because of the integrated signal that builds up from $z = 0$ where dark energy is at its most dominant, at an intermediate 'pivot redshift.' The Kolb et al. Dark Energy Task Force advocated a figure of merit for a dark energy experiment in terms of its ability to jointly constrain $w(z_{\rm pivot})$ and w_a.

2.2.3 Baryonic Acoustic Oscillations

Baryonic acoustic oscillations (BAO) originate as horizon scales whose lengths are now precisely determined from the WMAP microwave background experiment. They appear in the power spectrum of the galaxy distribution on scales of order 100 h^{-1} Mpc[1]. One of the principal aims of WFMOS in the area of dark energy research will be to use the BAO signature as a standard ruler in order to measure w based on data at redshifts $z \approx 1$ and beyond. This goal has been discussed extensively in the literature, including specifically in the case of WFMOS, as well as

[1] h refers to Hubble's constant measured in units of 100 km s^{-1} Mpc^{-1}

in the FS.

The fundamental limit to the precision with which we can measure the acoustic scale at any redshift is sample variance. To be competitive it is necessary to survey large areas of the sky and probe to faint limits. Both criteria favor WFMOS—it uniquely utilizes an 8-m–aperture telescope, and its 1.5 degree field of view dwarfs the competition (cf. 15 arcmin at Keck, 25 arcmin for the VLT). Thus, WFMOS is uniquely capable of providing new constraints on fundamental cosmology, particularly for redshifts beyond 1 where existing or planned wide field multiplexed spectroscopic instruments (e.g., AAT, BOSS) cannot probe.

2.2.4 Modified Gravity and Redshift Space Distortions

Given the puzzlement about what dark energy might be, there is increasing interest in the community in probing the validity of Einstein's General Relativity. The degeneracy between dark energy (e.g., a cosmological constant or a scalar field) and modified gravity is broken when we consider a perturbed universe and examine the relationship between matter and the potentials. In Einstein gravity the growth law for density fluctuations $\delta (= \delta\rho/\rho)$ is simple and can be represented via

$$f_g(a) = d\ln \delta / d\ln a \approx \Omega_m(a)^{\gamma}$$

where $\gamma = 0.55$. But for modified gravity, γ emerges as an important additional parameter in testing the standard framework.

The basis of our WFMOS dark energy proposal is two coupled galaxy redshift surveys designed to independently test the equation of state parameter w *and* the growth rate parameter γ. We believe designing WFMOS and its surveys to measure the combination of both parameters offers the greatest chance of an immediate breakthrough in our understanding of the cosmic acceleration. This is a major change from the strategy proposed in the FS.

We can test the growth of structure, and hence γ, using the clustering anisotropy on 10–20 h^{-1} Mpc scales measured using redshift space distortions (RSD). In redshift space, peculiar velocities induced by perturbations add to the apparent Hubble motion and cause us to mislocate galaxies in the radial direction. The 2-D power spectrum in redshift space is thus distorted from its form in true space, an effect known as 'Kaiser anisotropy.' The effect was first seen with high signal/noise in the local 2dF survey using 220,000 galaxies, and the first tentative detections are now being claimed at $z = 0.8$, opening the prospect for an initial test on γ (Figure 2.2-1).

RSD studies yield a measurement of f_g at the redshift of interest. In contrast, BAO data measure a combination of the local expansion rate $H(z)$ plus the angle subtended by the acoustic scale; this involves the angular diameter distance $D(z)$, which is an integral function sensitive to what happens to dark energy between redshift z and the present. But RSD measure peculiar velocities, which derive from the history of mass assembly at redshifts *beyond* that of the survey. Thus, in combination, the BAO and RSD techniques test the continuity of whatever dark energy might be over a wide range of cosmic time.

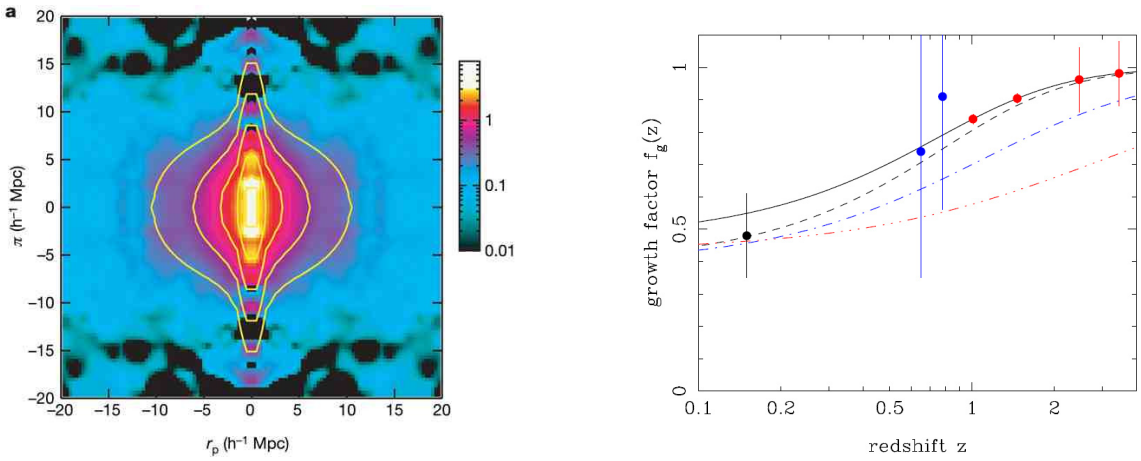

Figure 2.2-1: (Left) The redshift-space correlation function $\xi(r_p, \pi)$ at $\langle z \rangle = 0.8$, shown in false color to emphasize the Kaiser anisotropy at amplitudes $\xi = 0.1$ from the recent survey of Guzzo et al. (2008). The 'finger of God' radial stretching arises from virialized random motions at separations of a few Mpc, indicating the degree of dark matter clustering at that epoch. (Right) The growth rate function $f_g(z)$ inferred from redshift-space distortions using various existing and planned surveys (black/blue points) and the precision that can be expected from a WFMOS survey of 4×10^6 galaxies over $0.7 < z < 1.6$ and 100,000 galaxies at $z \sim 3$ (red points, each split into two redshift bins). See OCDD for discussion of the theoretical curves.

2.3 Proposed WFMOS Surveys

2.3.1 Survey Strategy: Changes Since the Feasibility Study

The FS proposed BAO surveys at both $z \sim 1$ and $z \sim 3$; the latter was an extremely expensive endeavor given the longer exposure times. In contrast we have found that since the pivot redshift changes only modestly in between these two surveys (from $z = 0.64$ to 0.98), unless dark energy is evolving rapidly, the case for an ambitious BAO survey at $z \sim 3$ is premature until we have some indication of rapid evolution from the data at $z \sim 1$. On the other hand, since density fluctuations grow by a factor of 2 between $z = 3$ and 1, there is a good degree of independence between the growth rate information $f_g(z)$ at these redshifts. Consistent with our argument to constrain w and γ independently to the highest precision possible, we argue for investing most of the observing time towards a 4×10^6 galaxy BAO survey at $z \sim 1$ that targets w (twice as ambitious as that proposed in the FS) with a much more modest survey of 100,000 galaxies at $2.5 < z < 3.3$ (6 times smaller than proposed in the FS) primarily aimed at targeting RSD and hence γ.

Focusing on the $z \sim 1$ survey, there is a further change since the FS, namely the funding of the SDSS-3 BOSS survey, which will define the landscape in low-redshift BAO studies over the next few years. The BOSS plan is to invest a significant fraction of 5 years observing time to constraining w using 10^6 luminous red sequence galaxies over $z < 0.8$. Although WFMOS as envisaged in the FS would offer a faster route to the same goal (or provide improved precision), we argue that it is more effective to fully utilize the 8-m aperture of Subaru to complement BOSS by tracing the distribution of a larger number of faint emission line galaxies to *higher redshifts*. By adopting red-sensitive deep-depletion CCDs, we have extended the wavelength coverage of the WFMOS spectrographs in order to follow the [O II] emission line in star-forming galaxies over $0.7 < z < 1.6$. In fact, the improved efficiency of our spectrographs means that although we have doubled the survey volume (cf. that proposed in the FS), the overall time requirement is compa-

rable. In a survey spanning 4×10^6 galaxies, this component of our dark energy survey will measure the acoustic scale to about 0.7% precision in this redshift range.

Ahead of a potential JDEM/Euclid mission whose launch can be expected in ~2018–2020, WFMOS will have no competition in the two proposed redshift ranges from any facility. The only possible competitor is the HETDEX project, which plans to survey Lyman α emitters in a blind manner in the $z > 3$ regime. If that survey proceeds, our high-redshift survey would still be valuable, complementing HETDEX by focusing on a different population of continuum-selected sources.

In summary, the proposed combination of galaxy surveys discussed in this proposal will:

- Measure the equation of state of dark energy using BAO over $0.7 < z < 1.6$ to a precision of 3% on constant w, better than the precision achieved by BOSS at lower redshift $z < 0.8$.
- Measure the evolution parameter, w_a, to a precision of approximately 0.3 (combining with Planck and existing supernova data), offering an interesting test of possible departures from a cosmological constant $w = -1$ over $0 < z < 2$. This represents a DETF figure of merit of close to 100, about 1.7 times better than expected from BOSS with the same assumptions.
- Measure the growth rate $f_g(z)$ over $0.7 < z < 3.3$ with unprecedented precision to test for departures from Einstein gravity. The $0.7< z < 1.6$ survey alone would measure f_g to about 1.5% precision offering the first convincing test of the standard model. The $2.5 < z < 3.3$ survey would add a second constraint over a larger time baseline to 7%.

As discussed in detail in the OCDD, the $0.7 < z < 1.6$ BAO/RSD survey will target $4{\times}10^6$ color-selected galaxies to $R_{AB} < 23.0$ over a survey area of 3,200 deg^2. Using the Keck DEEP2 survey data as a test case, we have developed techniques using BRI photometry that ensure a high success rate not only in selecting sources that lie in the required redshift range but also in indicating the sources likely to show strong [O II] emission, thus significantly improving the survey efficiency. Many ongoing and planned imaging surveys (DES, PanSTARRS, KIDS—in which our team's institutions are involved) will yield a photometric redshift accuracy better than that based on BRI photometry. The key issue is to ensure these surveys are sufficiently deep and located in an appropriate part of the sky for WFMOS with sufficient area. The simplest route is to augment the HSC weak lensing survey (likely ~2,000 deg^2) with DES, KIDS or Pan-STARRs data. Additional HSC imaging will not likely be required (see OCDD for discussion). Spectroscopic completeness is not a concern provided the survey is uniformly selected over a large cosmic volume. With exposure times of 15 minutes and minimal reconfiguration overheads, this survey is expected to require **832 clear Subaru hours (~83 nights)**.[2]

The $2.5 < z < 3.3$ RSD survey will target 100,000 galaxies to $R_{AB} < 25$ over a survey area of 100 deg^2. Targets will be found using well-tested *ugr* Lyman break selection methods. *gr* (or equivalent) imaging data will be readily available from the HSC weak lensing survey; the more challenging need is deep *u*-band data. Fortunately, the CFHT Legacy Survey has already obtained a significant (150 deg^2) amount of *u*-band data with adequate depth. Some is already public, and no doubt the remainder will be in a few years' time. With spectroscopic exposure times of 4 hours, the high-redshift survey will require **286 clear Subaru hours (~29 clear nights).**

Thus, in summary, the dark energy/modified gravity campaign can be accomplished in ap-

[2] We adopt the Gemini-recommended unit that 1 night = 10 hours

proximately **1120 clear Subaru hours (112 clear Subaru nights),** an allocation that is surely justified for such a profound cosmological quest. The expected achievements in constraining both w (via the precision on $D(z)$) and γ(via the precision on $f_g(z)$) with respect to existing and future facilities are summarized in Figure 2.3-1.

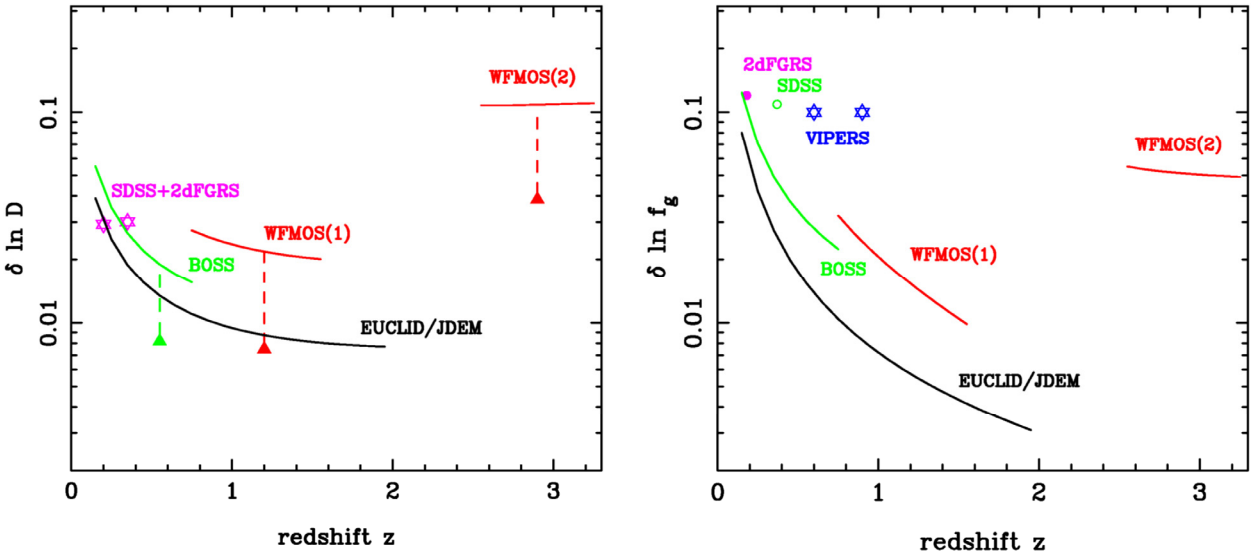

Figure 2.3-1: Fractional precision of various surveys. Left panel illustrates the expected fractional precision of various surveys in measuring the acoustic scale (using our own S/N formula, as discussed in the OCDD). Right panel shows the fractional precision in the growth rate (following White, Song & Percival 2008). The observed results for the 2dFGRS and SDSS at low redshift are plotted as points, together with the predicted accuracy of the VIPERS VLT survey. The lines are intended to show the precision expected in redshift shells of width 0.1. In the left-hand panel, we also show (triangle points connected by dotted lines) the average precision expected from the full volume of BOSS and of our WFMOS surveys.

2.3.2 Synergy with HyperSuprimeCam

HyperSuprimeCam (HSC) will provide an enlarged 1.5-degree diameter field and enter survey operations several years ahead of WFMOS. Our team has met with members of the HSC science community and discussed the obvious synergies between these two remarkable instruments. Although scientists have yet to agree on the plans for using HSC, we use this proposal to stake out two clear advantages of a coordinated effort.

Firstly, as discussed earlier, it makes great sense to coordinate the survey areas of both instruments and to use the HSC photometry to select targets for WFMOS. This involves very shallow imaging in 3 bands for some or all of the 3,200 deg^2 z ~1 BAO/RSD survey where BRI (or *gri*) photometry has a proven track record in selecting $0.7 < z < 1.6$ targets. Likewise for the z ~3 RSD survey, HSC data will be required to complement CFHT u data to select Lyman break 'dropouts.'

Secondly, the constraints on dark energy/modified gravity arising from WFMOS can, and should, be combined with those determined using weak gravitational lensing constraints provided from HSC. Subaru/HSC will provide the best weak lensing data prior to the launch of JDEM/Euclid. Combining weak lensing with photometric redshifts, calibrated via WFMOS spectroscopy, will enable 3-D weak lensing to constrain both the growth in the dark matter power spectrum and cosmic geometry. We quantify the benefits of this remarkable combination in more detail in the OCDD.

2.4 Galactic Archaeology

2.4.1 Near-Field Cosmology Comes of Age

Understanding the formation and evolution of galaxies remains one of the key questions in astrophysics. The complex processes that govern growth over cosmic history are imprinted on the Galactic structure see around us. WFMOS will be the premier instrument in the next decade capable of connecting a detailed inventory of the Milky Way galaxy and its assembly history with the rapid progress being made in probing the nature of the Universe on large scales and at high redshift.

The questions posed by this area of 'near-field cosmology' are as fundamental as those posed in unraveling the mystery of dark energy. What can our Galaxy tell us about the validity of the standard cosmological model and therefore the nature of dark matter and dark energy on small scales? What role does dark matter play in the assembly history of galaxies and what processes govern the interaction between dark matter and baryonic gas? Are these consistent with predictions of the standard model of cold, non-interacting dark matter? What can the fine structure of the stellar distribution tell us about the distribution and nature of dark matter itself? What was the sequence and process of formation of the Galaxy and how does our understanding of the history of the primary sub-components of the Milky Way (bulge, disk and halo and surviving satellites) influence our picture of how normal galaxies evolved? Finally, from studies of neighboring systems, can we be sure our inferences from the Milky Way are applicable more generally?

The key to progress lies in developing a detailed picture of the fossil record of past events, surveying stars to determine their *spatial, kinematic and chemical properties*. As galaxies are dynamically and chemically inhomogeneous, only by using the higher dimensionality afforded by combining kinematic and chemical measures can a full understanding of their constituent parts be determined. With its enormous multiplex advantage over an unprecedented wide field, WFMOS offers unique opportunities in this area. As introduced in the Feasibility Study (FS), information of two kinds is required. A deep Low-Resolution (LR) survey will chart the structural composition of the Galaxy using kinematic information and metallicities derived from absorption line indices. A higher-resolution (HR) survey will use 'chemical tagging' to identify sub-components as well as to unravel their detailed evolutionary history.

A number of developments have occurred in the subject since the FS was published in 2005. We have taken full account of these, both in defining our science requirements for the instrument and in fixing our proposed survey parameters. Foremost, we have placed significant emphasis on synergies with the upcoming Gaia mission; this remarkable satellite will provide parallax and proper motion information to limits well-matched to those of our WFMOS surveys. The combination will deliver, for the first time, six-dimensional velocity phase space essential for identifying galactic components. Secondly, we have taken into account the early progress made in surveying nearby galaxies, both satellites of the Milky Way and the neighboring M31 and M33 systems. Much work is needed to extend these preliminary investigations that are crucial to determine whether the conclusions drawn from our Milky Way apply generally to most massive spirals.

Finally, our team has been directly involved in progress made with Keck's DEIMOS and ESO's FLAMES spectrographs. The latter, in particular, has demonstrated clearly the optimal resolution for chemo-dynamical fingerprinting as a means to understanding the structure and evolution of nearby dwarf galaxies. As a result, our technical design and survey strategy have been significantly streamlined from those proposed in the FS.

The fundamental limit to progress in this area is the sheer number of high-quality spectra required. Utilizing Subaru's 8.2-m aperture, WFMOS, with its the extensive simultaneous wavelength coverage, has unique leverage to address the key questions in Galactic Archaeology. (Figure 2.4-1 demonstrates very clearly that WFMOS simply has no competition in its information-gathering power.)[3]

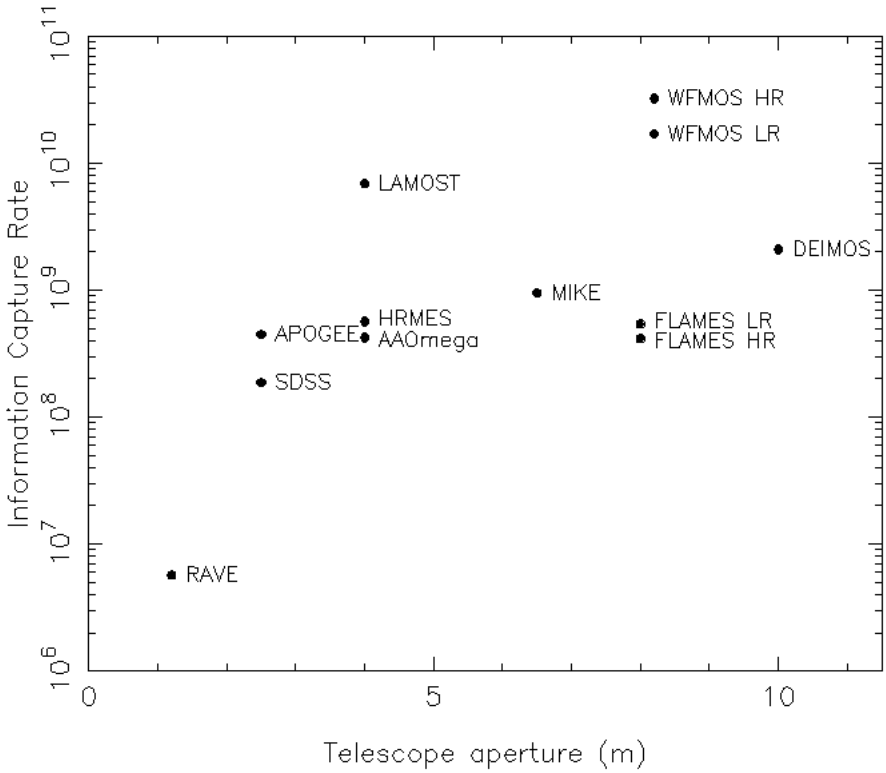

Figure 2.4-1: A measure of the impressive data-gathering power of WFMOS in comparison to other wide field spectroscopic facilities. The ordinate represents the product of the multiplex and number of resolved spectral elements above a fixed signal/noise per unit observing time. Our team has learned much from its extensive use of the FLAMES and DEIMOS instruments, and this has been reflected in our WFMOS requirements.

2.4.2 Survey Strategy: Differences with the Feasibility Study

The feasibility study provided an excellent starting point in highlighting the huge potential gains available for Galactic science. However, the ambitious nature of the program led to a rather imbalanced set of proposed surveys. We have reconsidered the program of Galactic Archaeology in detail, balancing the scientific outcomes with a realistic instrument and survey design.

2.4.2.1 Low-Resolution Galactic Survey

For the Low-Resolution (LR) survey, synergy with Gaia is crucial since full-phase kinematic measures and accurate distances are required for a complete analysis. Matching Gaia's survey limit of V = 20 is, therefore, a wise strategic choice. We have increased the spectral resolution over the original FS for sound scientific reasons. Analysis shows that a resolution of R = 5000 is needed to measure [Fe/H] to 0.1 dex precision and velocities accurate to 2 km sec^{-1}; these are required to provide an initial chemical tagging through overall metallicity measures and are es-

[3] We define the rate of information as the product of the number of spectral resolution elements ($R \times \lambda\lambda$ range), the number of fibers, the telescope diameter squared and the overall instrumental efficiency.

sential to fully isolate and probe dynamically cold tidal streams and other substructures. Furthermore, spectra that simultaneously encompass both the Mgb complex and the Ca II triplet ensure the LR survey will provide valuable data for all types of star and will not only generate more reliable stellar atmospheric analyses but also enable [α/Fe] abundance ratio estimates.

2.4.2.2 High-Resolution Galactic Survey

Experience with the ESO FLAMES and UVES instruments strongly suggests that the High-Resolution (HR) aspect of the Galactic surveys should be undertaken at R = 20,000. This is optimal in terms of maximizing wavelength coverage, recognizing the intrinsic line broadening in most stellar types. With a wide wavelength coverage and detailed line fitting, such spectra can recover substantial abundance measures previously thought only to be accessible with higher-resolution spectroscopy. At this resolution, our design provides a wavelength coverage ($\lambda\lambda$ 4,800–6,800 Å) enabling detailed abundance analyses of a wider range of species and will also facilitate improved links with spectral indices used in extragalactic studies.

In comparison with the original FS, where a HR survey of R = 40,000–50,000 was proposed, our redesign results in consequent economies in spectrograph design and survey requirements without significantly impacting scientific output. Furthermore, we dispensed with the 'nod and shuffle' technique proposed in the FS; as well as saving substantial CCD real-estate, our simulations and applications to real data demonstrate that a stable spectrograph with optimized sky subtraction leads to a factor 4 reduction in survey time.

The proposed WFMOS Galactic Archaeology program targets a number of Galactic and extragalactic components to address a range of scientifically important questions; the OCDD (Section 4) provides further details of how our surveys are strategically partitioned across Galactic science ranging from halo streams, nearby dwarf galaxies, the central Bulge and the outer disk and halo. In summary the LR survey totals **765 clear Subaru hours (~76 clear nights)** and the HR survey **1,125 clear Subaru hours (~112 clear nights).** The section also presents the case for future, large-scale surveys of M31 and M33; while this legacy program will require a substantial amount of further observing time, it will provide answers to the next big question in Galactic Archaeology, namely "Is the Milky Way unique?"

In summary, our Galactic Archaeology surveys total **1,890 clear Subaru hours (189 clear nights)** and are more acceptable in their scope than those proposed in the FS, yet offer more detailed information. They are also more balanced with respect to the dark energy request.

2.5 Additional Science

In this section we discuss the additional science that will arise, either from the proposed surveys presented earlier, or via further observations.

2.5.1 Determining the Neutrino Mass

Neutrinos are so far the only dark matter candidates known to exist. Although their non-zero mass is firmly established from solar, atmospheric, reactor and accelerator neutrino experiments, their absolute masses are still unknown. Through the suppression of the galaxy power spectrum arising from neutrino free streaming, an upper limit to the sum of neutrino masses can be determined. The key point here is that the behavior of the matter spectrum *P(k,z)* with redshift *z* is sensitive to neutrino mass in a manner that is distinctly different from that arising from the cold dark matter component. The current upper limit, obtained using WMAP, the distant supernovae data and BAO constraints from 2dFGRS and SDSS, is $m_{\nu,\,\mathrm{tot}} < 0.61$ eV (95% CL). WFMOS offers the prospect of reducing this upper limit significantly, possibly to the extent that the neutrino

mass itself could be measured. As there is a degeneracy between the neutrino mass and the dark energy equation of state parameter *w*, quantifying the neutrino mass is essential for most accurate measurements of dark energy.

We have investigated the evolution of density perturbations in the presence of massive neutrinos and find that the nonlinear matter power spectrum at $z \sim 1$ can be particularly effective. The nonlinear correction can improve the neutrino mass constraint by a factor of two compared with linear theory (which underpredicts the suppression). Using our $z \sim 1$ BAO survey we forecast a 1-sigma error of 0.097 eV on the $m_{\nu,\mathrm{tot}}$ from WFMOS. This means that if $m_{\nu,\,\mathrm{tot}} = 0.1$ in nature, WFMOS will be able to *detect* it at 1-sigma significance. This would be a development of profound importance for fundamental physics. On the other hand if the true neutrino mass is closer to zero, then we would obtain an upper limit of 0.19 eV (95% CL).

Although an important source of uncertainty in constraining neutrino mass from galaxy surveys is biasing, fortunately there are several independent ways of controlling this systematic effect : (i) modeling the biasing via halo model or semi-analytic simulations, and marginalizing over the biasing parameters; (ii) estimating the neutrino mass from galaxy power-spectra derived for different galaxy types and checking for consistency; and (iii) estimating the biasing empirically from weak-lensing map to be produced (e.g., from HSC).

2.5.2 Studies in Galaxy Formation

A key conclusion arising from discussions with Japanese astronomers and presentations made at both the international conferences mentioned in Section 2.1 is that WFMOS has enormous potential as a general-purpose, multi-object spectrograph in areas beyond dark energy/modified gravity and Galactic archaeology. One of the most exciting areas of great interest to the Japanese community is the spectroscopic study of distant field and cluster galaxies, particularly those identified in the ambitious direct imaging surveys planned with HSC. Using the existing Subaru imager Suprime-Cam, it has proved difficult for the Japanese community to secure necessary amounts of follow-up spectroscopy, primarily because the field of view of the camera (30 arcmin) is so much larger than that of the multi-object spectrographs to which they have routine access. The unique combination of HSC and WFMOS, instruments with nearly identical fields of view, offers a new synergy in science areas where the Japanese community is already very strong.

Recognizing this, we contacted an active group of Japanese extragalactic astronomers[4] and presented our instrument design in order to see if it was compliant with their likely future programs. With their assistance, we developed a number of sample programs that are feasible with our design. We hope this will serve to improve the reception to WFMOS in the Japanese community as well as to illustrate that survey instruments can achieve much more than their original goals. Section 5 of the OCDD describes these programs in more detail.

2.6 Conclusion

In summary, our team has taken the case for WFMOS forward significantly from that proposed in the Feasibility Study.

The quest for dark energy has developed substantially since 2005. Observationally, many new facilities have entered the race. Theoretically, the question of possible modifications to Einstein's gravity is now being taken seriously. We have designed an instrument and two associated surveys that maximize the impact of WFMOS in both the equation of state of a possible scalar

[4] M. Ouchi (convenor), T. Yamada, T. Kodama, M. Tanaka and K. Shimasaku

field *and* in evaluating the validity of Einstein's gravity via precision measures of the growth of structure. Our strategy takes maximum advantage of synergy with HyperSuprimeCam and complements the progress likely with the lower redshift survey undertaken with BOSS. Our surveys will give valuable input into the likely programs that will eventually be conducted with JDEM.

The subject of near-field cosmology has progressed likewise. Using our experience with Keck's DEIMOS and the VLT's FLAMES, we have proposed a more balanced and economic pair of Galactic surveys than those proposed in the FS. We have targeted the low-resolution survey closely to the upcoming Gaia mission, recognizing that synergy with parallaxes and proper motions will greatly enhance the science output. For the high-resolution survey, we have reduced the spectral resolution, arguing that increased wavelength coverage will, overall, increase the yield. Dispensing with nod-and-shuffle detectors reduces the overall request to a practical number of Subaru nights.

The four surveys—Low-Redshift Dark Energy (DELZ), High-Redshift Dark Energy (DEHZ), Low-Resolution Galactic Archaeology (GALR), and High-Resolution Galactic Archaeology (GAHR)—are summarized in Tables 2.6-1 and 2.6-2.

Table 2.6-1: Dark Energy Surveys

Low-Redshift Dark Energy Survey (DELZ)	
Redshift range	$0.7 \leq z \leq 1.6$
Number of galaxies	> 4,000,000
Target density for successful redshifts	1,245 / deg2
Incorrect redshift fraction	< 1%
Redshift precision, accuracy	$\Delta z < 0.001$
Spectral range	6,300–9,700 Å
Spectral resolution	3,500
Magnitude limit	$R_{AB} < 23.0$
Line S/N ratio	7
Estimated survey time	832 clear hours
High-Redshift Dark Energy Survey (DEHZ)	
Redshift range	$2.5 \leq z \leq 3.3$
Number of galaxies	> 100,000
Target density for successful redshifts	1,000 / deg^2
Incorrect redshift fraction	< 1%
Redshift precision, accuracy	$\Delta z < 0.001$
Spectral range	4,200–6,500 Å
Spectral resolution	1,500
Magnitude limit	$R_{AB} < 25$
Continuum S/N ratio	4
Estimated survey time	286 clear hours

Table 2.6-2: Galactic Archaeology Surveys

Low-Resolution Galactic Archaeology (GALR) Survey	
Area	2,000 deg^2
Number of stars	3×10^6
Resolution	5,000
Sensitivity limit	V = 20, S:N = 10-15 / Å
Wavelength coverage	8,150–8,850 Å 4,800–5,500 Å
Wavelength centering	0.1 Å
Continuum estimation accuracy	5%
Relative flux calibration	5%
Estimated survey time	765 clear hours
High Resolution Galactic Archaeology (GAHR) Survey	
Area	2,000 deg^2
Number of stars	1×10^6
Resolution	20,000
Sensitivity limit	V = 17, S:N = 150 / Å
Wavelength coverage	4,800–6,800 Å
Wavelength centering	0.1 Å
Continuum estimation accuracy	5%
Relative flux calibration	5%
Estimated survey time	1125 clear hours

3.0 Instrument Description

3.1 Rationale

The overriding factors in designing WFMOS for the science applications discussed in Section 2 are the need for *survey speed* and *positioner reliability*.

With the 8.2-m aperture of Subaru, emission line galaxies in the redshift range $0.7 < z < 1.6$ can yield sufficient signal to noise for a reliable redshift in only 15 minutes. This places stringent demands on the overhead for each exposure, and particularly that associated with reconfiguring 2,400 fibers for a subsequent field.

In the course of conducting the surveys discussed earlier, WFMOS will reconfigure itself over 3,000 times. Reliability of positioning and robustness of fiber units are key considerations.

In this section we present an instrument design that we believe represents a major improvement over that discussed in the Feasibility Study. The key advantages are:

- A positioner system that can reconfigure itself to the required precision in under 40 s. Each fiber is maneuvered at its tip, eliminating the need for tilting. The stout design of each unit leads to a robust system.
- A set of three high-efficiency spectrographs based on a Schmidt optical design, which offers an unrivalled combination of light beam area and acceptance solid angle at the detector (the A-Omega product). Recognizing the long-term utility of WFMOS, our spectrograph design can accommodate a range of gratings, each of which can be tilted, offering full flexibility in survey design.
- State-of-the-art, deep-depletion CCD detectors, ensuring optimal efficiency at red wavelengths for extending redshift surveys beyond $z \sim 1.3$ and measuring stellar dynamics using the Ca II triplet.

3.2 Instrument Overview

WFMOS is a fiber-fed spectrograph designed to be mounted at the prime focus of the Subaru telescope located on the summit of Mauna Kea, Hawaii. The instrument allows simultaneous low-resolution spectral observations of up to 2,400 astronomical targets. In high-resolution mode, WFMOS can observe 600 simultaneous targets.

The instrument system comprises several components. A block diagram appears in Figure 3.2-1. We summarize here the basic function of the components and their interactions; individual components are described in greater detail in following sections.

WFMOS comprises components mounted in several locations. System elements required to be at the prime focus of the telescope make up the Prime Focus Instrument (PFI) and are housed within a **Prime Focus Unit** (**PFU**). The three spectrographs, along with their detectors and support systems, will be located in a spectrograph room adjacent to the telescope, above the Nasmyth focus.

WFMOS will use several Subaru provided elements that are being developed for the **Hyper-SuprimeCam** (**HSC**) instrument. These include the HSC **Field Rotator**, **Hexapod**, structure, and a **Wide Field Corrector** (WFC).

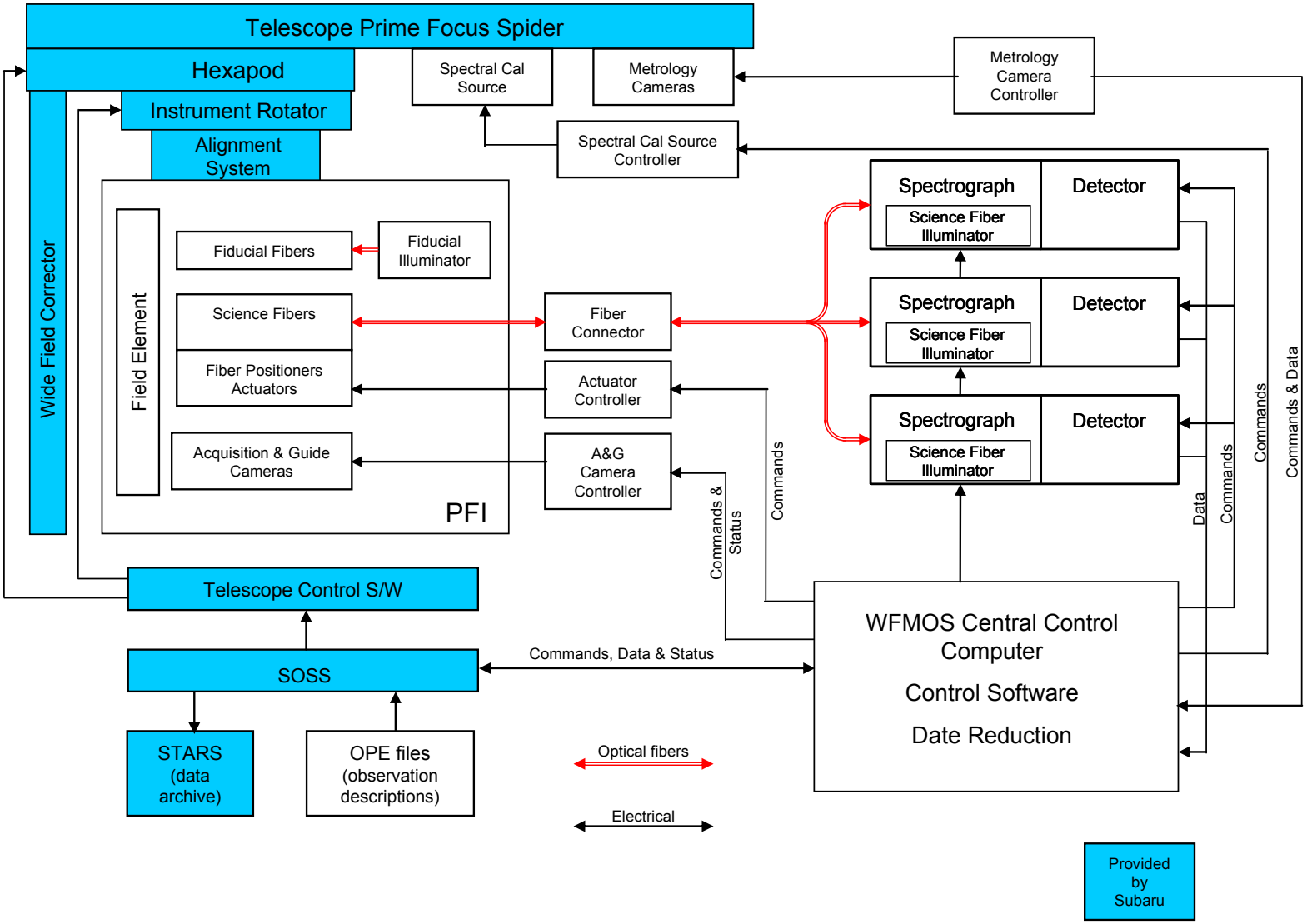

Figure 3.2-1: WFMOS Block Diagram

The filter and Dewar window used with HSC are replaced by the WFMOS **Field Element**, located close to the telescope prime focus. The Field Element is a flat window of 30 mm thickness and enables efficient coupling of the light from the WFC to the WFMOS fibers. It compensates for the removal of the Dewar window and filter that are part of the design for HSC. The Field Element also contains an array of small obscuring spots under which unused spectrograph fibers can be parked.

An array of 2,400 optical fibers is located in the PFU, with each fiber tip position being controllable in-plane by a piezo-electric **Fiber Positioner**, nicknamed "Cobra." Each fiber tip can be positioned within its 9.5-mm diameter circular patrol region. The patrol regions are in a hexagonal close-packed pattern, with 8-mm separation, and fill a hexagonally shaped 1.3-degree field of view. The overlap between adjacent patrol regions enables 100% sky coverage of this hexagonal field. The hexagonal shape of the field of view allows efficient tiling of the sky for large-area surveys.

The fibers can be reconfigured for new observation fields in 40 s, with each fiber tip placed to an accuracy of 5 μm (corresponding to less than 0.054 arc seconds on the sky). Fiber tips are translated (rather than tilted) within the image plane, providing uniform coupling efficiency for all configurations.

The small fraction of fibers that is not allocated to astronomical targets will measure the spectrum of the sky. In the case of the GAHR survey, which is cross-dispersed, three out of every four fibers are obscured by positioning the fiber tip behind a small dot on the back of the field element to avoid overlaying spectra or adding unnecessary sky background.

The **Fiber System** consists of 2,400 fibers that relay light incident at the instrument's focal plane to three spectrographs located remotely in a room adjacent to the telescope. The fibers are 60 m in length and are divided into three groups, each providing 800 inputs to a spectrograph. A key component of the fiber system is a **Fiber Connector,** which allows most of the fiber bundle to be permanently installed to the telescope while facilitating the removal of the PFU as necessary. The connector is located 5 m from the positioner end, allowing removal of the Top End Unit while leaving 55 m of the fiber bundle on the telescope structure.

After the science fibers enter the spectrograph room, they are divided three ways and arranged as linear arrays of 800 fibers at the input to each of three identical **Spectrographs**. The spectrographs provide the capability to simultaneously measure 2,400 spectra in low-resolution mode and 600 spectra in high-resolution mode. During high-resolution spectral observations, the unused fibers are positioned underneath **Blocking Spots** to reduce the sky background contribution to the spectra in the high-resolution mode. Each spectrograph uses a Schmidt optics system composed of a collimator, grating, and camera optics that are reconfigurable to support the four primary science surveys, which require different spectral resolutions and spectral ranges.

At the image plane of each spectrograph is a **Detector System** consisting of a pair of close butted 2,880 × 5,760 pixel CCDs inside a Dewar and associated cooling system. The 800 spectra are dispersed along the columns (5,760 pixels), so the gap falls between spectra. In the case of the GAHR survey, the 200 cross-dispersed spectra fill the detector array. The CCDs have exceptionally high quantum efficiency, which improves overall instrument efficiency.

The **Acquisition and Guide (A&G) System** is composed of four cameras located on the instrument optics bench in the PFU. Once calibrated to the fiber optic focal plane, the Acquisition and Guide System will provide feedback to update the telescope's pointing and field rotation by tracking on guide stars within the cameras' field of view.

There are four **Metrology** cameras, mounted on the prime focus support struts looking down at back-illuminated fiber tips via the primary mirror of Subaru. The metrology cameras determine the location of the fiber tips, allowing accurate positioning of the fibers on the selected science targets. Each metrology camera consists of imaging optics with a CCD detector and includes an internal flat-field source. Calibration of geometrical distortion inherent in the optics of the metrology cameras is achieved by having 154 illuminated fixed **Fiducial Fibers** whose positions are known accurately. Of the fixed fiducials, 91 are within the bounds of the hexagonal field of view, while 48 fixed fiducial fibers are at the perimeter of the hexagonal field. Beyond the perimeter of the hexagonal field, 15 fiducials are used to provide encoding of the rotator angle. The fiducial fibers also allow correction for geometric distortion in the WFC, through measurement and modeling.

The field of view of each Metrology camera is designed to image 1/4 of the optics bench fibers. The cameras image the backlit science fibers by viewing the optics bench through the telescope optical system, including the WFC and the primary mirror. The centroid of each fiber image is calculated and used to determine each science fiber position with respect to the fixed-fiber locations. This coordinate system is accurately referenced to the A&G camera, allowing accurate placement of astronomical targets on the science fibers.

The science fibers are back-illuminated by sources located inside the three spectrographs. Only one set of 800 fibers is illuminated at a time, in a manner allowing no ambiguity in determining fiber positions in the case that two fibers occupy a region of overlapping patrol regions.

The **Prime Focus Instrument** (PFI) consists of the Optical Bench, which contains the Field Element, Fiber Positioner System, Acquisition and Guide System, and components of the Fiber System Power Distribution System and Thermal System. The optical bench is mounted to the Rotator within the PFI via a bi-conic structure. This structure is tuned in stiffness to compensate for differential flexure between the WFC and the Rotator interface where the WFMOS components are mounted. The PFI is housed within the PFU, which can be installed and removed from the telescope as a single unit.

The **Power Distribution System** is located within the PFU to provide power conditioning and control to the electronics associated with the Fiber Positioner System, the Acquisition and Guide System, and the Metrology System. The distribution system interfaces to the telescope facility power and receives power control inputs from the System Control function. The **Thermal System** provides the interface between the telescope facility cooling system and the instrument systems located in the PFU to prevent excess heat from disturbing the telescope's viewing environment.

The **Spectral Calibration Lamps** provide the capability to measure the spectral response of the WFMOS instrument by providing a spectral source at the input to the telescope. The calibration lamps will be mounted on the telescope apart from the Prime Focus Unit.

The **System Control** provides the capability to manage an observation's preparation and execution. Preparation tasks include parsing large surveys into a series of individual observations, matching fibers to designated targets and selecting appropriate guide stars, predicting exposure times, and describing observations in a Subaru-format file. During telescope observations, the System Control orchestrates the instrument systems to achieve successful data collection, sequences the Metrology and Fiber Positioner Systems to achieve target acquisition with the fibers, interfaces to the Subaru Observatory Software System, and provides operator interfaces for quick-look data and instrument health and safety displays. The System Control also provides the

capability to perform high-level engineering tests to aid in instrument integration and trouble-shooting.

The **Data Reduction** function receives raw data read from the Detector System and uses it to produce calibrated spectra ready for scientific analysis. The Data Reduction function provides the capability to reduce data of varying spectral resolution and saves all spectroscopic and image files in the required data format. The Data Reduction function will also provide the capability to quickly assess the quality (completeness, signal-to noise ratio, etc.) of the data collected.

A typical observation proceeds as follows. After initialization, instructions are executed to configure the telescope and instrument for the desired observation. The details of each observation are pre-planned using software provided by the System Control to aid the researcher in orchestrating the survey. Using information derived from a catalog of astronomical objects, the field configuration, including the positions for each of the 2,400 fibers, is computed prior to the start of the observation. The spectrograph configuration is determined by which of the four primary science surveys is being executed. A typical observing night might use more than one spectrograph configuration in order to optimize survey efficiency as sky brightness or the seeing changes.

Execution of an observation begins with moving the telescope to the desired field center. While the telescope is slewing, the Fiber Positioning System executes commands from the System Control to simultaneously move each of the 2,400 fibers to its required position. The Metrology System is used to verify each fiber's position. The positioning process proceeds as follows:

1. The current position of each science fiber is determined relative to a set of fixed fiducial fibers. These fixed fibers are backlit by a dedicated calibration lamp. The backlit fibers are imaged by the Metrology System and the centroid of each fiber is calculated. Similarly, the 2,400 science fibers are backlit by calibration lamps in each spectrograph and imaged by the Metrology System. The centroids of each science fiber image are computed in order to determine their relative positions.
2. The System Control computes and issues the necessary commands to the Fiber Positioning System to move the 2,400 science fibers to the positions required for the observation. The metrology and the fiber movements are coordinated in 3 groups of 800 fibers. Some operations proceed in parallel.
3. Steps 1 and 2 are repeated several times to accurately position each fiber.

The positioning process is estimated to take less than 40 s from start of telescope pointing to completion of fiber positioning. In parallel with this process, the Acquisition and Guide System refines the pointing of the telescope. The Acquisition and Guide System provides feedback to the telescope pointing and rotator position during the observation. The hexapod is commanded to the appropriate position to maintain the WFC alignment in the presence of flexure in the PFU.

Once positioning is complete, the Detector System collects data. The Data Reduction System produces quick-look information on the completed observation so to that survey progress can be monitored.

3.3 Major Requirements

The OCDD defines the science requirements for WFMOS. These requirements in turn define the instrument requirements, as described in the FPRD. The WFMOS FPRD has over 60 requirements on the entire instrument and several hundred requirements on the subsystems. Not all

requirements are of equal weight; some impact the design much more than others.

We have identified those requirements that govern the design and established their connection with the WFMOS science requirements in Table 3.2-1, the Requirements Traceability Matrix. The table traces the flowdown of science objectives to measurement requirements, and then to instrument properties. The final column lists the instrument expected performance.

These requirements are abbreviated versions of the full requirements listed in the OCDD and FPRD, and are intended to summarize succinctly how high-level science requirements drive the design, and to identify the subsystems affected by high-level requirements.

Table 3.2-1: Requirements Traceability Matrix

	Science Objectives	Scientific Measurement Requirements	Instrument Functional Requirements	Predicted Performance
Provide a constraint on *w* to 3%.	Measure the distance to a mean redshift 1.2 with an accuracy of 0.6%.	• Redshift of the OII doublet at 373 nm from a redshift of 0.7–1.6 • Optimize visibility of OII doublet in OH night sky spectrum	• λ = 630–970 nm • R = 3500 • Line S/N $\geq$ 7	• λ = 630–970 nm • R = 3500 • Line S/N = 7
		• Observe > 4 × 10^6 galaxies	• $\geq$ 2,400 fibers	• 2,400 fibers
	Less than 2000 hours for DELZ and DELHZ	• Fast observations and high efficiency	• 80 s or less between observations • $\geq$ 2,400 fibers	• 40 s between observations • 2,400 fibers
Measure the growth rate of density fluctuations.	Measure this in 4 independent redshift bins between redshifts 1–3 to a precision of 0.02 near redshift 1 and a precision of 0.1 near redshift 3.	• > 100,000 galaxies observed • < 1% incorrect redshift • Redshift precision: dz < 0.001	• λ = 420–650 nm • R = 1500 $\pm$ 5% • Continuum S/N $\geq$ 4	• λ = 420–670 nm • R = 1500 • Continuum S/N = 4
Measure the mass, extent, substructure, of the Milky Way dark matter halo Conduct kinematic measurements of dSph candidates to confirm status, & measure masses, density profiles, and extent of dSphs. Measure the extent, (sub)structure, and kinematics of Milky Way stellar populations	Characterize radial velocity in approximately 30% of substantial stellar streams in the halo. Radial velocity precision of 2 km/s Proxy [Fe/H] measurements to 0.1 dex	• Observe > 3 × 10^6 stars w/ V $\leq$ 20 • R ~5000 • λ = 480–550 nm and 825–885 nm • Wavelength centering $\geq$ 0.01 nm • Continuum estimation $\geq$ 5%	• $\geq$ 2,400 fibers • R = 5000 $\pm$ 5% • λ = 480–554 nm and 818–885 nm • Spectral calibration lamps emit over λ = 480–544 and 818–885 nm. • Scattered light < 5%	• 2,400 fibers • R = 5000 • λ = 480–554 nm and 818–885 nm • Spectral calibration Lamps emit over λ = 480–544 and 818–885 nm. • Scattered light < 5%
Explore the fossil record of chemical evolution of stellar populations in the Milky Way.	Measure metalicity of stars with equivalent widths to better than 5 mÅ	• Observe > 1 × 10^6 stars w/ V $\leq$ 17 • R ~20,000 • λ = 480–680 nm • Wavelength centering $\geq$ 0.01 nm • Continuum estimation $\geq$ 5%	• $\geq$ 2,400 fibers • R = 20,000 $\pm$ 5% • λ = 480–680 nm • Spectral calibration lamps: λ = 480–544 and 818–885 nm. • Scattered light < 5%	• 2,400 fibers • R = 20,000 • λ = 480–680 nm • Spectral cal lamps: λ = 480–544 & 818–885 nm. Scattered light < 5%
	Less than 2500 hours for Galactic Archaeology Survey	• Fast observations and high efficiency	• 80s or less between observations • $\geq$ 2,400 fibers	• 40 s between observations • 2,400 fibers

3.4 High-Level Assumptions

This section describes the high-level assumptions used to finalize the proposed design of WFMOS (Table 3.4-1). A full list of assumptions appears in the Detailed Technical Design.

We received documents defining the performance of the Subaru Wide Field Corrector (WFC); however, we do not have design details that can be used in the system-level analysis. Based on the conceptual design provided, which shows the number of optical elements and qualitative curvature of each optical surface, we developed a working model of the WFC consistent with the provided performance specifications. The mechanical tolerances in our positioner design and the design of the field element are based on our assumed WFC model.

We assumed that a portion of the PFU would be shared between HSC and WFMOS, that the instruments would need to be de-mated from the PFU before the other instrument can be mated, and that this process would take approximately a day. If it takes substantially longer than a day, it will affect the observing timelines. We also assumed that it would only take three people to remove or install WFMOS from the telescope and move it to the TUE room. We further assumed that Subaru could staff this task without hardship. A related assumption is that we have two interfaces between WFMOS and the PFU: one at the rotator and one at the top of the hexapod.

Another important assumption concerns the stiffness and mechanical design of the HyperSuprimeCam PFU. We assumed that the instrument hexapod can use a static look-up table to compensate for the flexure in the PFU structure. We further assumed that there will be non-negligible differential flexure between the WFC mounting interface and the interface where the fiber positioning system must mount. Further details are given in Section 3.9.

We assumed the performance parameters for some aspects of the Subaru telescope and the elements common to HSC and WFMOS would not dominate the error budgets and assumed values were used as shown in Table 3.4-2. As a measure of caution, whenever we encountered an unknown parameter, we increased the level of margin held in the budget.

We assumed that the HSC wavefront sensor will produce lookup tables that will control the PHSC hexapod accurately enough for WFMOS, as suggested in the Interface Control Documentation (90.00.00.01_15.10.00.00_ICD_PHSC). Our computations using the reversed engineered WFC model showed that we need the focus of the WFC to be accurate to 50 μm.

We assumed that we will be able to send focus updates to the hexapod to adjust the focus of the WFC relative to the Subaru primary. We likewise assumed we will be able to send updates and offsets to the Instrument Rotator with a high speed communications link. Our Acquisition & Guide System will modify both focus and rotation.

Table 3.4-1: Major Assumptions

Assumption	Basis	Technical Impact
Differential flexure between WFC interface and positioner interface	HSC design and WFC mass	Need for a passive flexure compensation mechanism.
WFC vignetting and telecentricity	WFC performance provided, JPL model of WFC	Field corrector design
PFU interface	HSC design	Fiber placement accuracy
PHSC hexapod performance and stability	HSC design	Fiber placement accuracy and stability
Ability to send focus updates to the hexapod to adjust the focus of the WFC relative to the Subaru primary.	HSC design	Optical coupling efficiency to fibers
Ability to send updates and offsets to the instrument Rotator	HSC design	Fiber placement accuracy and stability

Table 3.4-2: Assumed Telescope Performance Throughput Values

	420 nm	440 nm	550 nm	640 nm	790 nm	970 nm
Component / Subcomponent	**Component Throughput**	**Component Throughput**	**Component Throughput**	**Component Throughput**	**Component Throughput**	**Component Throughput**
Atmosphere	0.83	0.83	0.89	0.90	0.90	0.90
Secondary Obscuration	0.95	0.95	0.95	0.95	0.95	0.95
Primary Reflectance	0.87	0.87	0.87	0.85	0.82	0.82
WFC Throughput	0.88	0.88	0.88	0.88	0.88	0.88
WFC Vignetting	0.83	0.83	0.83	0.83	0.83	0.83
Uncorrected Atmospheric Dispersion	0.995	0.995	0.995	0.995	0.995	0.995
Misalignment between WFMOS/HPFU	*0.95*	*0.95*	*0.95*	*0.95*	*0.95*	*0.95*

We assumed we will get the following documents at the start of any contract. These assumptions have driven our cost and schedule estimates for the build phase.

- Complete Subaru Interface Control Documents.
- Optical Prescription to the Wide Field Corrector.
- Complete Subaru and Gemini requirements.
- Finite Element Analysis for the WFC/PHSC interface.
- Dynamic environment from telescope movement at spectrograph room and at Prime Focus

During the course of the build phase we assumed we will get:

- SOSS Software Interfaces by Control System PDR.
- The Gemini Pipeline Reduction System CDR Documentation by Data Reduction Pipeline PDR.
- The Gemini Pipeline Reduction System Software by Data Reduction Pipeline CDR.

3.5 Instrument Trades

An important aspect of any study is tracing the high-level design trades that lead to the proposed design. Table 3.5-1 provides a summary of the trades considered for various subsystems with the selected option highlighted and a brief description of the rationale for that choice. Throughout our design, we have optimized throughput subject to cost and risk constraints.

Table 3.5-1: Summary of Major Instrument Trades. The left column lists the trades along with options considered. The selected option is shaded light blue. The right-hand column describes the rationale for the selected option.

Trades and Selected Option	Rationale
Fiber Size	
107 μm core (custom)	Optimizes fiber performance with low (3%) cost increase over standard fibers. Numerical aperture is 0.22
100 or 110 μm core (standard)	
Detectors	
Custom 450 μm LBL w/ delta doping, custom TiO2/SiO2 coating	Increased performance w/ custom CCD. Estimated QE > 90% between 450-970nm, > 96% between 480–950nm
300 μm thick Hamamatsu CCDs	
Spectrograph Design	
Reconfigurable dichroic system	
Schmidt configuration - VPHG reconfigurable, identical	Major advantage is reduction of complexity and number of optics. Large beam size minimizes effect of blockage and allows increase in resolution if desired.
Positioner	
Articulate fiber tip—Cobra	Places control on the point of interest -fiber tip. Does not require corresponding optics (POSM)
Articulate fiber base	
Robot pick and place	
Fixed fibers, actuated mirror to direct light into fiber	
Plug plate	
Metrology Cameras	
Four 4.5k by 4.5k back illuminated full frame CCD detectors	Low risk, cost effective
Four 4.5k by 4.5k front illuminated full frame CCD detectors	Perform early testing. Cost savings over back illuminated version if requirements are met
Two 2k by 2k back illuminated full frame detector scanned by several hundred pixels	
Single large format 10.5k by 10.5k pixel back illuminated full frame detector	
Corrector Plate	
Plano-plano	Simple, inexpensive, equivalent performance
Spherical	

3.6 Metrology Camera System

The function of the metrology system is to measure the position of the fiber heads on the focal plane so that each can be repositioned to a given location to an overall accuracy of 10 μm (L2.300). The metrology system itself must be able to locate the fibers on the positioner focal plane to better than 3.2 μm (L3.2720).

The proposed system has four cameras, mounted on the prime focus spiders looking back at the back-illuminated fiber heads via the primary mirror of Subaru (Figure 3.6-1). Each camera

has a 4k × 4k CCD detector with imaging optics and will look at a quarter of the positioner focal plane. Calibration of the camera distortion and mapping to the focal plane will be achieved by imaging backlit fixed fiducial fibers of known position located on the prime focus positioner plane.

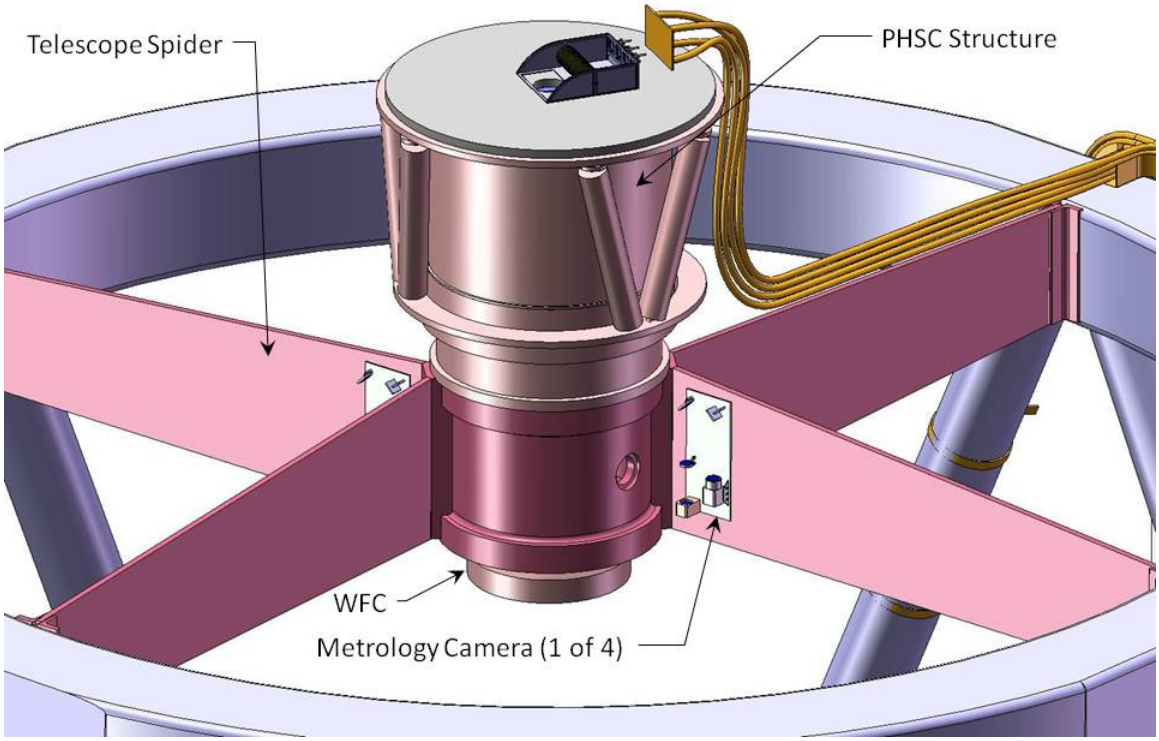

Figure 3.6-1: Schematic of Single Camera on the Prime Focus Support Strut

To reposition the science fibers onto a new object field, each metrology camera takes an image of a quarter of the focal plane. This is achieved by pulsing the LED light sources of the backlit science and fiducial fibers.

Since the patrol fields overlap, multiple images of the focal plane with different illuminated sets must be taken in order to identify the fibers uniquely. One-third of the science fibers are backlit at a time using an LED source in the spectrograph, and metrology imaging is performed three times. The science fibers are then moved to new positions based on predicted positions of the chosen targets. The metrology camera then takes a new set of images, and the positions of the science fibers are measured in the same way as before. The error from the required position is then calculated and the fibers moved again. This process is repeated six times.

The stringent subpixel centroiding requirement means back-illuminated CCDs are preferred to front illuminated ones, as they offer better subpixel uniformity. The baseline detector is the 1100S camera from Spectral Instruments, Inc with a E2V230-84. The camera read-out time is 2 s, and the centroid computation time is 1 s.

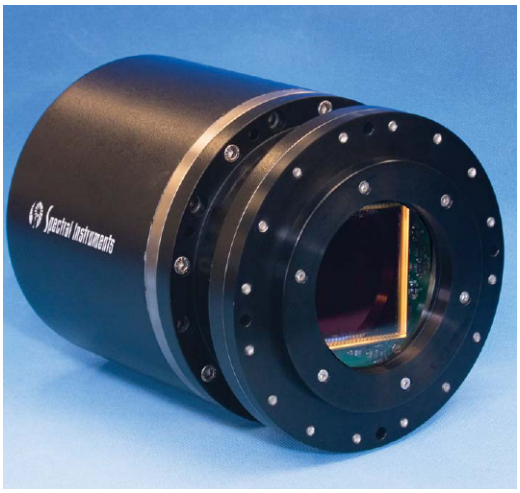

Figure 3.6-2: 1100 Series Camera from Spectral Instruments, Inc.

The optical design of the camera and its position on Subaru is shown in Figure 3.6-3. Since the camera is looking back at the fiber field via the primary, the camera is focused at infinity. The system is designed to be compact while giving very good image quality across the field with little field distortion. The CCD detector window is coated with a narrow-band filter to reduce chromatic and stray lights effects. The backlit fiber sources are matched to the narrow band filter and are visible for daytime work on the telescope.

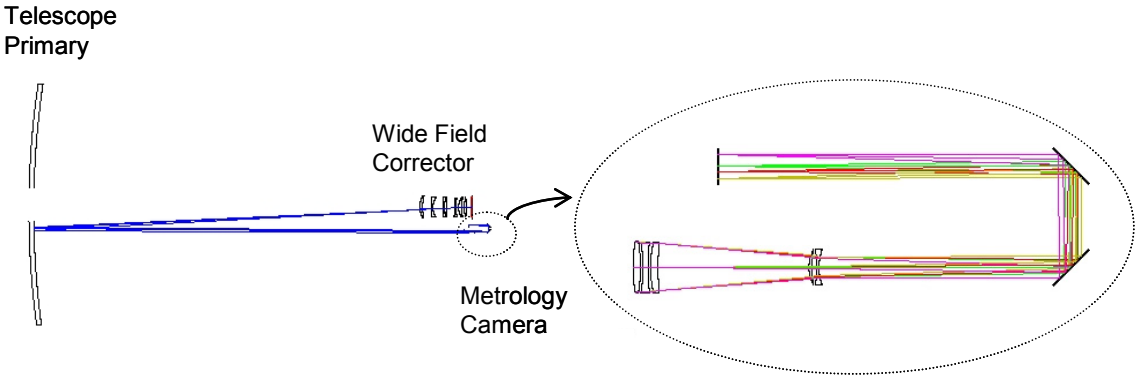

Figure 3.6-3: Optical Layout of the Subaru Telescope and the Metrology Camera

3.7 Field Element

The Wide Field Corrector design assumes a filter and Dewar glass window of 30-mm diameter. When WFMOS is installed, the WFC remains, but the filter and Dewar window inherent in HSC are removed. A trade study was performed to consider whether alternate designs would provide significant advantage over the flat window. The factors considered were flat image plane, coupling efficiency, ease of fabrication, image quality, tolerances and ease of applying blocking spots. While no replacement window would be the least expensive, a simple shift in the focal plane is not sufficient to provide good coupling to the fibers, due to the residual spherical aberration and field curvature. Our design, therefore, incorporates a flat optical element that serves as a replacement for HSC's Dewar window and filter.

An important aspect of the optical performance of the WFC is the lack of "telecentricity": the chief ray is not normal to the focal surface at the edge of the field. We evaluated the loss of fiber

coupling efficiency due to this effect and the potential of additional optical elements to compensate. Through our optical modeling, we have determined that the loss of throughput due to lack of telecentricity is very nearly identical to the loss of light from vignetting in the WFC. Additional optical elements designed to improve telecentricity do not actually significantly improve the throughput and have, therefore, not been incorporated in our design.

The WFMOS Field Element coupling efficiency at the fiber tips is shown in Figure 3.7-1. The blue line indicates the coupling efficiency without the as-built performance of the Subaru Primary and WFC. The red line gives the overall coupling performance including the Primary, WFC and average seeing of 0.7 arc seconds. The black line shows the goal of 0.80 coupling efficiency.

In addition, the Field Element has 2400 small, opaque spots ("Blocking Spots") deposited on the side closest to the fiber positioners. There is one Blocking Spot per patrol region and each Blocking Spot obscures a tiny fraction (<0.1%) of each positioner patrol region. The presence of the Blocking Spots allows the positioner to park unused fibers underneath these spots during high resolution spectral observations, which in turn reduces the sky background during these observations.

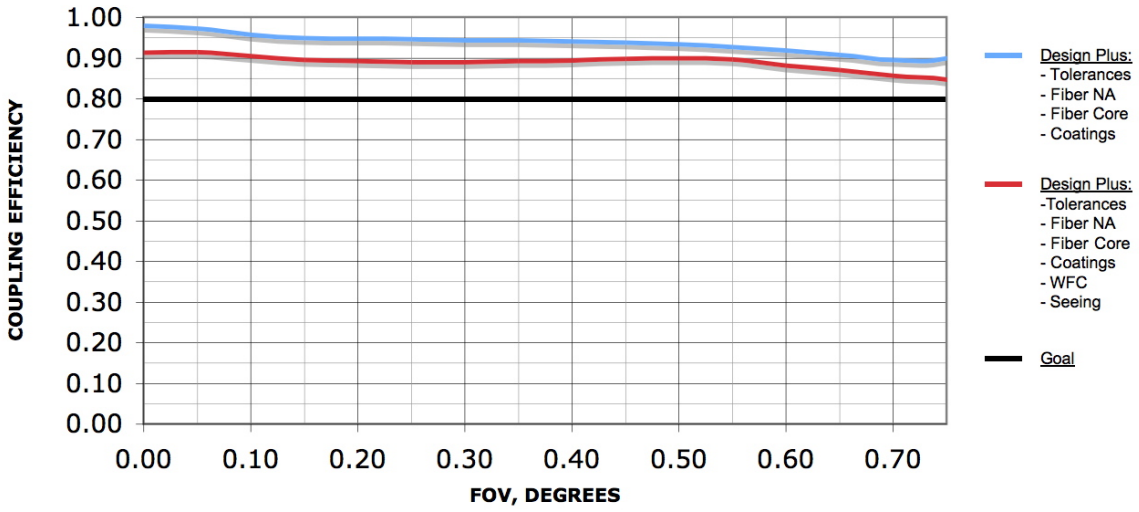

Figure 3.7-1: The WFMOS Field Element–to–Fiber Tip Coupling Efficiency

3.8 Acquisition and Guide Camera

The WFMOS Acquisition and Guide (A&G) System serves two purposes: during initial target acquisition, it locates the appropriate guide stars; once the stars have been acquired, the A&G system sends positional updates to the telescope and the image rotator in order to maintain alignment of the fibers with the science target.

We have based the A&G system for WFMOS on the highly successful A&G system for Autofib-2 on the William Herschel Telescope on the Canary Islands (Goodsell et al. 2003; Parry et al. 1994). WFMOS will use four coherent fiber bundles, each made up of thousands of individual fibers. Each fiber bundle relays the image from the focal plane to one of four CCD cameras. The image of the fiber bundle needs to be reimaged onto the detector. Figure 3.8-1 summarizes the configuration of the A&G system for WFMOS.

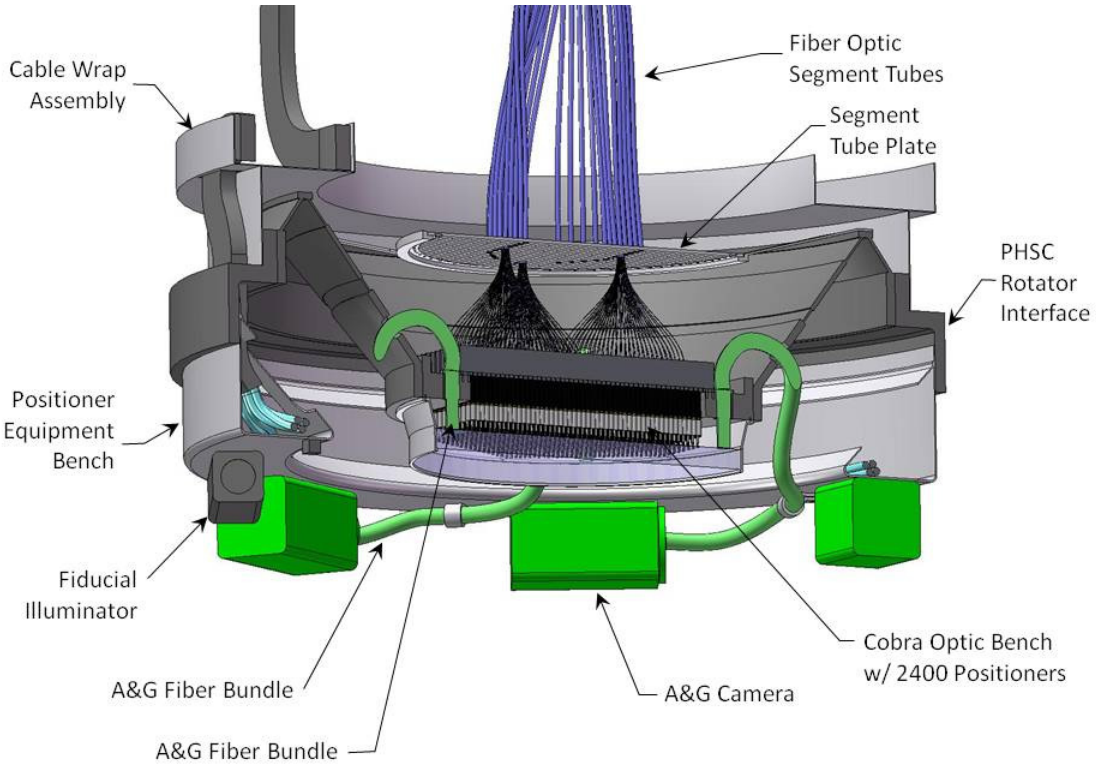

Figure 3.8-1: The proposed configuration of the WFMOS A&G System. A coherent fiber bundle reimages the focal plane onto the A&G Camera.

3.9 Prime Focus Instrument

The elements just described—the Acquisition and Guide Cameras, the field element, the positioner subsystem and the other telescope-mounted components except the metrology cameras—form the Prime Focus Instrument (PFI) and are mounted on the PFI structure that interfaces to the PFU) (Figure 3.9-1). The critical function of the PFI structure is to establish and maintain alignment of these subsystems to the WFC. There are two major elements of the PFI structure: the rotating portion that interfaces to the PHSC rotator and the fixed portion that interfaces near the upper end of the PHSC hexapods.

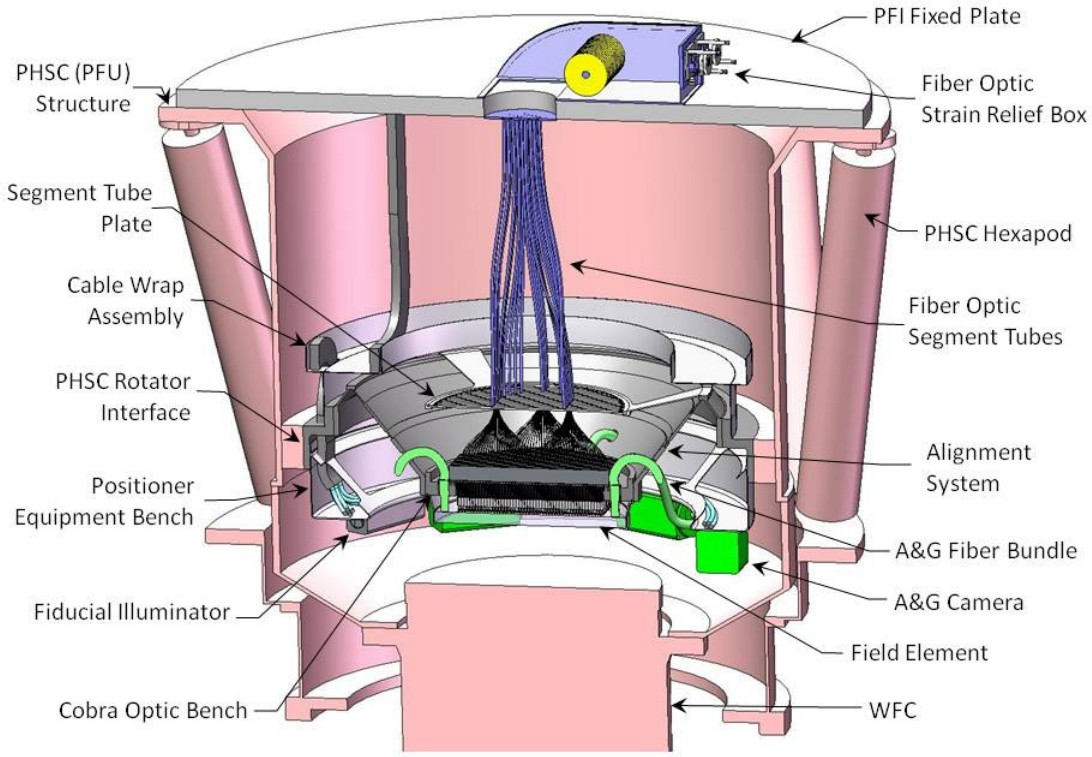

Figure 3.9-1: The Prime Focus Instrument

The rotating portion interfaces to the PHSC Rotator with a bi-conic structure and supports the Positioner Assembly and associated fibers, the fixed fiducial system, and the acquisition and guide cameras (Figure 3.9-2). The bi-conic structure provides initial alignment of the positioner to the WFC and is tuned in stiffness such that the defocus, decenter, and pointing of the Positioner Assembly matches that of the WFC within the required limits. The most critical alignment requirement is the focal plane tilt of 34 arcsec with respect to the WFC. This appears to be readily achievable since this is on the same order as the predicted WFC tilt with respect to the telescope over its 60 degree operational elevation.

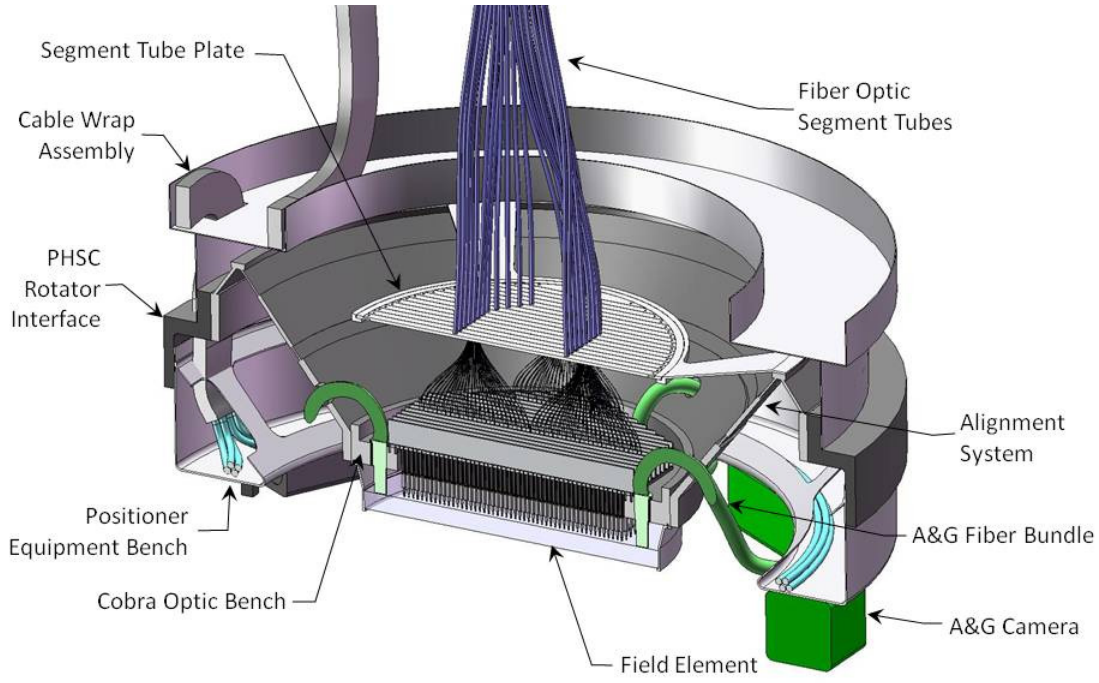

Figure 3.9-2: The Rotating Portion of the PFI

The PFI Fixed Plate supports the optic fiber cables, the Strain Relief Box, power and data cables, and the Cable Wrap Assembly (Figure 3.9-3).

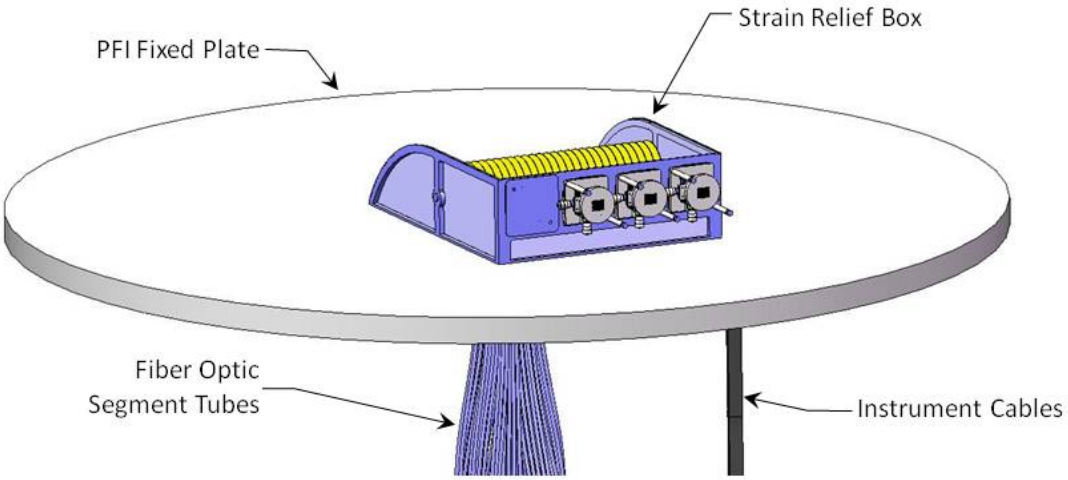

Figure 3.9-3: The PFI Fixed Structure

The Fiber Optic cable is routed between the fixed and rotating parts of the PFI, such that the 500-degree rotator range is accommodated by twisting along the rotation axis rather than bending around a spool. This improves throughput by reducing the bundle length by approximately 4 m, while the effect on throughput and FRD via twisting is offset by the cable not having to bend around a spool or cable chain.

The thermal control approach is to remove heat locally from the heat-generating components of the system—the A&G Cameras, and the Metrology Cameras—using the glycol coolant loop.

These components are commercially available with glycol cooling, which may be modified to remotely locate the field joint on the secondary ring.

One of the major integration phases occurs at JPL where the positioner assembly, Acquisition and Guide Cameras, and Fixed Fiducial are integrated onto the PFI structure using a temporary structure for the PHSC. As a risk-mitigation strategy, a fit check of the Rotator Interface Ring and the PHSC Rotor is done before it is integrated into the instrument. A turnover/rotation fixture is used to build up the PFI starting from the rotator interface. As soon as the alignment system and positioners are integrated onto the Rotator Interface Ring, the fixture is used to test performance in multiple orientations with respect to gravity.

3.10 Positioner

One of the key features of WFMOS is the positioner assembly, which places the tips of the fiber optics at specified locations on the focal plane to route the light from the astronomical objects of interest to the spectrograph. Previous generations of multi-object spectrographs have allowed simultaneous spectra of many hundreds of objects. Techniques employed for these spectrographs have included humans placing fibers by hand in automatically machined plates (e.g., SDSS), and robotic pick-and-place of magnetically attached fibers (e.g., 2dF). As our ambitions rise to simultaneously measuring many thousands of simultaneous spectra, a reconsideration of the full array of viable techniques is required.

After examining a number of alternatives (Detailed Technical Design, Section 2.3.16), the selected approach, the “Cobra” positioner system, populates the focal plane with 2,400 positioners that fill a hexagonal field (Figure 3.10-1). Each positioner moves a single fiber to its target position in its planar patrol region. Translating the fibers through the patrol region using these actuators allows rapid, direct placement of the fiber tip with a mechanism that is robust in terms of stability, accuracy, and life. Its planar movement eliminates losses due to fiber tilt and tests replicating the fiber path through the positioner confirm that there is no loss due to fiber twist or bend.

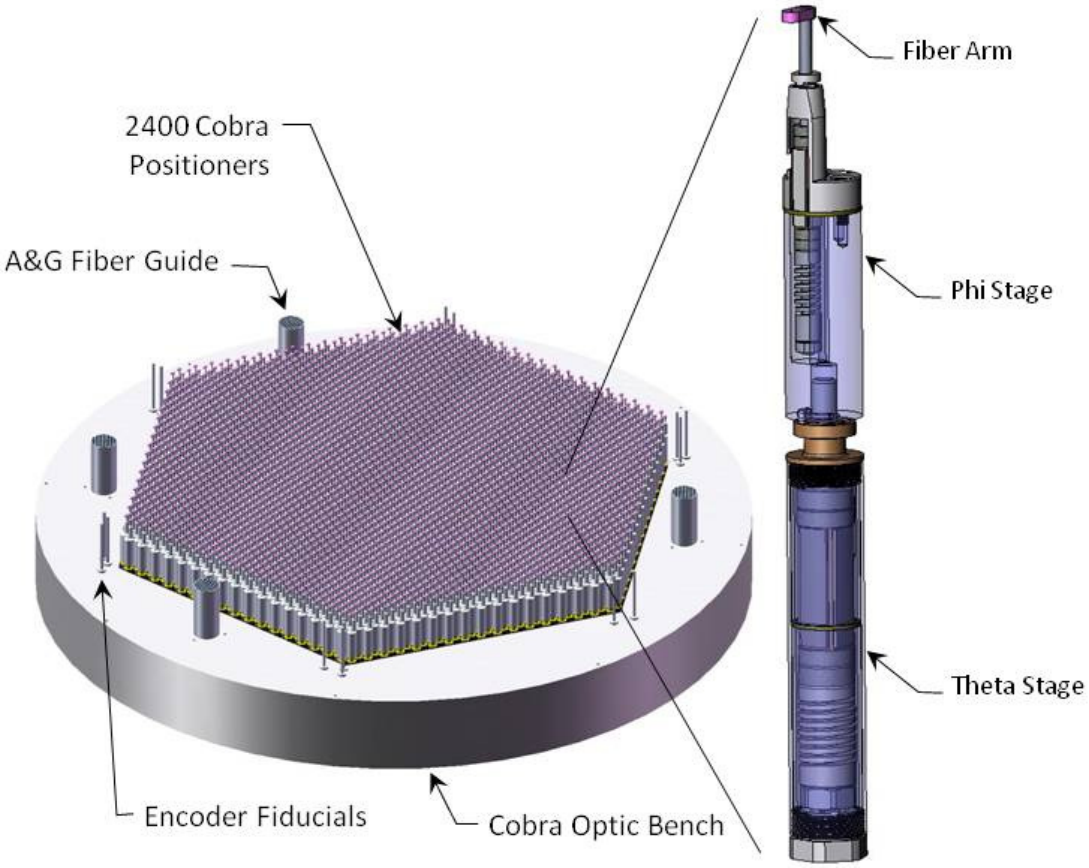

Figure 3.10-1. Positioner Bench Populated with One Module and a Single Positioner

Each fiber tip can be placed anywhere within a circular region, the patrol region, using a set of two piezo-electric motors. Figure 3.10-2 shows how the focal plane is covered with overlapping patrol regions. In this figure, the blue segment and the circle it sweeps out shows the travel of the first (theta) stage; the orange segment and its swept circle shows the coverage of the second (phi) stage. The second stage rotates the fiber arm. The combination of these movements provides coverage through the larger enclosed circle with radius, R.

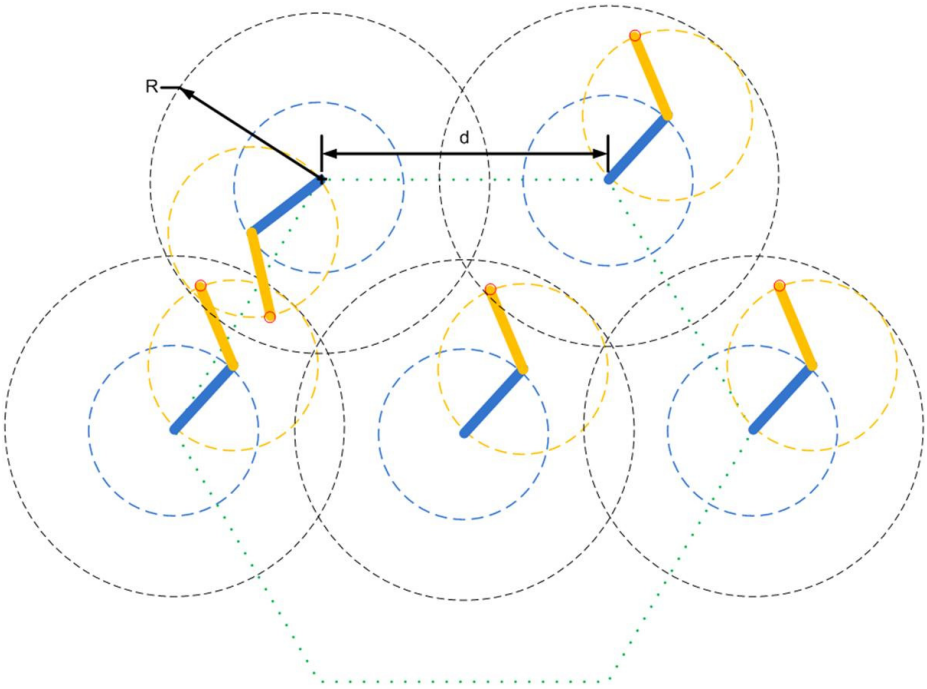

Figure 3.10-2: Positioner Patrol Region Overlap. The black dashed lines indicate the patrol regions of adjacent positioners, showing there is complete coverage of the populated field of view. The distance between adjacent positioners, *d*, is 8 mm, while the diameter of the Patrol Region, 2*R*, is 9.5 mm. Blue and orange represent the two stages of the positioner motors (see text).

The positioner is designed to locate the fiber tip to within 5 μm accuracy in less than 10iterations (FPRD L3.790), with all commanded moves taking less than 1 second (FPRD L3.800). Meeting these timing and accuracy budget allocations means the throughput loss from the positioners is less than 10%. Fiber repositioning — taking into account the other steps such as the metrology loop (Table 4.2-1) — will be accomplished in less than 40 seconds. This maximizes observing time and efficiency. A prototype was built by New Scale Technologies and recent testing at JPL demonstrated this first unit was able to converge on 90% of the targets to within the 5 microns accuracy in 6 iterations and had 100% convergence after 8 iterations, all at the required speed. Additional details of this test are discussed later in this section and in the Detailed Technical Design, Section 2.3.14.

The Cobra Positioners are mounted in an optical bench at the focal plane and are placed 8 mm apart to create a 2,400-positioner field in a hexagonal pattern to allow efficient tiling of the sky region of interest. Each positioner has a circular patrol region of 9.5 mm; this, combined with the 8-mm spacing, ensures complete coverage of the populated area of the focal plane. The populated area fully covers a 1.3-degree field over the area of the focal plane with higher throughput, resulting in more efficient use of the positioners (Figure 3.10-3).

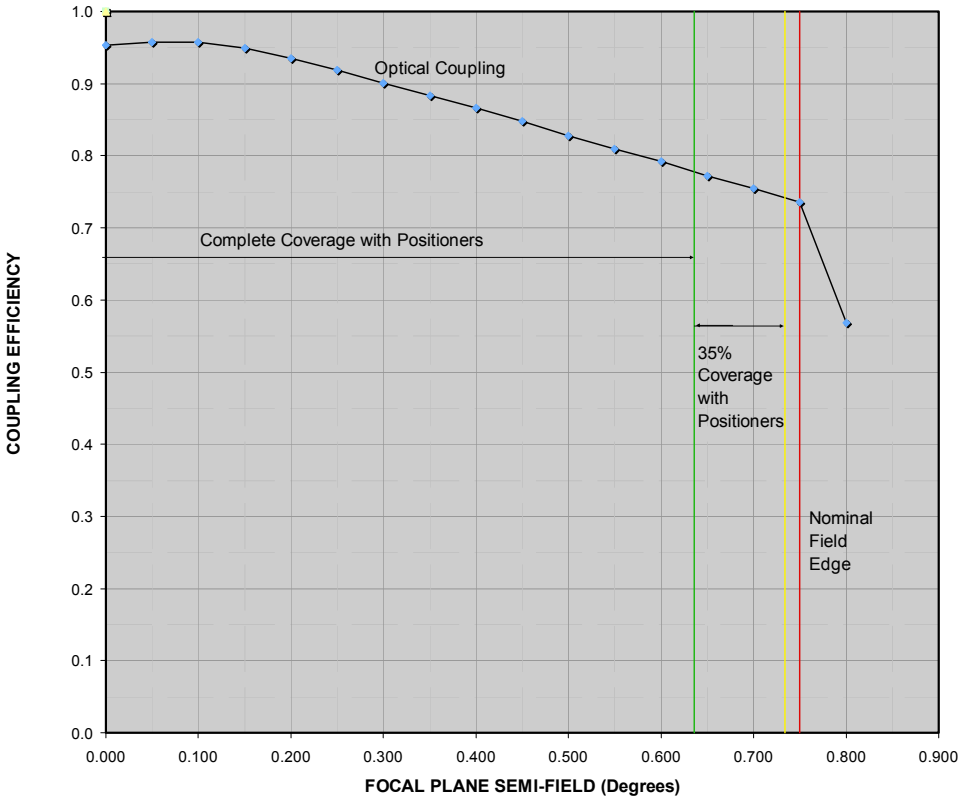

Figure 3.10-3: Optical coupling efficiency versus distance from the center of the field of view. The plot shows the field coverage of the positioner array. Coupling includes the optical performance of the WFC and the numerical aperture of the fiber, but does not include seeing or WFC internal flexure.

The actuators are controlled in an open-loop mode with position information obtained after the fiber field is moved. Their positions are verified by back illuminating the optical fibers and measuring its location using a CCD metrology camera.

The key to achieving rapid and accurate target acquisition are the Cobra Fiber Positioners, Figure 3.10-4. Cobra's small size, high speed, and high resolution make it a key component of WFMOS. The critical technology is a new class of rotary motors, called Rotary Squiggle Motors, which were developed specifically for WFMOS by a small team of engineers at JPL and New Scale Technologies (NST). These motors set new benchmarks for small size and resolution performance which has not been achieved in electromagnetic motors. This simple, robust rotary piezo tube motor has been scaled to 3.3 mm diameter, without significant loss of power efficiency. JPL's experience in high reliability spaceflight mechanisms combined with New Scale Technologies existing linear motor design and analysis skills as well as mass production capabilities is the perfect teaming relationship for the needs of WFMOS. The teams collaborated in a rapid 8 month development of the Cobra Positioner that successfully surpassed the requirements for positioning accuracy and speed.

Figure 3.10-4: The Prototype Cobra Fiber Positioner

The motive force of the Rotary Squiggle Motor is provided by two pairs of piezo plates mounted on a flexible tube that are actuated in a coordinated "hula" fashion to produce rotary motion (Figure 3.10-5). The Cobra Positioner is made up of a 2.4-mm motor and a 4.6-mm motor, which match the sizes required to ensure the WFMOS survey speed.

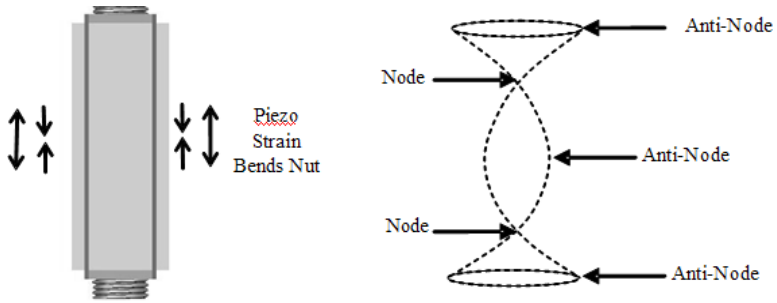

Figure 3.10-5: Rotary Squiggle Motor Motive Force Schematic

The Cobra unit is a 7.7-mm diameter, theta-phi style, 2-axis fiber positioner, with the dependant axis offset from the independent axis, enabling the optical fiber to be placed anywhere in a 9.5-mm patrol region, as shown in Figure 3.10-6.

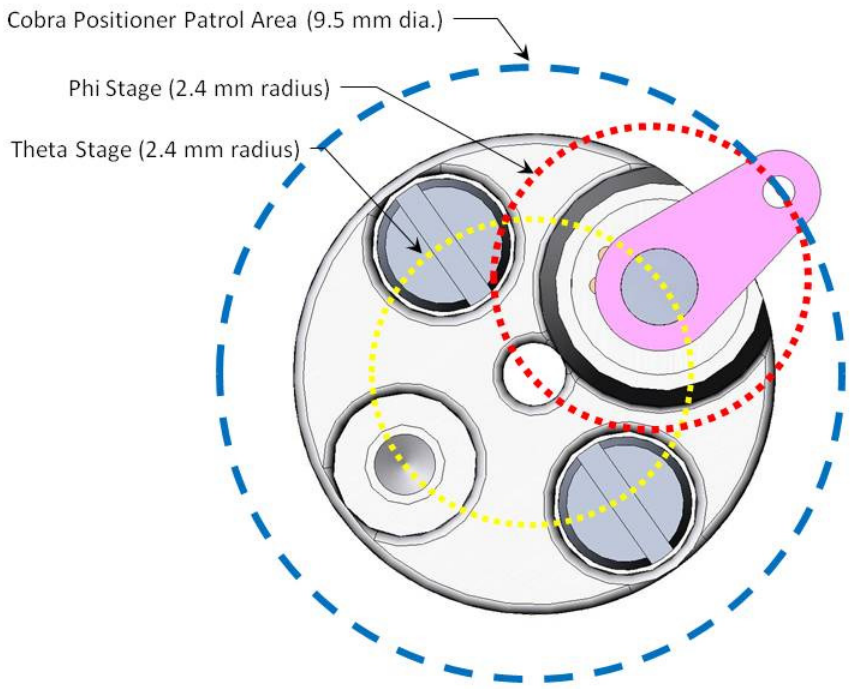

Figure 3.10-6: Patrol Region of a single fiber positioner (top view). The two motors in each positioner have axes that are offset from one another, allowing the fiber tip to travel anywhere within the patrol region.

Features have been included in the Cobra Positioning system to make integration and test more efficient. The Cobra Positioners are fabricated and assembled with tolerances that keep the patrol areas sufficiently parallel to the focal surface to eliminate all but one manual adjustment during assembly. Also, the positioners are divided up into separable modules to make integration, testing, and servicing easier. Each module has its own electronics module, making verification of mechanical and electrical function and performance possible early in the construction phase. These features are in line with the overall project strategy to allow early and complete testing of subsystems.

The Cobra Electronics uses a distributed-driver approach. This approach facilitates maximum motor movement flexibility with minimum wiring. A block diagram of the approach is shown in Figure 3.10-7. The Positioner System key component is the Positioner Module. This Module consists of a unique addressable FPGA and a driver per motor in the module.

The basic approach has three steps:

1. Motor drive information is created in the positioning computer from data generated by the Metrology System. This consists of the Unique Module ID, the motor number in the module, the duration of the motors operation, and the direction CW or CCW of the motor.
2. This information is transmitted through an optical Ethernet connection to the Ethernet Interface, which reconverts the Ethernet Data format back into data commands that are forwarded to the proper Positioner Module FPGA.

3. The FPGA generates the signals that have the proper duration frequency and phasing to cause the motor to rotate properly.

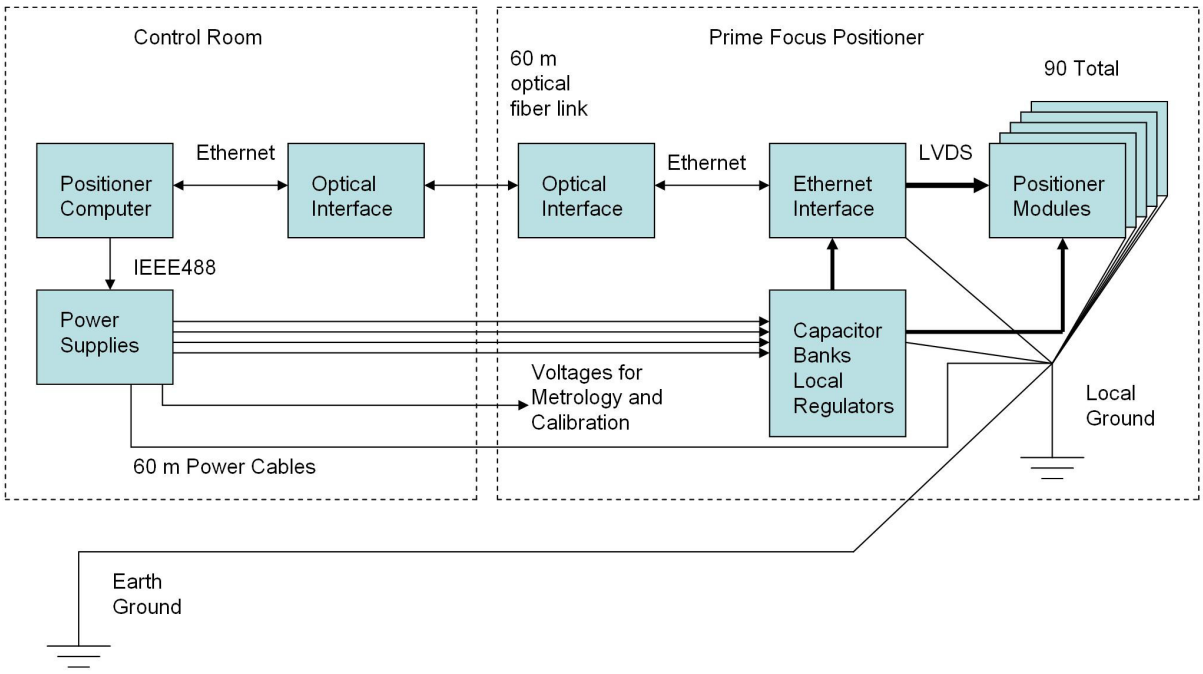

Figure 3.10-7: Positioner System Block Diagram

Proper packaging design and techniques are necessary to make the 2.5-volt signals from the FPGA compatible with the 120-volt square wave out of the drivers. To accomplish the electronics packaging, chip on board (COB), automated assembly, and automated testing techniques will be utilized. Testing will be performed to ensure noise and cross-talk issues are addressed. Sufficient resources have been allocated to allow early testing (by Positioner PDR) and multiple design cycles to characterize the performance of the electronics and bring the design to maturity.

Once assembled and verified, the Cobra modules are then integrated to the Cobra Optic Bench, which interfaces to a tilt/rotation test fixture via the Positioner Alignment System. When the entire bench is assembled and the electronic modules are daisy chained together, the bench is functionally validated. The deformations due to temperature and gravity are acceptance tested before the components are integrated and verified at higher levels of assembly.

Integration of fibers into the modules can be done in parallel. The design and schedule allows for integration of the fibers through the center of the positioners; this is a configuration that has been tested and meets the throughput requirements. However, schedule and workforce can be recovered by routing the fibers externally to the positioner. Early testing will determine whether the throughput requirements are met. If the requirements are met, the integration approach can be simplified and accelerated.

The WFMOS control system provides the positioner movement planning software (MPS) with the target and the current fiber locations—as measured by the WFMOS Metrology System—of the individual optical fibers, specified in the coordinate system of the WFMOS instrument measurement plane. The MPS computes the motor drive information and generates an output file consisting of the sequence of movements for the embedded controller software to

command each positioner motor to move the fibers to the target position.

After each sequence of maneuvers, the MPS will receive an updated map of the positioner fiber locations and generate a new command sequence to reduce the error between the target and actual positions. The software includes a learning algorithm to incorporate the history of movements of each positioner with respect to parameters such as starting position, length of move, or temperature in planning the next move. The Cobra Positioners have a 9.5-mm patrol region, but are spaced only 8 mm apart. This overlap ensures complete coverage by the positioners, but also means that adjacent positioners may collide if their sequence of maneuvers is not carefully coordinated. When computing the sequence of motor commands for an individual Cobra positioner, the MPS considers current locations of the six adjacent positioners with which its patrol region overlaps. The simple solution is to run each positioner radially when transiting common patrol areas to avoid collisions.

A prototype testbed was constructed to demonstrate the performance of the Cobra Fiber Positioner. The testbed was set up with a back illuminated fiber and a metrology feedback camera system analogous to the system being proposed for WFMOS (Figure 3.10-8). Even though this was a rapid, low-cost development, this first unit was able to position within 5 μm within six iterations, 90% of the time.

Although this performance exceeds the requirements, mechanical and software control improvements have been identified in anticipation of performance degradations not captured in the prototype test. Differences in large scale production, driver design, subsystem communication, lifetime, neighboring positioner collisions, and environment all may have effects on the number of iterations to achieve convergence. We will make improvements in the design where they come at little or no cost. Optimization of torque versus resolution, the rotor-stator interface design, control algorithm maturation and improvements in manufacturing and assembly techniques will lead to better resolution, greater reliability, and/or reduced manufacturing costs and gives confidence the requirements will be met.

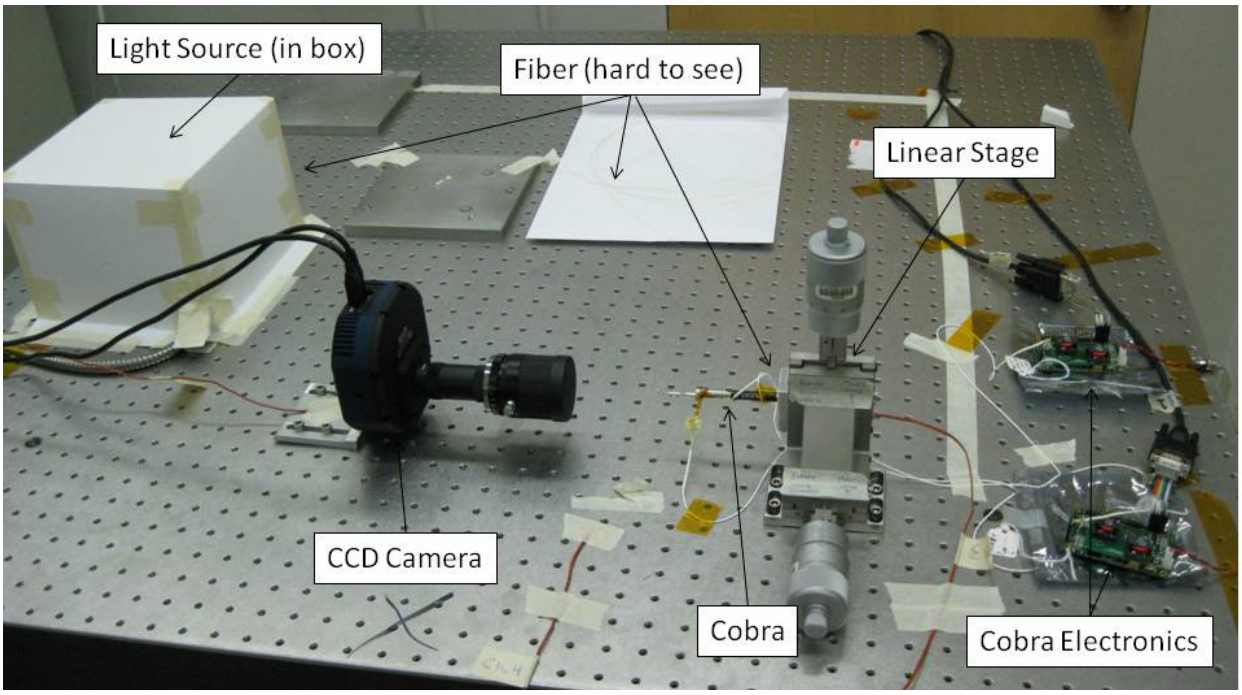

Figure 3.10-8: Prototype Positioner Testbed. A light source illuminates a fiber optic mounted in the Cobra positioner unit under test. A CCD camera accurately measures the position of the fiber tip.

3.11 Fiber System

The function of the Fiber System is to collect light from the prime focus and deliver it to the three spectrometers located off the telescope. Based on science needs, the optimum fiber is a step-index, silica fiber with core diameter of 107 μm, cladding diameter of 140 μm and numerical-aperture (NA) of 0.23. Several commercial vendors, such as Polymicro Technologies, Nufern, and OFS/Furukawa, are willing to provide such custom fibers. Preliminary fiber-routing design indicates that 60-m long fibers would be needed from the prime focus unit to the spectrometer. Figure 3.11-1 shows key elements of the fiber system. Though the fibers, and the application they are being used for, may be unique, it behooves us to use technology and processes developed by the telecom and fiber-optics industry. We will, therefore, rely heavily on industry standards and practices to build cables and connectors; we will rely on custom fabrication only where appropriate.

From a system performance view, the key requirement on the fiber system is its throughput. Based on preliminary design, the fiber system throughput ranges from 0.4 at the blue end of the spectrum to 0.65 at the red end of the spectrum (see Figure 3.11-2). Three dominant factors affect the throughput of the fiber system: 1) attenuation, 2) focal ratio degradation (FRD), and 3) connector losses.

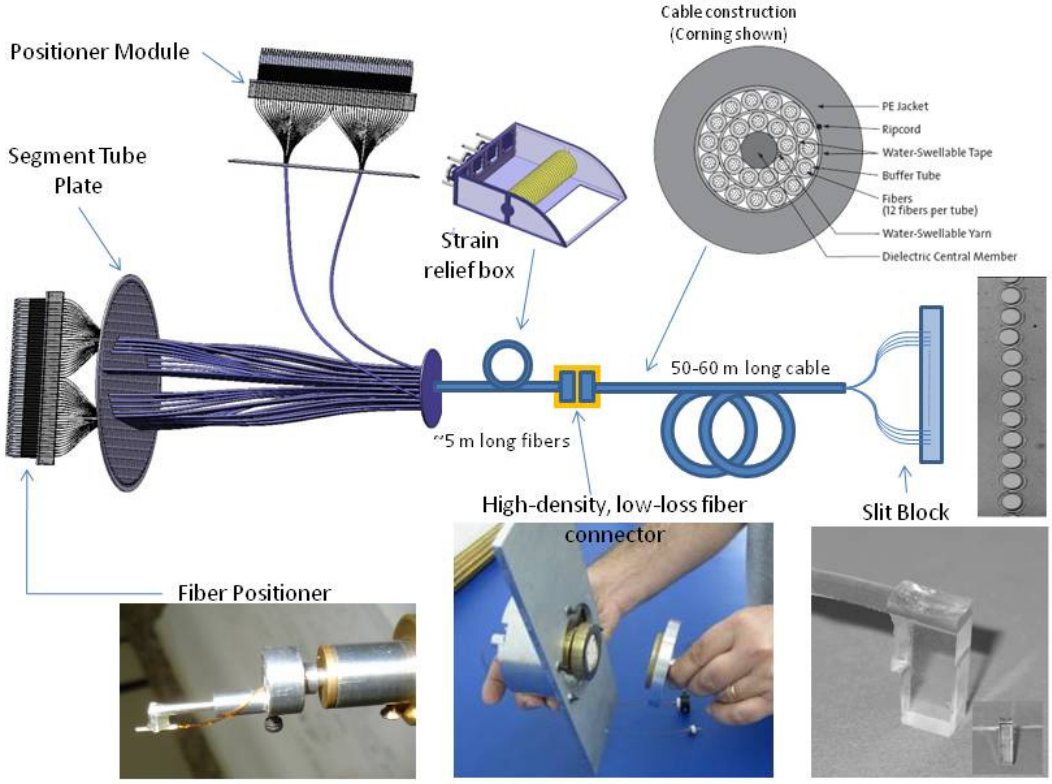

Figure 3.11-1: Schematic of the fiber system from the positioners to the spectrograph. Pictures of key hardware from risk-reduction activities are also shown.

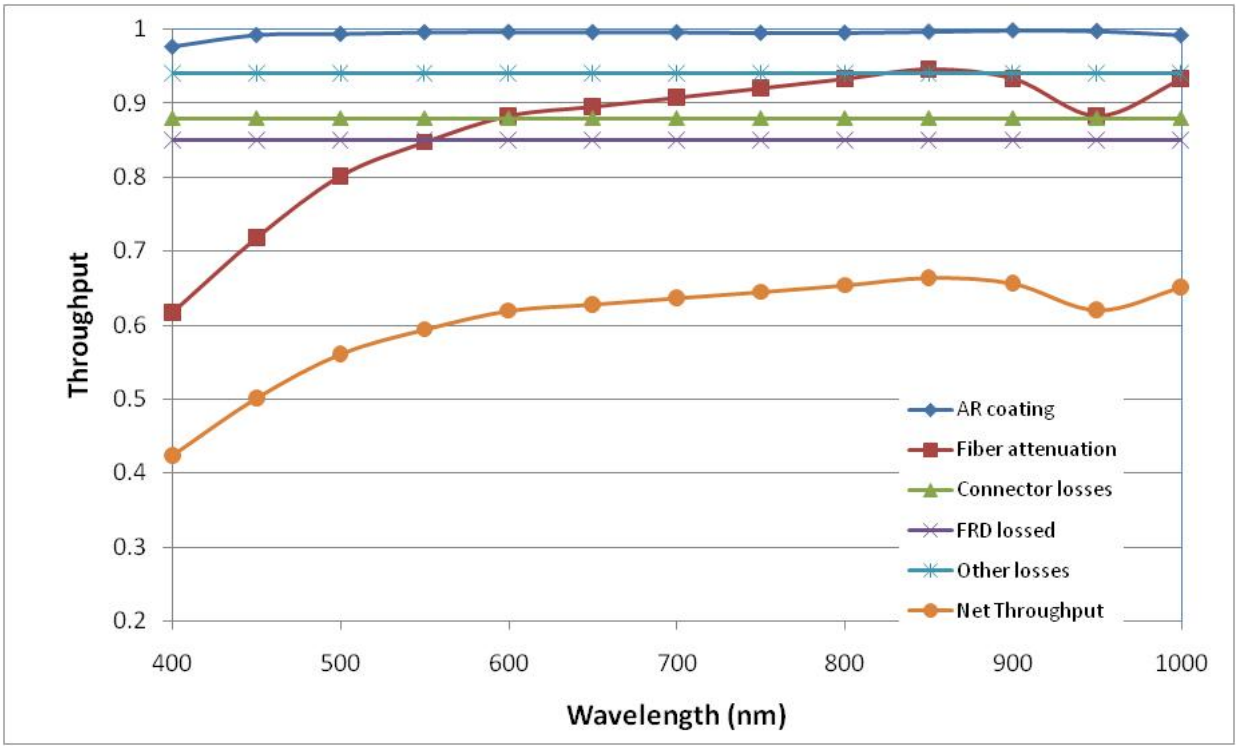

Figure 3.11-2: Fiber Throughput and the Contribution from Various Components

The bulk attenuation of low-OH silica fibers, typically specified as loss in dB/km, is highly wavelength dependent in the 400–1,000–nm band. This bulk attenuation is well characterized and is practically independent of vendor or core size.

To facilitate WFMOS installation and maintenance, fibers need to be sectioned and arranged for interconnection, which in turn introduces insertion losses. To connect up 2,400 fibers in a reasonable time, multi-fiber connectors are necessary. Fabrication of custom very-high-density fiber connectors with 30 rows of 28 fibers (rectangular pattern with fiber pitch of 200 µm) are planned to support WFMOS. To support 2,400 fibers, three such mating connector pairs will be fabricated, and the extra fibers will be used as spares or for alignment monitoring. LNA has built and tested a 5 × 5-fiber connector as part of preliminary risk-reduction activities. Test results indicate that the custom connectors meet requirements and that they can be scaled to the desired fiber counts. In the current baseline, there will be just one connector in each cable, and the throughput budget assumes an achievable connector efficiency of 88%.

To minimize insertion loss degradation with repeated mate/de-mate cycles, we plan to use a dynamic connector scheme, in which one connector (mounted on a 3-DOF stage) is actively aligned to the other connector during installation. Tests on prototype indicate that positioning accuracies of <1 µm are achievable. Before settling on the current design we evaluated available commercial connectors. Readily available MPO/MT connectors support as many as 72 fibers and provide fiber positioning accuracies of 3 µm with mechanical guide pins. For a 100-µm core MMF, insertion losses are expected to be below 0.4 dB (or better than 90% throughput) with a degradation of <0.2 dB insertion loss after 500 mate/de-mate cycles. Unfortunately, most of the commercial products (including MPO/MT connectors) only support 125-µm cladding fibers, and not the 140-µm fibers baselined for WFMOS. One of the descope options available to us is thus the use of commercial products along with 105/125-µm fiber.

Focal ratio degradation (FRD), the third major source of throughput error, is a measure of how well the fiber preserves the angular distribution of the input light. FRD is often hard to quantify and depends to a large extent on fiber geometry (core diameter and core/cladding concentricity) variation and details of the routing (bends, twists, stresses on fiber). Proper NA matching between the telescope, fiber, and spectrometer is critical to avoid losses from overfilling or under-filling the fiber or the spectrometer. Fiber mismatch at the connector interface can also introduce FRD. LNA has devoted substantial effort to understanding and minimizing losses from FRD. Figure 3.11-2 shows some early results.

Besides the above major contributors there are other loss terms. Fresnel losses (~4%) at both ends of the fiber can be substantially minimized (to ~1%) with broadband anti-reflective (BBAR) coatings. This is relatively easy to do at the slit-block end. AR coating fibers at the positioner end presents logistical challenges; therefore, those ends will be left uncoated. There are also losses (evanescent field decay) from bending and twisting of fibers. We have allocated 5% losses due to these effects.

The fibers at the positioner end are placed and bonded in a custom ceramic ferrule that is mounted to the actuator. As the fiber is moved, it twists and coils, either of which can cause FRD. To understand this, 15 mock-ups of the actuator assembly were built to simulate articulation of fiber in the same manner as the proposed design. Test results indicate that twisting does not appear to induce an increase in FRD.

To present light to the spectrometer, 800 fiber tips will be lined up in a linear array with a pitch of 230 μm. Each "slit block" will contain 80 fibers, and 10 slit blocks will be assembled end-to-end to build one "slit" for each of the spectrographs. In risk-reduction activities, 80 rows of fibers were epoxied (with EPOTEK 301) to quartz blocks. Several PTFE blocks were used to hold the position of the fibers accurately during epoxy curing. Once the fibers were bonded, the "slit block" was lapped and polished. For WFMOS, an additional cover plate, with BBAR coating on one side and index-matching gel on the other side, will be placed against the slit block surface to minimize Fresnel losses.

To protect the fibers from handling and environment, they are enclosed first in a protective tube and then are grouped into the segmented tubes which act as a protective conduit. The filled volume of the segmented tubes is calculated to prevent any crushing of the fibers.

As mentioned earlier, the fiber cables are separated into two sections:

- The short, approximately 5-m, cables go from the positioners to the top of the PFU through a strain relief box. The strain relief box is designed to protect the fibers from the motions of the telescope. This short section stays with the PFU and instrument.
- The long, approximately 55-m, cables run from the connectors on top of the PFU all the way to the spectrograph located in the adjacent room. Part of this long cable—from the spectrograph to the telescope structure—is permanent.

The remaining section is connected to the PFU during instrument operation and stored away (tied to the telescope structure) when not in use.

3.12 Spectrograph

Our WFMOS spectrograph subsystem design comprises a set of three identical general-purpose spectrographs capable of carrying out all four required surveys (see Section 2) as well as offering the flexibility for many other types of observation. The spectrograph requirements and basic parameters are summarized in Tables 3.12-1 and 3.12-2.

The WFMOS surveys demand a large multiplex gain and large wavelength coverage. This, combined with the 8.2-m Subaru aperture, demands a very large A-omega, the product of the area of the light beam and its solid angle as measured at the detector. The A-omega of an instrument is an important figure of merit, defining both the information-gathering power and the difficulty of the optical design and, hence, its cost. A-omega for WFMOS is an order of magnitude larger than that of current large-survey MOS systems (2dF, AAOmega and SDSS) and comparable to that of the multi-IFU MUSE for the VLT.

We have been able to obtain the required A-omega with three spectrographs that have f/1.07 cameras and CCD detectors of 93 mm × 93 mm. We are proposing to use custom CCDs from LBL. The proposed design (see Figures 3.12-1 and 3.12-2) uses Schmidt optics and meets all survey requirements. It has a large beam diameter (500 mm) to minimize the central obstruction losses, give high spectral resolution (as required by the GAHR survey) and keep the field angles within the camera within sensible limits to maintain good image quality. Schmidt optics is the most cost-effective approach, providing the greatest A-omega per dollar. In our design, Volume Phase Holographic Gratings (VPHGs) are used in transmission mode to maximize throughput and versatility. Our design allows spectral resolutions of up to R ~30000.

Table 3.12-1: Spectrograph requirements based on the four surveys. The first three rows are a repeat of the science case. The other rows are derived requirements.

Requirement	DELZ	DEHZ	GALR		GAHR
			Blue	Red	
Min λ (nm)	630	420	480	818	480
Max λ (nm)	970	670	544	885	680
Resolving power	3500	1500	5000	5000	20000
SRE width (Angstroms) *	2.82	3.63	1.03	1.70	0.29
Number of SREs per spectrum	1488	688	680	412	6897
Number of spectral orders per fiber	1	1	1	1	4
Length of a single spectral order (mm)	80	37	37	22	93
No. of spectrographs required	2.6	1.2	1.2	0.7	3.0
% of detector area used	86.3%	39.9%	36.3%	22.8%	100%
* *SRE – Spectral Resolution Element*					

Table 3.12-2: Basic derived spectrograph parameters. These are driven by the GAHR survey, which is the most demanding of the four surveys.

Detector format for one spectrograph	93 mm × 93 mm
Format of a single CCD	93 mm × 46.5 mm, buttable along the long side
Number of spectrographs	3
Collimator f-ratio	f/2.12
Camera f-ratio	f/1.07
Minimum beam size	~300-mm diameter
Fiber pitch at slit	230 µm, center to center
Projected fiber size at detector	54-µm diameter
SRE* width (µm at detector)	54.0 µm
SRE height (µm at detector) = projected fiber pitch	116.25 µm
* *SRE – Spectral Resolution Element*	

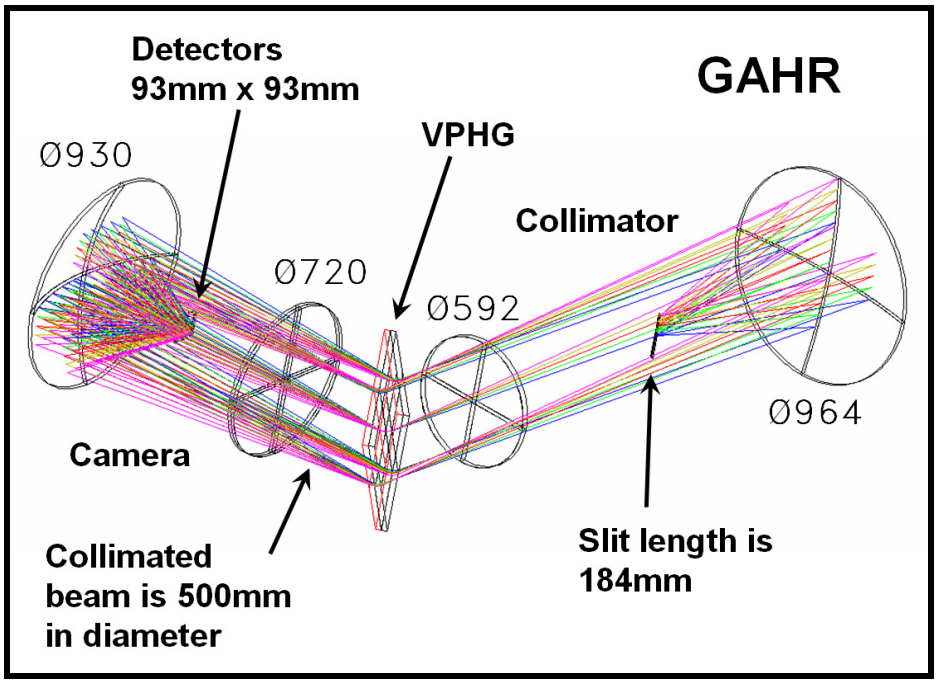

Figure 3.12-1: The optical design of a single WFMOS spectrograph, shown here as configured for the GAHR survey. The diameters of the major optical elements are shown in millimeters.

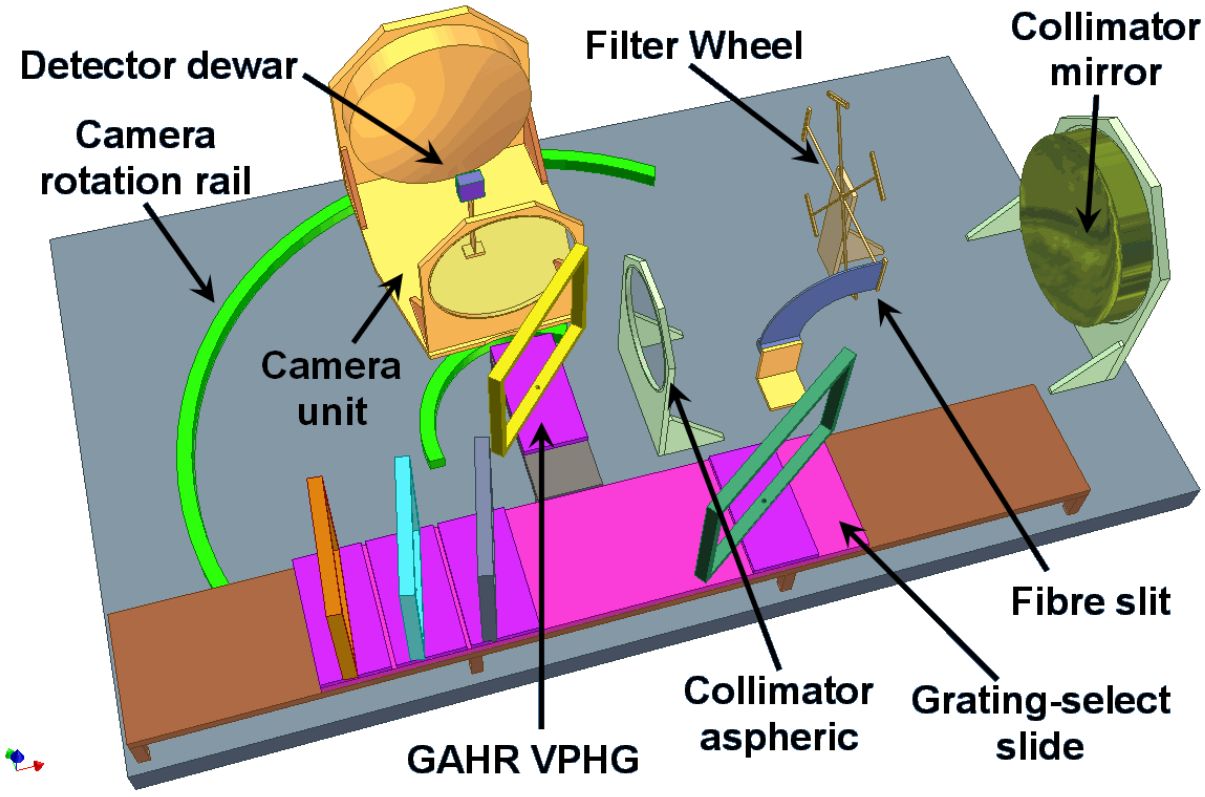

Figure 3.12-2: CAD model of one of the three identical spectrographs, shown here as configured for the GAHR survey. The table is approximately 5 m × 3 m.

Changing survey modes requires the following:

- Changing the camera–collimator angle. The spectral resolution R is directly related to this angle, with the lowest R corresponding to the straight-through position.
- Changing the VPHG by moving the active VPHG out of the beam on to the selector-slide, moving the slide to the position for the new VPHG and then moving the new VPHG in to the beam (see Figure 3.12-3).
- Changing the band-pass filter by rotating the filter wheel.

This process is fully automatic and can be done in less than one minute.

The WFMOS design uses VPHGs for all four surveys. VPHGs have several advantages over the ruled gratings traditionally used in astronomical spectrographs. VPHG peak efficiency is in excess of 90%. For both the DELZ and DEHZ surveys, the gratings will be used in first order. For the two Galactic Archaeology surveys, higher orders are used.

The design is extremely versatile and general-purpose. The survey gratings can potentially be used at other wavelengths and resolutions by changing the camera–collimator angle. For example, the GAHR grating gives R ~30,000 at the maximum camera–collimator angle, and any wavelength sub-range (about 30-nm long) in the 420-nm–970-nm range can be selected by selecting the appropriate order with a band-pass filter. The band-pass filters are small and inexpensive. A great advantage of a VPHG spectrograph with a variable camera-collimator angle is that the gratings can always be used so that they satisfy the Bragg condition and, therefore, work at their peak efficiency. The design has additional flexibility in that it is possible to install new gratings for future observations.

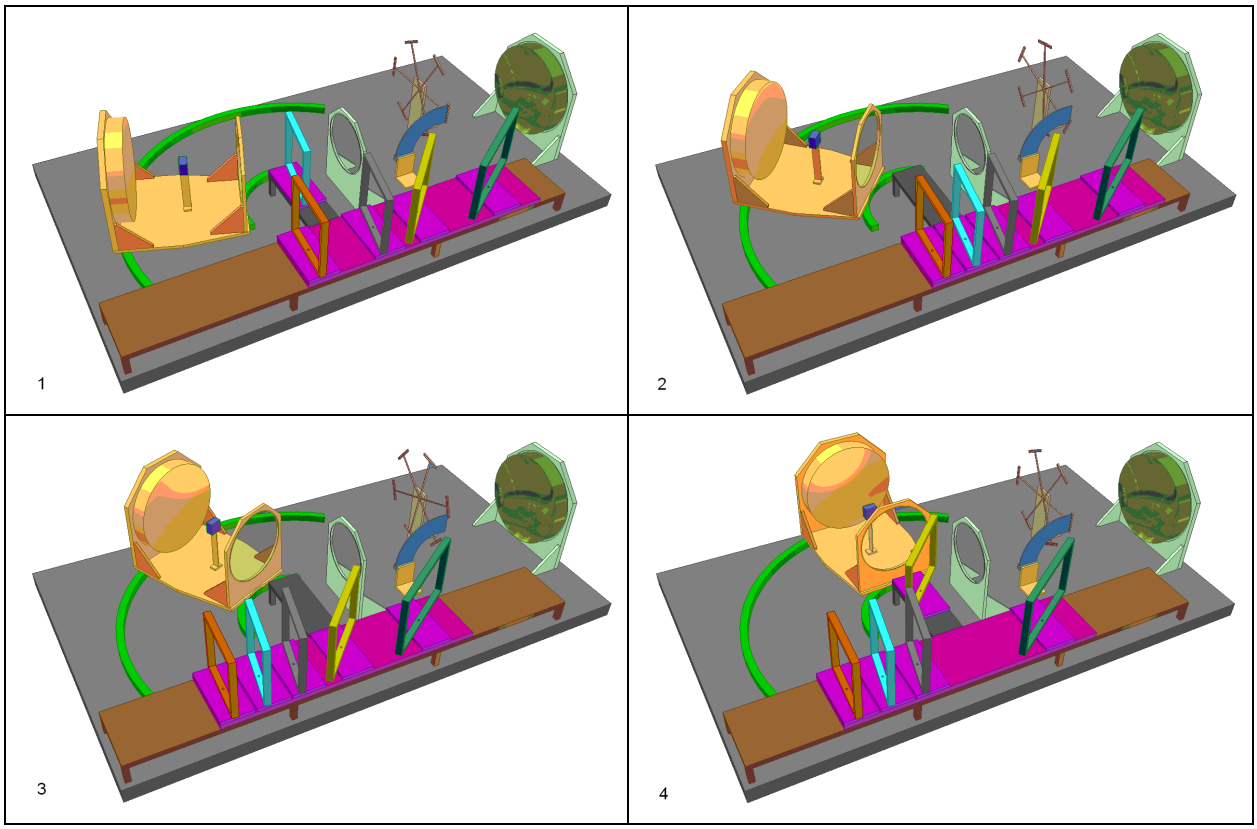

Figure 3.12-3: A time sequence showing the system reconfiguring between the DELZ mode (top left) and the GAHR mode (bottom right). Note that camera, the filter wheel and the grating exchanger all move at the same time.

3.13 Detector System

A mosaic of two close-butted CCDs will be located at the prime focus of the reflective f/1.07 spectrograph camera of each of the three WFMOS spectrographs. Four hundred spectra will be projected on each CCD with fibers spaced at the slit to avoid the small gap between CCDs. A plano convex field flattener in close proximity to the CCDs will serve as the window to a very compact vacuum housing surrounding the CCD mosaic connected by a slender duct to a low vibration Joule-Thompson cooler placed outside the spectrograph beam. The design minimizes beam obstruction on axis and is tapered to avoid additional beam obstruction off axis. Since the spectrograph is gravity-stable and vibration isolated, the CCD cabin is supported only by the rectangular duct. The entire vacuum enclosure with the exception of a Kovar window frame will be constructed from stainless steel, electropolished and cold coated on the interior for low emissivity. The exterior finish will be matt black and have a stepped profile to eliminate most grazing incidence reflections. Image ghosting is minimized by the very low reflectivity of the multi-layer coated CCD, by AR coatings on the field flattener, and by spacing the field flattener 1.7 mm from the CCD. The use of stiff materials and minimization of cantilevered mass pushes the lowest resonant frequencies to 27 Hz and 83 Hz and 184 Hz. These figures can be significantly improved by further tuning of the design so that significant attenuation will be achieved by the spectrograph's vibration damping mounts, which will have 2 pole roll off above 1.5 Hz.

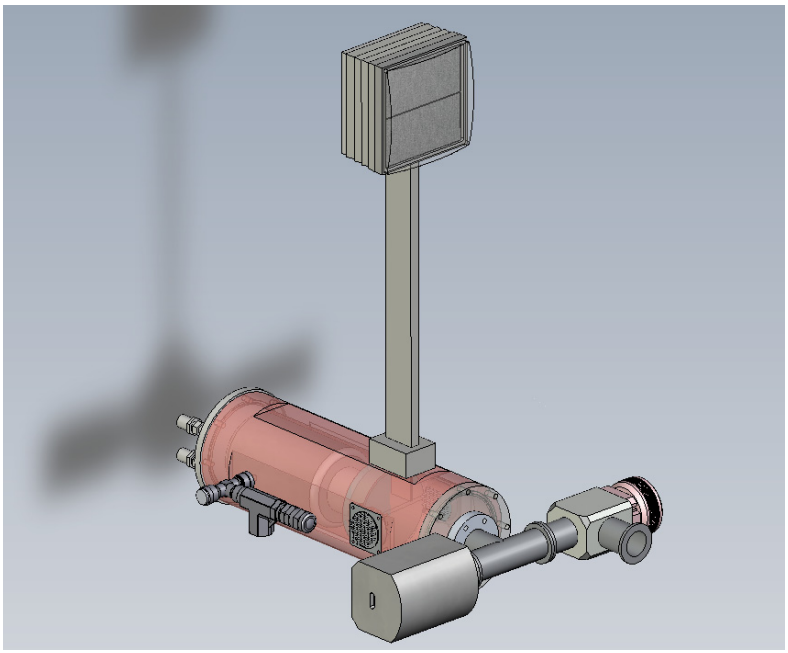

Figure 3.13-1: The CCDs will be located within an evacuated enclosure supported by a narrow duct carrying a cold finger from a Joule Thomson (low vibration) closed-cycle cooler outside the spectrograph beam.

CCD columns will be oriented parallel to the dispersion direction to allow faster region-of-interest readout for DEHZ and GALR surveys, which use only half the detector area. This orientation also supports rapid binning of spectra to just a few lines to support rapid measurement of total flux during raster scans for calibrating positioner coordinates.

A custom CCD will be procured, since this offers significant CCD performance and optical advantages. The optimal CCD size for good optical performance and minimum spectrograph cost is about half way between the standard large-format CCD size (61 mm) and a mosaic of two such CCDs. To minimize the speed of the camera and thus improve optical performance, the CCD size has been increased to 46.5 mm by 93 mm, the maximum allowing two CCDs to fit into the available 138 mm diameter on a 150 mm silicon wafer. The 16 μm pixel size has been optimized for the best compromise between resolution (for high signal-to-noise GA surveys) and S/N for the DE surveys where exposures are shorter and read noise has some impact. This leads to CCD dimensions, 2,880 columns and 5,760 rows, with 3 to 3.5 pixels across the FWHM of the image of the fiber after aberrations and lateral charge diffusion are taken into account.

Quantum efficiency is projected to be very high over the entire 420-nm–970-nm wavelength range (Figure 3.13-2) and compares favorably to competing CCDs, particularly at the extremes. This remarkably high QE will be achieved by combining several recent, but proven, innovations:

1. Thick (450 μm), fully depleted p-channel CCDs, designed by LBL and fabricated by DALSA, will substantially enhance the QE at the longest wavelengths. Full depletion for such thick CCDs has been made possible by LBNL's now mature design, which supports particularly high backside bias voltages (tested to 220 V). Notwithstanding the greater thickness, lateral diffusion and defocus with absorption depth can be shown to be negligible compared to the size of the fiber image.

2. The delta doping process developed by JPL specifically for these p-channel CCDs will be applied to eliminate the absorption in the backside contact, providing reflection-limited blue response not otherwise seen shortward of 500 nm.
3. JPL will deposit a custom dual-layer sputtered TiO_2/SiO_2 coating to reduce reflectivity to less than 4%, from 420 nm to 970 nm.
4. The low dark current seen in the delta doped LBL detectors allows them to be operated at –100°C or warmer, providing enhanced red QE due to the shorter absorption length at higher temperatures.

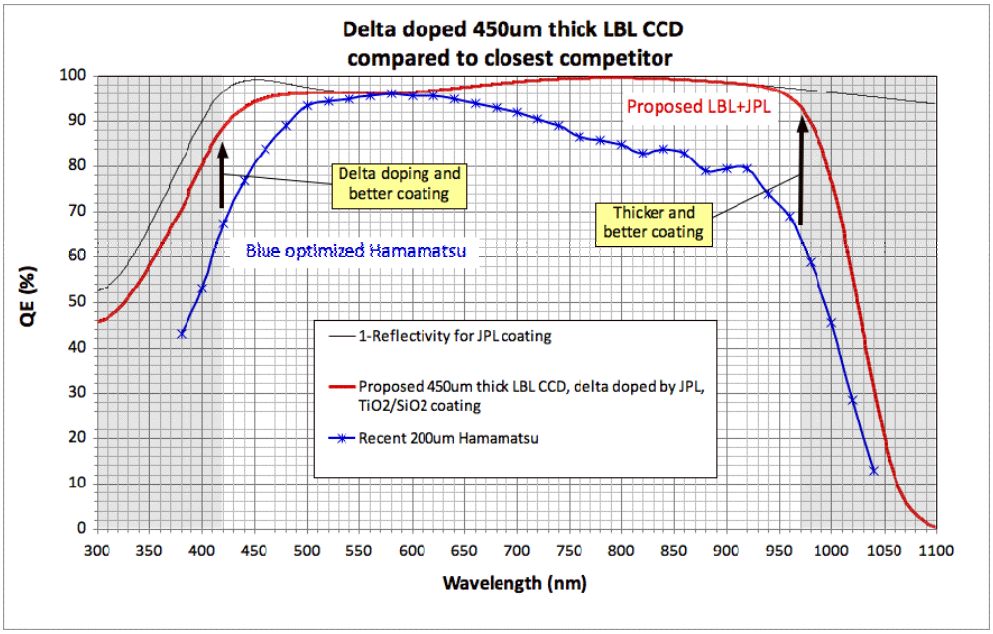

Figure 3.13-2: Theoretical 1-R and lower bound on QE compared to next best competitor. The Hamamatsu can be improved in the red by increasing thickness but only to 300µm, and by applying the $Ti0_2/SiO_2$ coating designed by JPL.

LBL will perform cold wafer probing prior to backside processing and packaging. Packaging by JPL will assure less than 10 µm height variation across the mosaic of two detectors, while providing for small gaps between each CCD and its neighbor (or vacuum housing). Caltech will characterize and integrate the CCDs into the cameras.

Full-frame readout time will be reduced to 16 s to match the fast reconfiguration time of the Cobra fiber positioner, while also reducing overheads between multiple exposures on the same field to <5%. This will be achieved by reading through 20 amplifiers per CCD to compensate for the low pixel rates (~50 kHz) required to achieve very low noise (Figure 3.12-3).

Yield loss due to the high amplifier count will be concealed by providing 40 amplifiers per CCD and selecting 20. An amplifier will be located at each end of each of 20 serial register segments. The best amplifier will be selected for each segment by setting by clock and video jumpers to determine the serial clocking direction. In addition to improving yield, this will tighten the noise distribution, eliminating outliers, and will reduce the mean noise.

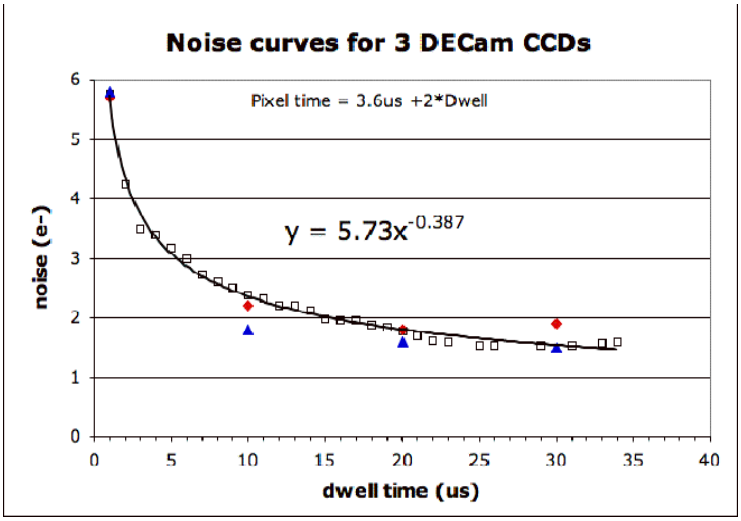

Figure 3.13-3: Read noise versus dwell time for three DECam CCDs manufactured by LBNL/DALSA. Courtesy of Juan Estrada, Fermi Lab.

Fabrication and testing of 84 CCDs has been budgeted to produce 6 science-grade devices, safely more than the yield experienced by the 62 CCD Dark Energy Survey Camera. Images will be dithered in the spatial direction so that cosmetic defects will be removed along with cosmic rays, allowing specifications for cosmetic defects to be relaxed. Three hundred-μm thick Hamamatsu CCDs without delta doping (but possibly with JPL's multilayer coating design) are offered as a technology fallback option, although this route appears to be more expensive (unless wavelength coverage or multiplex advantage is sacrificed) and delivers lower performance at both wavelength extremes.

3.14 System Software

The WFMOS software is responsible for:

- Preparing and managing WFMOS observations in advance.
- Selecting the observations to be made each night.
- Top-level control of WFMOS observations at the Subaru observatory.
- Providing engineering and test software.
- Batch processing of WFMOS data in real time to monitor survey data quality.

3.14.1 Observation Preparation

WFMOS will be capable of observing 2,400 science targets simultaneously in a single observation and, in total, a given WFMOS survey will yield data for up to 4 million science targets. Observers need a means of automating the generation of their surveys. The WFMOS observation preparation software will provide the observer with facilities for selecting the science targets that make up a WFMOS survey and arranging those targets into a collection of schedulable observations. It will also provide configuration software for matching targets efficiently to fibers. The end product of the observation preparation software is a database of observation commands waiting to be scheduled.

3.14.2 Observation Management

The WFMOS software provides facilities for managing prepared observations. Priorities can be assigned, extra science targets can be added to observations that have spare fibers, and obser-

vations can be modified to bring them up to date with any changes in instrument capabilities. Nights of WFMOS observations are scheduled by the Subaru observatory.

3.14.3 Observation Execution

The WFMOS control software runs at the Subaru observatory and interacts with the local computer infrastructure through Subaru's SOSS software. Descriptions of the WFMOS observation descriptions required for a particular night are extracted from the database created by the observation preparation software and may be executed by the observer or observatory staff member.

The WFMOS control software is responsible for coordinating all the underlying WFMOS subsystems. The control hierarchy and block diagram are shown in Figures 3.14-1 and 3.14-2, respectively. The control software manages the sequence of operations needed to make each observation, acquire the data and save it to the data store. A typical sequence would be:

- Acquire the target field with the telescope and configure the spectrograph.
- Use the feedback provided by the metrology camera to configure the fiber positioner.
- Acquire guide stars using the autoguiders.
- Acquire data with the science detectors.
- Collect and store FITS header information.
- Send the data to the data pipeline.

The sequencing steps are overlapped wherever possible to maximize the survey efficiency; for example, the next target can be acquired while the science detectors are still reading out.

The WFMOS control software will manage the subsystem interfaces shown in the block diagram and ensure all the interfaces meet the required standards of maintainability. A Python-based communication infrastructure will be provided.

3.14.4 Engineering and Test Software

Engineering software will be used to set up and calibrate the instrument during integration and testing, and when WFMOS is installed on the Subaru telescope. The end product of the instrument calibration software is an instrument description that is shared with all the WFMOS software systems. The engineering software will allow the instrument description to be kept up to date; for example, if any fibers or positioners break or if the spectrograph has new components installed.

The WFMOS software will provide diagnostic and testing facilities that can be used throughout the development and testing phases of the instrument. Automatic test scripts will ensure that instrument components are tested frequently and rigorously. The engineering facilities will remain after delivery to provide diagnostic tools for investigating any faults and problems.

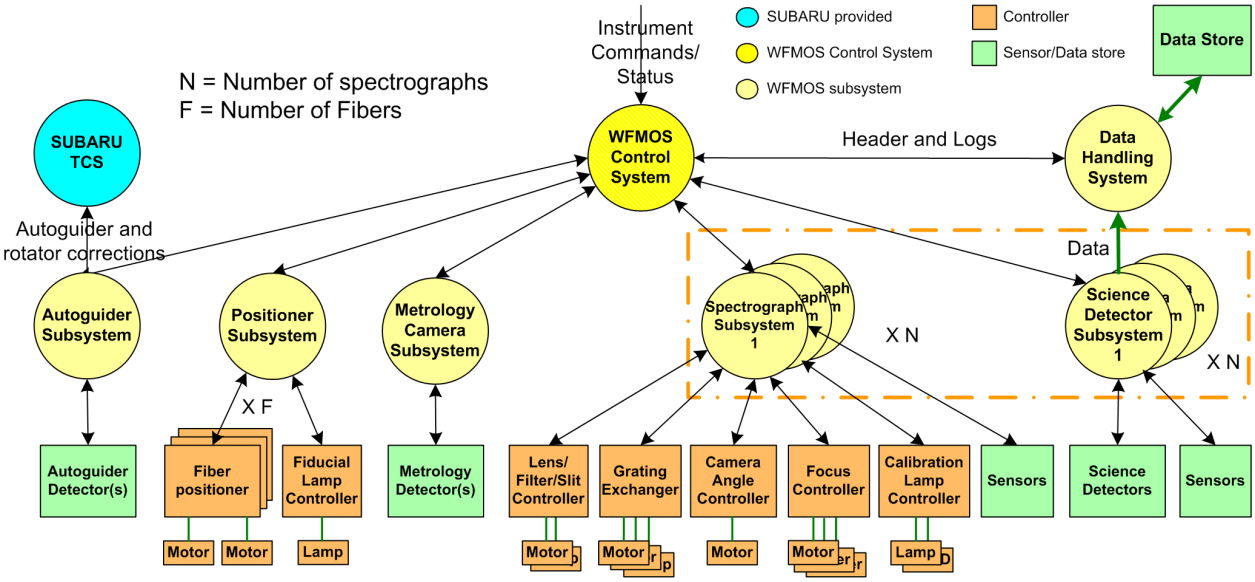

Figure 3.14-1: Control Hierarchy

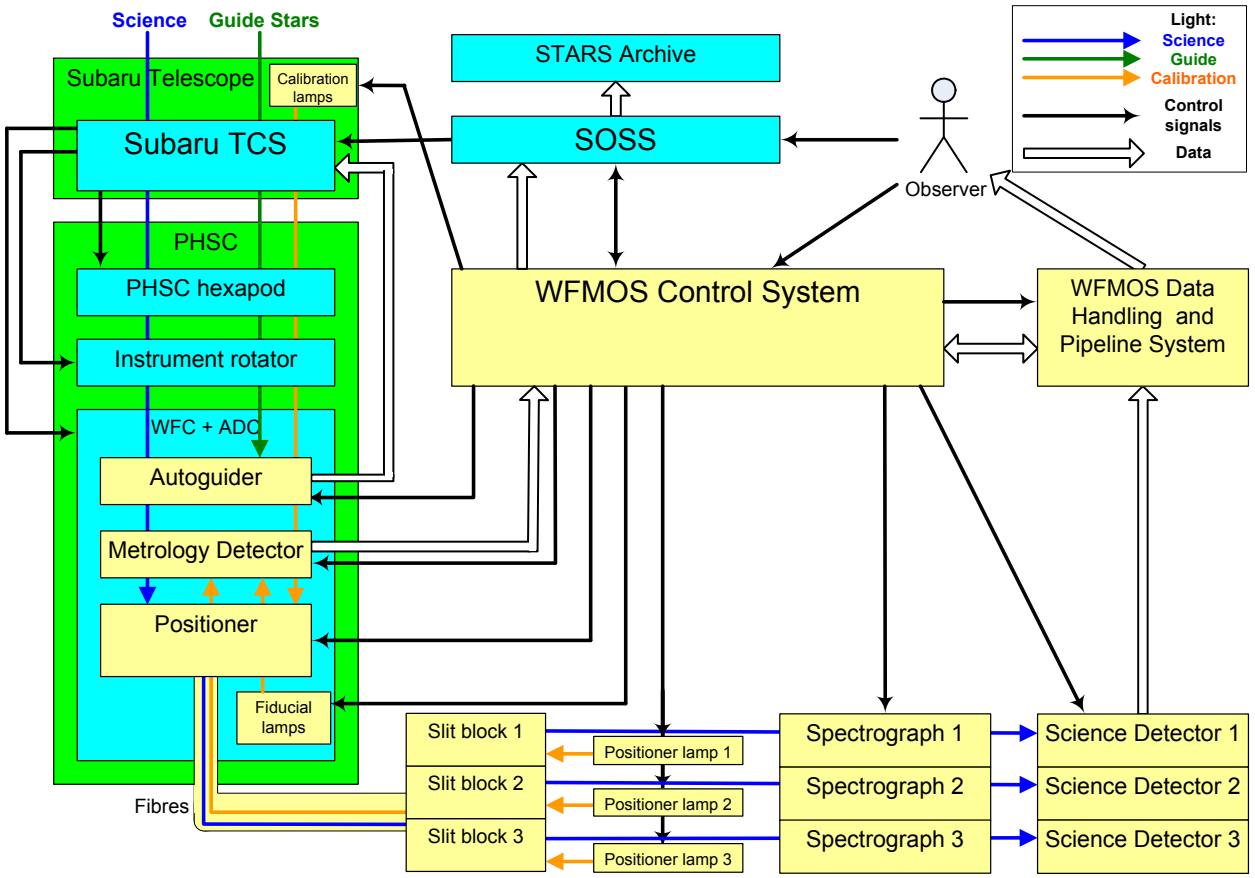

Figure 3.14-2: Block Diagram. Subaru infrastructure is shown in green, Subaru-supplied components are shown in cyan, and WFMOS-supplied components are shown in yellow.

3.15 Data Reduction

The Data Reduction (DR) Subsystem comprises four basic sub-components:

- A data handling system (DHS).
- An infrastructure for running DR.
- Quick-look data visualization.
- Data reduction routines.

The subsystem directly interfaces to the Detector Controller(s) (to whom it provides data storage facilities) and to the Software Control subsystem, which provides overall control and handles all external interfaces.

The bulk data interface will be provided by Network Attached Storage (NAS) system; the data store will be directly available through mount points to the other systems. Control interfaces will be provided as Python wrappers; in this way, the other systems can be insulated from the underlying communication system. The underlying communications will be handled either by an ORB (if the design re-uses the Subaru SIMCAM software communications) or by a common message bus (if the Gemini Pipeline Reduction System - PRS communications are preferred). Communications with the Quick-look tools will be possible either by direct access to the NAS or via IVOA Spectral and Image access protocols, thereby allowing any VO-compliant tool (VOSpec, SPLAT, etc.) to be able to access the data.

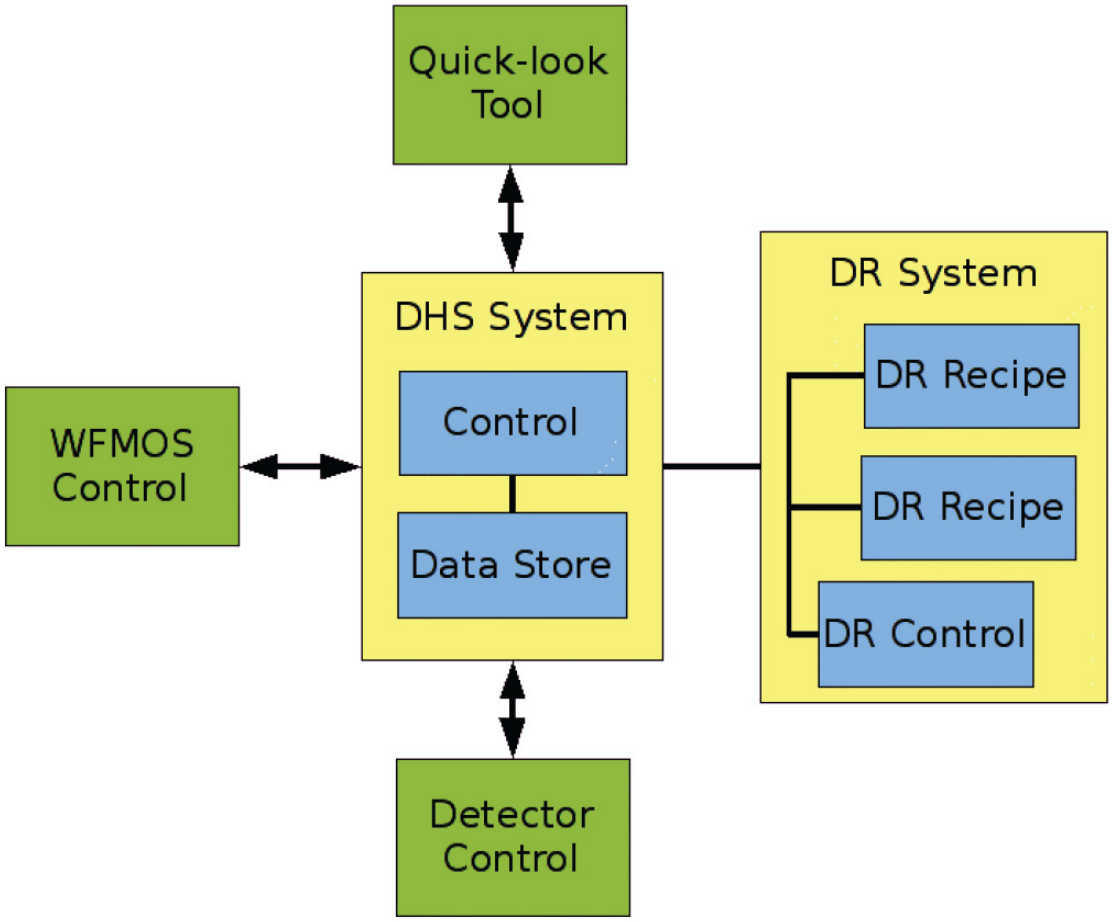

Figure 3.15-1: DR Subsystem Block Diagram and Interfacing

The Data Reduction routines themselves have been split into two packages; Package A (standard spectroscopic data reduction that provides "science ready" data) and Package B (that provides scientific quantities, such as red-shift, from the spectra). Package A follows the data flow shown in Figure 3.15-2:

- First the data are amalgamated and identified, and the relevant calibrations selected.
- The image data are flat-fielded and bias corrected.
- The orders are traced on the image, then extracted to form spectral data.
- The spectral data are wavelength calibrated.
- The data are then made available for further DR (Package B), QC checks and archiving.

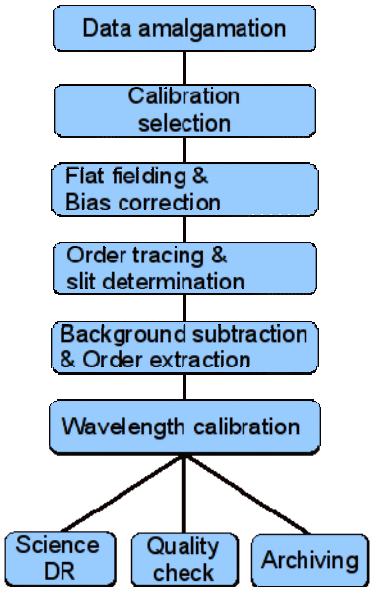

Figure 3.15-2: DR Data Flow

4.0 Instrument Performance

4.1 Optical Throughput

Throughput is a key parameter as it ultimately governs how quickly observations can be made. The Optical Throughput allocation, where each element of the design was assigned a throughput to match or exceed was created and these values are included as requirements in the FPRD. As requirements, these values represent the minimum performance; the instrument design strategy is to maximize performance and the Current Best Estimate (CBE) is presented here. As the instrument design matures, continued improvement is sought through subsystem design choices and balancing resources throughout the instrument system to maximize total throughput.

The instrument CBE is presented in Table 4.1-1 and is supplemented with the estimated throughput from external factors such as the telescope primary, the WFC, and atmospheric dispersions. The instrument performance estimates, also include the variations between the different surveys. For example, the Dark Energy surveys require a different order sorting filter type from the Galactic Archaeology surveys and produce a different throughput estimate for each survey type. The throughput is presented at the wavelength extremes of 420 nm and 970 nm and several wavelengths in between.

Table 4.1-1: Throughput budget for Dark Energy and Galactic Archaeology surveys. The spectrograph efficiency differs for the two survey types because of differences in the order sorting filter. The bottom line throughput number for the Galactic Archaeology surveys reflects this difference. The throughput does not include optical coupling at the fiber entrance as this depends on seeing and the target (e.g. galaxy size). These factors are accounted for separately in exposure time calculations. The entry for the WFC vignetting is an average across the field.

Component	Wavelength (nm)					
	420	440	550	640	790	970
	Throughput					
Atmosphere	0.83	0.83	0.89	0.9	0.9	0.9
Secondary Obscuration	0.95	0.95	0.95	0.95	0.95	0.95
Primary Reflectance	0.9	0.9	0.9	0.9	0.85	0.85
WFC Throughput	0.88	0.88	0.88	0.88	0.88	0.82
WFC Vignetting	0.83	0.83	0.83	0.83	0.83	0.83
Uncorrected Atmospheric Dispersion	0.995	0.995	0.995	0.995	0.995	0.995
Corrector Plate Throughput	0.98	0.98	0.98	0.98	0.98	0.98
Misalignment between WFMOS/HPFU	*0.98*	*0.98*	*0.98*	*0.98*	*0.98*	*0.98*
Obscuration of pupil by Metrology System	0.995	0.995	0.995	0.995	0.995	0.995
Obscuration of pupil by Spectral Cal System	0.995	0.995	0.995	0.995	0.995	0.995
Fiber Positioners	0.89	0.89	0.89	0.89	0.89	0.89
Fiber System	0.55	0.55	0.61	0.66	0.68	0.68
Spectrograph	0.689	0.689	0.689	0.689	0.689	0.689
CCD QE	0.895	0.931	0.957	0.973	0.997	0.931
DE Instrument throughput	**0.29**	**0.29**	**0.34**	**0.38**	**0.40**	**0.37**
GA Instrument throughput	**0.23**	**0.25**	**0.29**	**0.32**	**0.34**	**0.26**
DE Total throughput	**0.15**	**0.15**	**0.19**	**0.21**	**0.21**	**0.18**
GA Total throughput	**0.12**	**0.13**	**0.16**	**0.18**	**0.18**	**0.13**

4.2 Reconfiguration Time

In addition to instrument throughput, the other driver of observing efficiency is observational overhead. In order to minimize overhead, parallel activities are planned. Immediately after the previous exposure is complete, we begin reading out the three science detectors. Simultaneously we begin slewing the telescope to the new target location and repositioning the fibers. This involves illuminating the fibers, imaging the fiber tips with the Metrology camera, computing the centroids of the imaged fiber tips, and moving the fiber tips. The repositioning sequence is repeated until the fibers are within tolerance of the object coordinates. The time budget allows six iterations for fiber positioning.

The fibers are back-lit from the spectrographs and are arranged in the focal plane so that no two adjacent fibers are illuminated from a single spectrograph. This allows unambiguous identification since there are overlapping patrol regions. Table 4.2-1 illustrates the activities happening in parallel. Once the metrology cycle is complete, the Acquisition and Guide System acquires the guide targets. When the A&G system notifies the Control System that it has a lock, the instrument starts a new exposure. The entire process will take less than 40 s.

Table 4.2-1: Positioner Configuration Timeline

Start Time	Duration (s)	Steps being Taken in Parallel			
0	1	Move A-1			
1	2	Image A-1	Move B-1		
3	2	Compute A-1	Image B-1	Move C-1	
5	2	Move A-2	Compute B-1	Image C-1	
7	2	Image A-2	Move B-2	Compute C-1	
9	2	Compute A-2	Image B-2	Move C-2	
11	2	Move A-3	Compute B-2	Image C-2	Read out of Science Detectors
13	2	Image A-3	Move B-3	Compute C-2	
15	2	Compute A-3	Image B-3	Move C-3	
17	2	Move A-4	Compute B-3	Image C-3	Move Telescope to New Position
19	2	Image A-4	Move B-4	Compute C-3	
21	2	Compute A-4	Image B-4	Move C-4	
23	2	Move A-5	Compute B-4	Image C-4	Acquire Target w/ A&G system
25	2	Image A-5	Move B-5	Compute C-4	
27	2	Compute A-5	Image B-5	Move C-5	
29	2	Move A-6	Compute B-5	Image C-5	
31	2	Image A-6	Move B-6	Compute C-5	
33	2	Compute A-6	Image B-6	Move C-6	
35	2		Compute B-6	Image C-6	
37	1			Compute C-6	
38					

4.3 Allocation Efficiency

An important aspect of any positioner scheme is the efficiency with which the individual positioner elements can be allocated to the targets of interest for spectroscopy. This allocation efficiency is a measure of how effectively the spectroscopic capability of the instrument is being used. WFMOS has been designed to provide high allocation efficiency for both the low and high spectrograph modes. If the number of targets is very large compared to the number of positioner elements, then every element will have many targets available to choose from and the positioner

allocation success rate will be high. If there are few targets, then most positioner elements will not have a target available. At intermediate target density, the success rate will be moderate, and will depend on the degree of overlap of adjacent patrol regions. A full discussion of the allocation efficiency issues and trade-offs appears in the OCDD, Section 6.

4.4 Exposure Times and Survey Time Estimate

As discussed above, WFMOS provides high throughput and high positioner allocation efficiency, allowing the primary surveys to be accomplished in modest telescope time. Table 4.4-1 summarizes the required exposure times and survey times for the primary surveys. More extensive detail of the survey efficiency and exposure time calculator appear in the OCDD.

Table 4.4-1: Exposure and survey times for the low-redshift Dark Energy survey (DELZ), the high-redshift Dark Energy survey (DEHZ), the low-resolution Galactic Archaeology survey (GALR), and the high-resolution Galactic Archaeology survey (GAHR).

Survey	Resolution	Mag	S/N	Obs (min)	Survey time (hrs)
DELZ	3500	RAB < 23.0	Line = 7	15	832
DEHZ	1500	RAB < 25	Cont = 4	240	286
GALR	5000	V = 20	10–15 / Å	30	765
GAHR	20,000	V = 17	150 / Å	60	1125

4.5 System Versatility and Upgrades

The conceptual design of the current instrument has been tuned to delivery optimal performance for the Gemini surveys (DE/GA) while attempting to keep costs low. However, as introduced in Section 2, as the unique capabilities of WFMOS will have major impact in many areas of auxiliary science, we have borne this in mind in our design study.

There are significant features in the major elements of this design, the fiber positioner assembly and the spectrograph, that ensure versatility and permit possible upgrades. The key to keeping upgrade options open is clean interfaces between subsystems and design modularity.

The highlights of potential upgrades are:

- Increase in the total number of positioners—possible because of the design of the individual positioner and the spectrograph design.
- Increase in spectral resolution of the spectrographs.
- Survey changes with different gratings.

4.5.1 Positioner

The current design has 2,400 positioners arranged in a hexagonal pattern centered on the focal plane that covers 1.2 to 1.4 degree field. This configuration was selected to optimize the data collected with respect to cost. The outer edges of the 1.5 degree focal plane are affected by vignetting reducing the throughput and subsequently making those fibers beyond 1.4 degrees less efficient (Figure 3.10-3). However, even taking this vignetting effect into account, a decrease in observation time can be obtained by fully populating the focal plane with positioners. The number of positioners can be increased to 3,200 with no change in the design of the existing Cobra positioner, its control system, or its electronics architecture.

4.5.2 Spectrograph

The spectrograph design easily allows an increase in the number of positioners as well as other design upgrades. Since each spectrograph is identical, adding a fourth spectrograph would

accommodate more positioners. No recurring engineering costs are added.

The spectrograph beam size is 500 mm in diameter, and the range of camera-collimator angles is 0 to 110 degrees. A grating can be designed for any angle in this range, giving a range of spectral resolutions from 0 to 30,000. The width of the detector in SREs (spectral resolution elements) is constant—there are always 1724 of them. So as the resolution increases the wavelength coverage decreases. The whole wavelength range 420 nm–970 nm is obtained at R ~2178 at 12 deg, whereas 31.6 nm of spectral coverage in a single order is obtained at R ~30,000 at 100 degree. The spectrographs can, therefore, be used to do other science programs if new gratings are purchased. Furthermore, the gratings purchased for the four surveys can be used at different angles to give different wavelength ranges.

Our system will have significant sensitivity below 420 nm and above 970 nm, which will definitely be of great interest for auxiliary science.

5.0 Integration and Test

5.1 Integration Approach

Our history in delivering science instruments has enabled us to develop a systematic approach to I&T where it is common to have subsystems developed and tested by different groups. Emphasis on early validation at the subsystem level with clear definitions of interfaces allows verification of functionality and identification of problems early and minimizes the problems encountered when the instrument is finally assembled and tested as a system. Initial sub-system level validation also provides early test data to confirm interfaces, especially data content and form. The verification process of the instrument begins with the development of the Acceptance Test Plan (ATP) to define the series of tests, inspection, and analyses used to validate the instrument requirements. This plan will emphasize subsystem level tests and subassembly tests to verify functionality and performance early and to identify any problems and minimize telescope time for acceptance tests. At each stage we weigh the differences in response or performance when simulating an interface against the complexity of higher level tests, time and personnel necessary to debug higher level assembly tests, and finally telescope time at the full system level to determine when each requirement should be validated.

The strategy in developing the ATP is:

- Develop tests with clear objectives and success criteria.
- Validate as many requirements as possible at the lowest level.
- Select representative tests to confirm tests at the previous stage after the next integration step.
- Select simple interfaces and identify risks associated with use of simulators and support equipment compared to a higher system-level test.
- Minimize telescope time for Acceptance Tests by identifying the minimal set of tests that, in conjunction with previous tests and analysis, will fully validate the instrument.

An example of how this process works for the PFI is described in Section 2.14.6 of the Detailed Design Document. A similar approach is developed for every assembly and subsystem. These tests are defined as the design progresses to ensure features needed for I&T are built into the software and hardware and the necessary laboratory facilities are available at the appropriate time.

Examination of the instrument block diagram (Figure 3.2-1) shows this instrument can be integrated along two paths: one involving the telescope-mounted hardware and the other for the spectrograph, detectors and data pipeline. The software control system will be installed and tested at both integration sites. All of this occurs prior to integration onto the telescope, and the only test missed is the overall optical throughput, which can easily be calculated from individual tests. These parallel paths will also be followed in the initial telescope installation work before the final on-sky work commences. The advantages of this approach are minimizing the risk to schedule by allowing parallel independent progress and flexibility for as long as possible and maximizing the total resource available to the integration Phase by using two integration sites.

The full plan is detailed below and shown schematically in Figure 5.1-1. The System Software will require careful management as modifications and bugs will be appearing simultaneously from two sites/time zones.

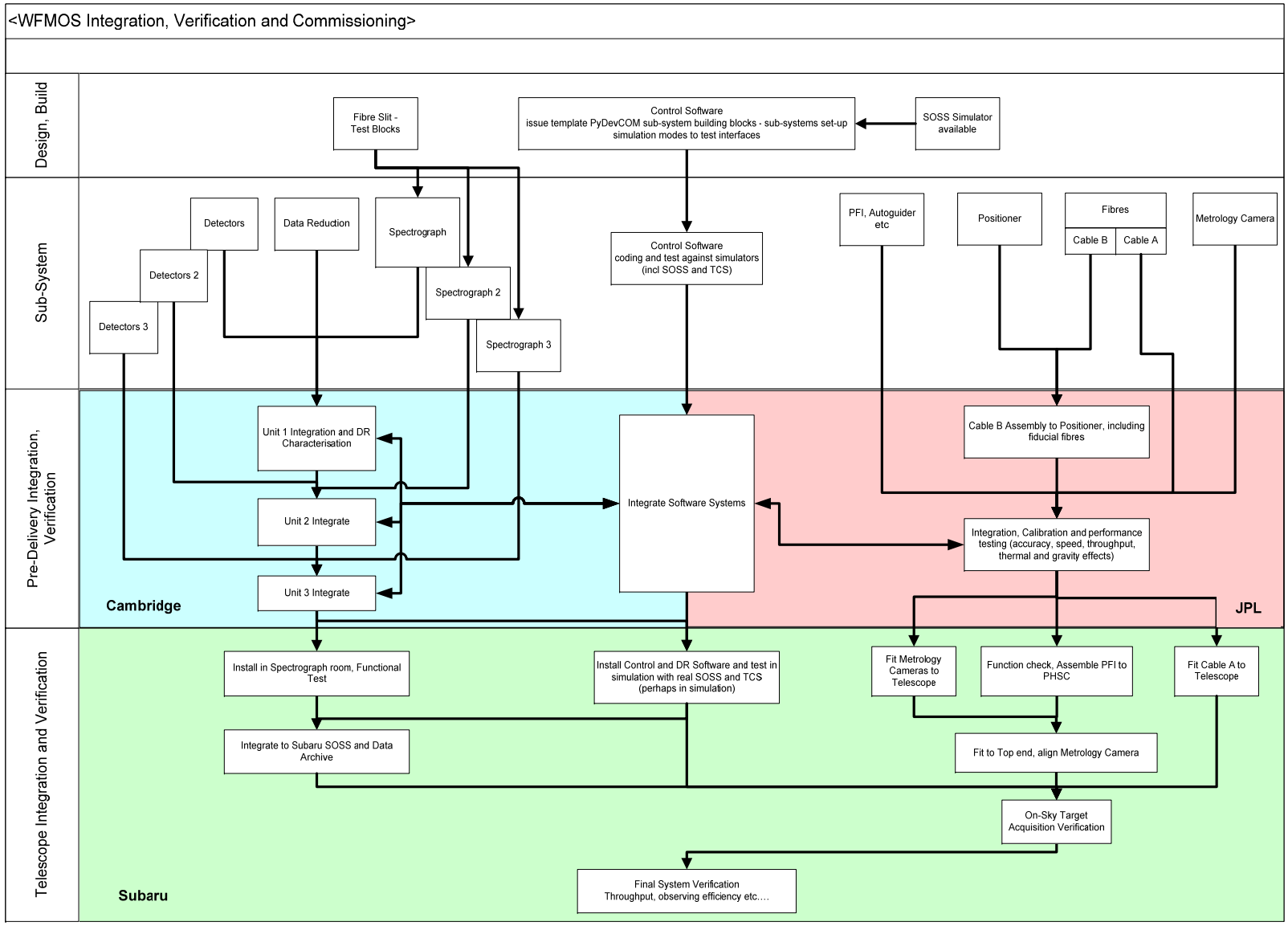

Figure 5.1-1: The Instrument Integration and Test flow follows two parallel paths before final integration onto the telescope: spectrograph/detector/data pipeline integration and PFI/metrology integration.

5.1.1 Spectrograph/Detector/Data Pipeline/WFMOS Control Subsystems' Path

This integration work will be located at the Institute of Astronomy at the University of Cambridge. The main tasks are:

- Mechanical Assembly and alignment of the Detector system to the spectrograph optics. Confirm cryogenic performance of Detector System in Spectrograph.
- Connect Detector to Data Pipeline Software and confirm files/data are being passed.
- Confirm three systems work properly together using the System Software—it is assumed individual systems will have already tested their interfaces to the System Software.
- Measurement of the optical performance in 'imaging mode.'
- Measurement of the optical performance in all 'spectrometer modes' and calibration of grating/spectrograph angles.
- Confirm the performance of on-line data reduction against known spectra.

After formal customer acceptance, the hardware will be disassembled where necessary, packed and shipped directly to the Subaru telescope.

5.1.2 Prime Focus Instrument (PFI) Path

The second path for the instrument integration and test will be located at the Jet Propulsion Labs in Pasadena. Prior to this phase, the 'Cable B' fibers (the shorter section of the fiber cable) have been integrated into the positioners and the positioning accuracy, repeatability, and timing have been validated. The primary remaining task for the PFI/Positioner/Metrology loop is to integrate the metrology system using the system software.

The main tasks of integration and testing at JPL are:

- Test of the System Software control loop with the Positioner Assembly and Metrology Cameras. They will be configured to mimic the instrument setup on the Subaru telescope with the four metrology cameras placed in approximately the same location relative to the PFI, as they would be on the Telescope (Figure 5.1-2). Two tilted spherical fold mirrors can then be used to represent the primary mirror of the telescope for testing and to compensate for the absence of the Wide Field Corrector. The metrology system is calibrated to quantify error in the position measurements of the fiber tips.
- Final test will be an optical throughput measurement from positioner to Slit Block (at Spectrograph) and will confirm the repeatability of that performance over several Connector matings.

Once again, after formal customer acceptance, the hardware will be disassembled where necessary, packed and shipped.

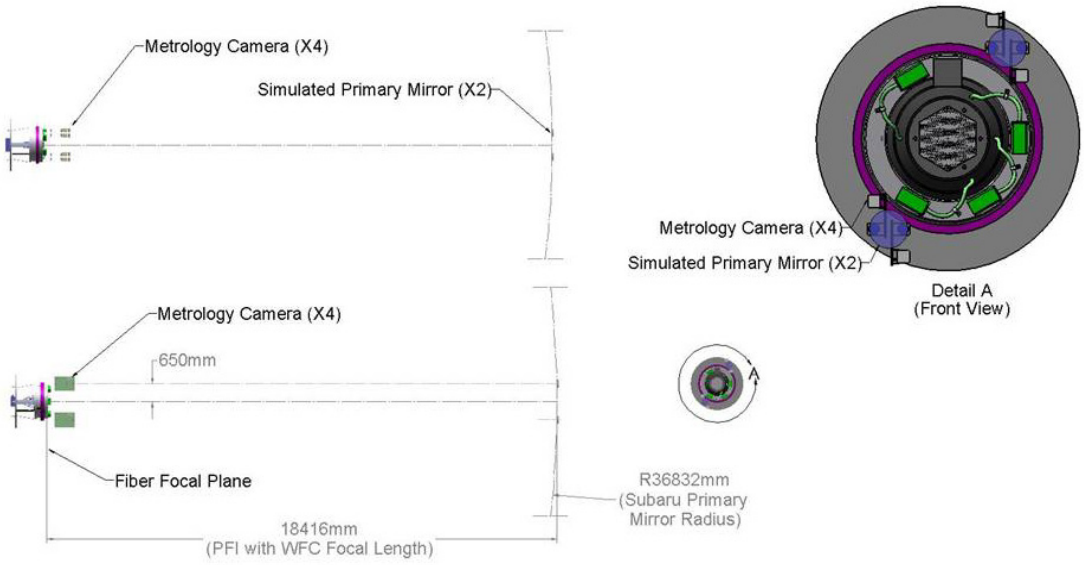

Figure 5.1-2: Test Configuration of the Metrology, Positioner and PFI Loop at JPL

5.1.3 Integration and Verification at Subaru Telescope

Apart from final verification, a key goal of the work at the Subaru Telescope will be to minimize downtime for the telescope. The final test plan will be revised to benefit from lessons learned during integration of other instruments at Subaru that occurs before WFMOS delivery (e.g., HyperSuprimeCam and FMOS).

Initially there are three parallel activities which are not expected to need telescope shutdown: 1) re- assembly and test of the spectrographs in their assigned room in the dome, 2) integration of the System Software and Data Reduction Pipeline, and 3) re- assembly and test of the PFI elements followed by assembly to the PHSC to make a Prime Focus Unit. System Software Integration can probably be done both at sea level or at the summit of Mauna Kea. We expect all spectrograph-related hardware to be delivered directly to the Telescope site. The integration site for assembly of PFI elements into the PHSC will require negotiation with Subaru. These three activities are shown in the flow diagram and include visual inspection, functional checks (each subsystem will have the capability of performing a self diagnostic test) and a limited repeat of the acceptance test which closed out work prior to shipment.

Two other activities occur during this period, namely preparing the telescope structure for and fitting of fiber Cable A (the longer section of the fiber cable) and the Metrology Cameras. These ought to be possible with daytime engineering only.

It is at this point that the two integration paths finally join together as the Prime Focus Unit is installed on the telescope and the fibers are connected to the Spectrograph. This is when coordination with the telescope staff is crucial to develop procedures and schedules which optimize the test flow but minimize telescope down-time and cost. The key tasks of this final phase are to:

- Validate operation of metrology camera using the primary mirror, WFC, and PHSC to position the fibers.
- Validate operation of A&G cameras on sky.
- Demonstrate and validate target acquisition on sample fields.
- Verify on-sky tracking performance.

- Verify optical throughput and measure sensitivity.
- Verify data pipeline on real targets.
- Verify software integration to the telescope.
- Final customer acceptance test.

The instrument is then ready for science commissioning and the main contract would be complete.

6.0 Operations

We have designed the WFMOS instrument and science surveys for efficient, streamlined operation. There are several components of operations that are necessary for realizing the scientific return of WFMOS. The "Package A" data reduction pipeline is included in this construction proposal and its associated costs. This pipeline produces calibrated spectra, and is described in Section 3. In this section, we summarize the additional components of operations required to complete the Dark Energy and Galactic Archaeology surveys. Additional detail on the scientific surveys and operational modes of the instrument appear in the OCDD; additional technical detail on the instrument appears in the Detailed Technical Design. The components of operations fall into the following categories:

- Construction of data reduction "Package B"
- Conducting the DE and GA science surveys
- Installation and removal of WFMOS from the Subaru Prime Focus.

We examine each of these categories in turn.

6.1 Data Reduction Package B

The Package B pipeline use the calibrated spectra from Package A and produces automated, high level science products ready for further analysis. For the DE survey, this consists primarily of extracting redshifts from the galaxy survey through the identification of the [OII] feature for the low redshift survey, and through continuum fitting for the high-redshift survey. Galaxy typing will be done for the better s:n targets. We will use a small team of scientists together with professional programmers to produce the DE portion of Package B. Associated costs appear in the Management and Cost volume. The PI delegates scientific management of the effort to Professor John Peacock.

For the GA survey, Package B includes extraction of velocities and metallicities (low resolution) and abundance determination (high resolution). Tasks include 1) automated estimation of global stellar atmosphere parameters, 2) automated continuum estimation, multi-component line fitting, and abundance analysis from line lists, 3) automated radial velocity estimation, and 4) using optical plus near-IR photometry (and distances if available, e.g., from Gaia) to produce model atmosphere fits to spectra. Associated costs appear in the Management and Cost volume. The PI delegates scientific management of the effort to Prof. Mike Irwin.

Some of the Package B tasks have significant overlap between the DE and GA surveys. These include:

- Optimizing sky subtraction methods.
- Scattered light modeling using blocked-off fibers.

The apportionment of these tasks will be made at the beginning of the Package B effort.

6.2 Conducting the Dark Energy and Galactic Archaeology Science Surveys

The two primary science surveys are described in detail in the OCDD. Each survey comprises the following steps:

- Preparing observations.
- Monitoring survey progress.
- Analysis of results and publications.

Preparing observations involves selecting targets from existing catalogs, optimizing fiber al-

location efficiency, evaluating survey completeness, deciding tiling strategy, and prioritizing observations considering sky brightness and seeing. An observing tool that allocates targets to fibers will be provided as part of the system software during the construction phase. The additional steps described here involve interacting with this tool and performing any necessary additional optimization.

The survey preparations and survey monitoring have many common elements in the two primary surveys. A number of scientists will participate in the survey phase of WFMOS, and the primary surveys will be conducted over the course of approximately five years (depending on the yet-to-be-negotiated agreement with Subaru). The bulk of the day-to-day effort will be conducted by post-docs under the direction of members of the current science team. The estimated cost for this phase appears in the Management and Cost volume.

6.3 Installation and Removal

We anticipate that WFMOS observations will be interleaved with observations using other instruments, including the HyperSuprimeCam. Removing WFMOS from the telescope will necessitate the removal of the Prime Focus Unit from the telescope, disconnection of the fiber connector, storage of a portion of the fiber optic cable on the side of the telescope, and possible removal of the metrology cameras. Removal of WFMOS components from the Prime Focus Unit will be required to allow the Prime Focus Unit to be reconfigured with HyperSuprimeCam. Installation of WFMOS is essentially the reverse of this process. We estimate the Prime Focus Unit can be removed from the Subaru prime focus in less than three hours and be accomplished entirely with Subaru personnel in a manner similar to standard top-end unit exchanges.

The initial installation of WFMOS components in to the Prime Focus Unit is described in the Prime Focus Instrument section of the Detailed Technical Design. Routine swaps of HSC and WFMOS will be a streamlined version of this process. WFMOS is designed to allow the swap of HSC and WFMOS components within the PFU to take approximately one full work day. This estimate depends sensitively, however, on the detailed HSC design. Two members of the WFMOS instrument team will be required to supervise the first two swaps. It is also prudent to budget an additional few days for the first two swaps. Subsequent swaps would be accomplished entirely with Subaru Observatory personnel. The detailed procedure and timeline for this process will be developed before the WFMOS preliminary design review.

6.4 Additional Considerations

In addition to the Dark Energy and Galactic Archaeology survey observations proposed here, there will be classically allocated non-survey observations. Although not formally requested to do so by Gemini, we believe it prudent to consider the operational scenarios for these potential additional observations. We envision that many of these surveys will have long-term status and be queue scheduled. The rest will be a broad range of observing programs proposed by PIs from within the Gemini and Subaru communities. These could also be queue scheduled, or the observers may be given fixed nights and visit the telescope. WFMOS can accommodate these observations with no additional software cost by using the System Software observing preparation tools and the Package A data reduction pipeline. The operation of WFMOS will not be very different from that of other fully automated multi-fiber spectroscopic survey instruments, such as FMOS, 2dF+AAOmega, and FLAMES.

7.0 Management and Cost

7.1 Management and System Engineering

Instruments on the scale of WFMOS have few precedents in the domain of ground-based astronomy. Indeed, the cost and complexity of WFMOS are more typical of space-based astronomy instruments and missions. As such, the management approach to WFMOS should be appropriate to the complexity of this development and draw on lessons learned from the management of other developments of this scale

The WFMOS team has chosen the Jet Propulsion Laboratory to be the lead partner institution to manage and coordinate these activities. In this role, JPL provides overall project management and project systems engineering in addition to its technical contributions to WFMOS. JPL has broad experience in project management on a range of projects for both NASA and non-NASA projects and has delivered over 40 spaceflight, airborne, balloon, and ground instruments in the $10 M–$100 M range over the past 20 years. Based on this experience, JPL has identified practices that are applied through the project phases to ensure that WFMOS will successfully deliver within schedule and budget:

1. Detailed planning during pre-project phases, including detailed schedules, budgets, and resource requirements.
2. Identification of cost containment strategies, including descope lists.
3. Identification of potential risks and mitigation strategies.
4. Provision for adequate budget and schedule reserves.
5. Clear statements of roles and responsibilities for key project members (PI, PM, PSE, PS) and decision-making.
6. Early identification of project communication and coordination strategies.

Managing an instrument developed by multiple international partners requires additional effort and is routinely done at JPL. This requires detailed knowledge of the development of the instrument in order to correctly assess progress and identify trends in schedule or cost growth quickly to take corrective action. Experience has shown the key to managing this type of project is through continuous communication with all partners, focused attention on the cost and schedule, and adherence to requirements and ICDs for design structure. JPL is committed to delivering this instrument on time and at cost and, during the development, providing complete insight on the instrument progress to Gemini. This is done through the monthly reports that include technical status, milestone status, cost and schedule detail, and any issues and mitigation.

A recent example of an instrument delivered on time and on cost is the Moon Mineralogy Mapper (M3), an imaging spectrometer designed to map the surface mineral composition of the moon for the Chandrayaan-1 Indian Space Research Organisation mission. This instrument was a JPL in-house development managed by Mary White, the WFMOS project manager. The original proposal cost was $23.6 M and final costs after delivery and preliminary integration on the spacecraft was $25.1 M, with the increase due to delays from the spacecraft provider. Completing M3 at cost required constant interaction with the spacecraft provider, detailed assessment of development progress against schedule, and implementing design changes in a timely manner.

JPL involvement with ground instruments includes the Keck Interferometer and the M1 Control System (M1CS) for the Thirty Meter Telescope (TMT), and the calibration system for Gemini Planet Imager (discussed in section Management Proposal Section 12.1). JPL is also support-

ing TMT on the design and development of the Alignment and Phasing system, telescope system engineering, the Planet Formation Instrument feasibility study, and the telescope optics.

WFMOS aligns with JPL's Astronomy and Physics Directorate (APD) strategic plan for increased development of ground and space-based optical instruments and JPL is committed to its success. Ground instruments allow the development of complex systems with technologies that can also be applied to space-flight instruments. JPL is a large, diverse organization accustomed to handling complex, multi-disciplinary challenges and can provide critical resources in various forms to support WFMOS. The support from the APD has been evident through the study phase through communication on the study progress and in the coordination and support in the proposal review and preparation process. In addition to management support, the JPL infrastructure provides mechanisms and resources for cost and schedule management, document organization and storage, and configuration control. This project has the advantage of selecting the desired tools and functions without having to meet the more stringent practices of a flight project.

The WFMOS organization chart is shown in Figure 7.0-1.

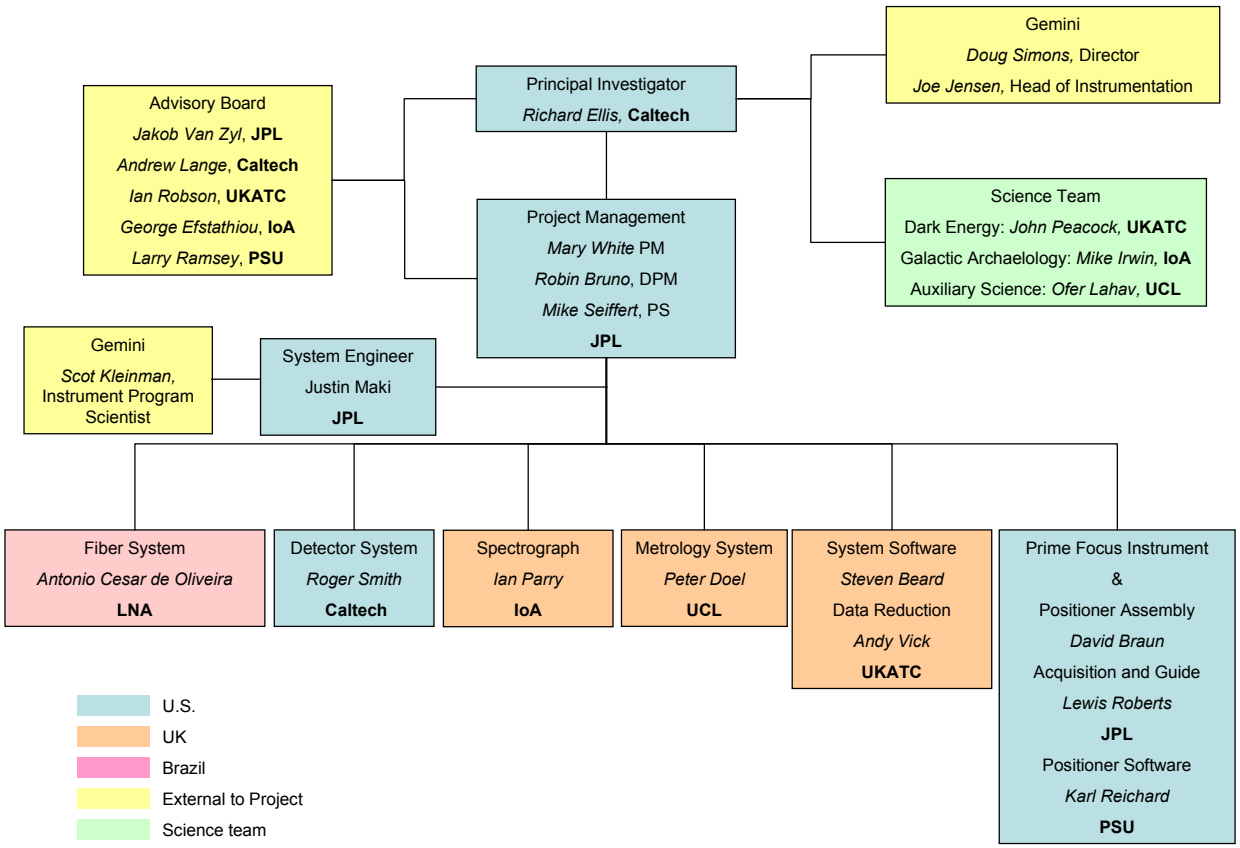

Figure 7.0-1: WFMOS Organization Chart

The management team consists of the PI, Project Manager, Deputy Project Manager, Project Scientist, and System Engineer.

- **The role of the PI** is to lead the development of the science case and to act as the final authority to confirm that the instrument design and build meets the science goals. This includes coordination of the full science team to ensure the goals of the DETF are met and interaction with the technical team to ensure the instrument development is meeting cost, schedule, and performance commitments. This interaction with the technical team is

primarily with, but not limited to, the project manager, project scientist, and instrument system engineer.

- **The project manager** is responsible for delivering an instrument that meets the requirements on schedule and at cost. Responsibilities include communication with Gemini and JPL program management, coordination of the technical team, and managing resources. In this case, the instrument has a firm cost cap, so a critical feature of the program manager's role is to anticipate any cost overruns and, if necessary, implement descopes in a timely manner. These actions must be communicated clearly to the PI and to Gemini if they affect any requirements from the OCDD Level 1 Requirements or Instrument Level.
- **The project scientist's** role is to provide the modeling and assessment necessary to ensure the instrument capability is consistent with the science objectives derived in the OCDD. In addition, he fulfills the role of providing a strong tie between the science and engineering team as the design and build of the instrument progresses. In this role, he is a key player in assessing trades that affect instrument performance and determining and quantifying the impact on the science objectives.
- **The system engineer** reports to the project manager, leads the technical architecture of the instrument and makes sure the subsystem development is balanced with respect to technical risk and complexity. In addition, the system engineer is responsible for risk management. All of this requires a comprehensive and in-depth knowledge of the instrument development and interaction between subsystems so that system-level trades in design or approach can be made effectively. The formalization of these decisions is through the management of the Level 2 and Level 3 requirements. In addition, the system engineer is responsible working with the Subaru technical representative to obtain the telescope ICDs and requirements. Finally, the system engineer manages and enforces configuration control over all governing documents.

7.2 Instrument Cost

The key elements in cost management are accurate cost estimates, detailed cost tracking, and timely actions for cost control. The total estimated cost for the WFMOS instrument is $68.5M, which includes a baseline cost of $58.3M and $10.2M in reserves (20%). The reserves do not include the Gemini-held reserves of 15%. Table 7.2-1 shows the costs by partner and Table 7.2-2 provides the costs by top-level WBS. The partner contracts held with Gemini include 15% reserves, which are included in the total cost column in table 7.2-1. Reserves above 15% are included in the JPL total cost to allow management of reserves across the project. The process used to estimate necessary reserves is presented in section 5.2 of the Management and Cost Volume and in section 7.5 below. Half of the instrument cost should meet the Gemini partner shares requirement as shown in Table 7.2-3. The project partners are comprised of the U.S., UK, and Brazil; half of the project costs are distributed to the partners as shown in Table 7.2-3.

Table 7.2-1: WFMOS Costs by Partner

Partner	Baseline Amount, $K	Total Cost w/ Distributed Reserves, $K
JPL	27,237	34,385
Cambridge	10,383	11,940
PSU	563	647
Caltech	2,578	2,578
LNA	3,550	4,083
UK-ATC	4,355	5,009
UCL	1,639	1,885
Subaru Provided Elements	8,000	8,000
Baseline Total	58,305	
Reserves	10,222	
Total w/ Reserves	**68,527**	**68,527**

Table 7.2-2: Cost by Top-Level WBS

		Cost by Year, $K								
WBS Element	**Institution**	**yr 1**	**yr 2**	**yr 3**	**yr 4**	**yr 5**	**Total Cost, $K**	**Reserves, %**	**Reserves, $K**	**Cost w/ Reserves, $K**
1.0 Science	Caltech/JPL	317	210	215	218	221	1,181	20.0	236	1,418
2.0 Management	JPL	895	1,273	1,310	1,212	904	5,594	10.0	559	6,153
3.0 System Engineering	JPL	485	528	530	509	276	2,328	17.3	404	2,732
4.0 Instrument System		7,791	11,702	11,068	4,566	2,284	37,411	24.1	9,022	45,534
4.1 Spectrograph	Cambridge	1,847	3,278	3,698	959	601	10,383	20.0	2,077	12,459
4.2 Positioner	JPL/PSU	2,490	3,410	1,765	288	324	8,276	23.9	1,453	9,729
4.3 Detector System	Caltech/JPL	729	1,337	982	147	183	3,379	28.3	870	4,248
4.4 Fiber System	LNA	1,231	952	625	441	302	3,550	20.0	710	4,260
4.5 Prime Focus Instrument	JPL	701	1,628	2,871	2,157	561	7,918	26.0	2,120	10,038
4.6 System Software	UKATC	391	400	692	526	257	2,266	25.0	567	2,833
4.8 Metrology/Calibration system	UCL	403	697	435	48	56	1,639	20.0	328	1,967
5.0 Instrument Integration and Test	JPL	0	0	284	794	624	1,701	28.3	481	2,182
6.0 Data Systems	UKATC	318	555	839	230	148	2,089	20.0	418	2,507
7.0 Subaru Provided Elements	Gemini	1,655	1,655	1,655	1,655	1,379	8,000	0.0	0	8,000
TOTAL		**11,462**	**15,923**	**15,901**	**9,184**	**5,836**	**58,305**	**20.3**	**10,222**	**68,527**

Table 7.2-3: Partner Shares and WFMOS Cost Distribution

Country	Required, %	WFMOS, %
United States	46.80	58.94
United Kingdom	28.15	35.45
Canada	13.60	0.00
Brazil	4.45	5.60
Argentina	4.65	0.00
Australia	2.36	0.00
Total	**100.00**	**100.00**

Details of the cost estimate are provided in the Management and Cost Volume. The cost estimates obtained are bottoms up estimates from the doing organizations supplemented with cost analogies for similar instruments or subsystems. Cost guidelines were developed and distributed to ensure consistency and completeness in the estimates. Vendor quotes have been obtained for major procurements. Each estimate has been through the originating institution's financial office so that all rates and overheads are accurate. A series of informal and formal reviews were conducted by JPL, STFC and an external review board during the development of the proposal. The reserves for each subsystem were estimated based on design complexity, design heritage, team experience, development effort, fidelity of vendor quotes, and overall risk in delivery.

Cost tracking and management will be critical on this project. The PM is responsible for managing and reporting the project schedule and costs with support from the Business Management Team. Although Earned Value Management (EVM) is not required for the WFMOS project, the fundamental principles of EVM will be applied. The cost and schedule management will be implemented and controlled using JPL's business management system, which provides an integrated project management system for defining work, organizing the work, assigning responsibility, developing schedules, authorizing work, establishing budgets, measuring performance, analyzing variances, controlling costs, and summarizing the technical, schedule, and cost information required for effective control of a project.

For tracking, monthly financial reports from each partner will be submitted and then consolidated for management review. To minimize overhead, each partner will submit their standard institutional financial report, and the Project Resource Analyst (PRA) will assemble a project-level report with key features used by the Project Manager for review. An accurate understanding of the design status with respect to the schedule is critical for assessing the cost status. The status of major milestones with expected costs is a good global indicator of cost trends.

In addition, a project lien list will be developed and maintained to track cost changes and potential increases. The lien list contains items that may require additional funds, the decision date for execution, and the steps necessary to finalize the decision. This lien list is used by the management team as a means to assess cost trends and they will approve liens based on cost, instrument performance, technical risk, and schedule risk.

Cost management is critical on this project, and the management approach reflects that by assigning clear responsibilities and allocating sufficient time for cost, schedule, and risk analysis. Any cost trends that indicate likely overruns and the realization of costs incurred through executed liens will be managed through the implementation of descopes and allocation of reserves. Decisions made to control costs without impacting instrument performance typically come in one of several forms: 1) reduced expected performance while still meeting the requirements (minimum performance), 2) elimination of design options that could have led to improved perform-

ance, or 3) added risk. A list of descopes and trigger dates will be used to balance any cost overruns within the framework of balancing risk in the instrument. The most important feature of this approach is to implement the descope in a timely manner. Features maintained in the descope list are:

- Descope options, with implementation approach
- The resulting acceptable reduced performance or risk position.
- The schedule milestones related to the required decisions.
- The budget impact if the options are exercised at the identified milestones.
- The survey success impact.
- Reserve Management.

This strategy has been used successfully on other projects that have faced similar cost caps such as M3, recently delivered, and the Nuclear Spectroscopic Telescope Array (NuSTAR) project, currently in Phase C/D. A formal process that may include a trade study to review the impact and final approval from the management team is required to exercise the descope. The advisory board may be involved if the change is significant and Gemini will be consulted on any descope that affects a Level 1 or Level 2 requirement. The challenge is that the time to exercise a descope effectively is often early and there is a tendency to want to defer in order to maintain all features of the original design. A descope list will be developed further at the start of the study, but at this time two high-level descopes are to reduce total number of positioners and to use standard spectrograph CCDs instead of custom CCDs. For the positioners, there are several execution dates: 1) start of positioner contract, 2) parts procurement, 3) positioner assembly, and 4) bench assembly. At each stage, the cost savings decreases, but this allows the flexibility to maintain the baseline design as long as possible. We can also generate multiple trigger dates in the procurement of custom CCDs. Similarly, cost savings decrease with time, but the option retains the advantages of the system for as long as possible.

Both of these descope options described effectively increase the survey time. Science goals are still achievable, but the instrument is less efficient.

Table 7.2-4: Descope Options

Item	Decision Date	Performance Impact	Likelihood of Performance Impact	Other Subsystems Affected	Cost Reduction	Comment
Use COTS CCDs instead of custom CCDs	Project start, parts order, integration	30% reduction in wavelength coverage or resolution, depending on survey	High	Spectrograph	$260K	
Reduce number of positioners from 2,400 to 1800	Positioner CDR, parts order, start of positioner integration	Decreased observing efficiency	High	Spectrograph, fibers, detectors	$1.2M	Coupled w/ reducing spectographs to 2. Costs only reflect reduction number of positioners. Additional savings in integration and test
Reduce number of spectrographs from 3 to 2	Spectrograph CDR	Decreased observing efficiency	High	Positioners, fibers, detectors	$2.5M	Coupled w/ reducing number of postioners to 1800.
Reduce the number of metrology cameras in JPL I&T	Metrology CDR, JPL I&T	Decrease in throughput	Low	Software, thermal system	$490K	After early testing, it may be possible to go to one 4K x 4K camera. Additional error in measuring postioner locations results in loss of throughput

7.3 Schedule

The baseline schedule is 58 months as shown in Figure 7.3-1. The baseline costs are developed against the 58-month schedule; project reserves are sufficient to cover development and build risk as well continuing workforce if schedule reserves, estimated at 5 months, are used. If the schedule reserves are used fully, the total project timeline is 63 months for a final delivery date of December 13, 2014. This schedule shows the critical path is through the fiber system. However there are two major paths leading to instrument integration; this schedule shows these two major tested subsystems delivering to the telescope within two months of each other.

Some of the major milestones are:

- Kickoff Meeting.
- Project System Requirements Review (SRR).
- Project and subsystem Preliminary Design Reviews (PDR).
- Project and subsystem Critical Design Reviews (CDR).
- Integration and Test Readiness Review.
- Delivery of test slit blocks with fibers to the spectrograph.

- Positioner EM completion.
- Detector delivery to JPL for coating and delta doping.
- Software delivery to spectrograph and positioner/PFI I&T.
- Spectrograph/detector system ship to Subaru.
- All final subsystem hardware deliveries to I&T.
- Software and Data Pipeline delivery to Subaru.
- Positioner/PFI ship to Subaru.
- Completion of ATP.

Successful completion of major reviews according to the standards associated with SRR, PDR, CDR, and PSR are good indicators of overall progress as well as the completion of significant tests and delivery of hardware assemblies. The detailed set of milestones along with clear definition of success will be developed further at the start of the study.

Schedule tracking and management are important to this project as they are directly related to cost. Any schedule slip in one area can result in not only additional effort in that area, but holding personnel longer in other subsystems if it also impacts the final delivery date. A similar approach to the cost tracking is taken, collecting schedule status from all the partners on a monthly basis and using a single integrated project schedule to assess the trends.

Options for schedule recovery are also actions that typically do not impact performance, but may increase development risk. These can be items such as increasing workforce to accelerate tasks, replacing analysis with test, eliminating lower-level tests and capturing those objectives at higher level tests, staggered deliveries, and descopes. Depending on project costs, expedite fees to vendors may be used.

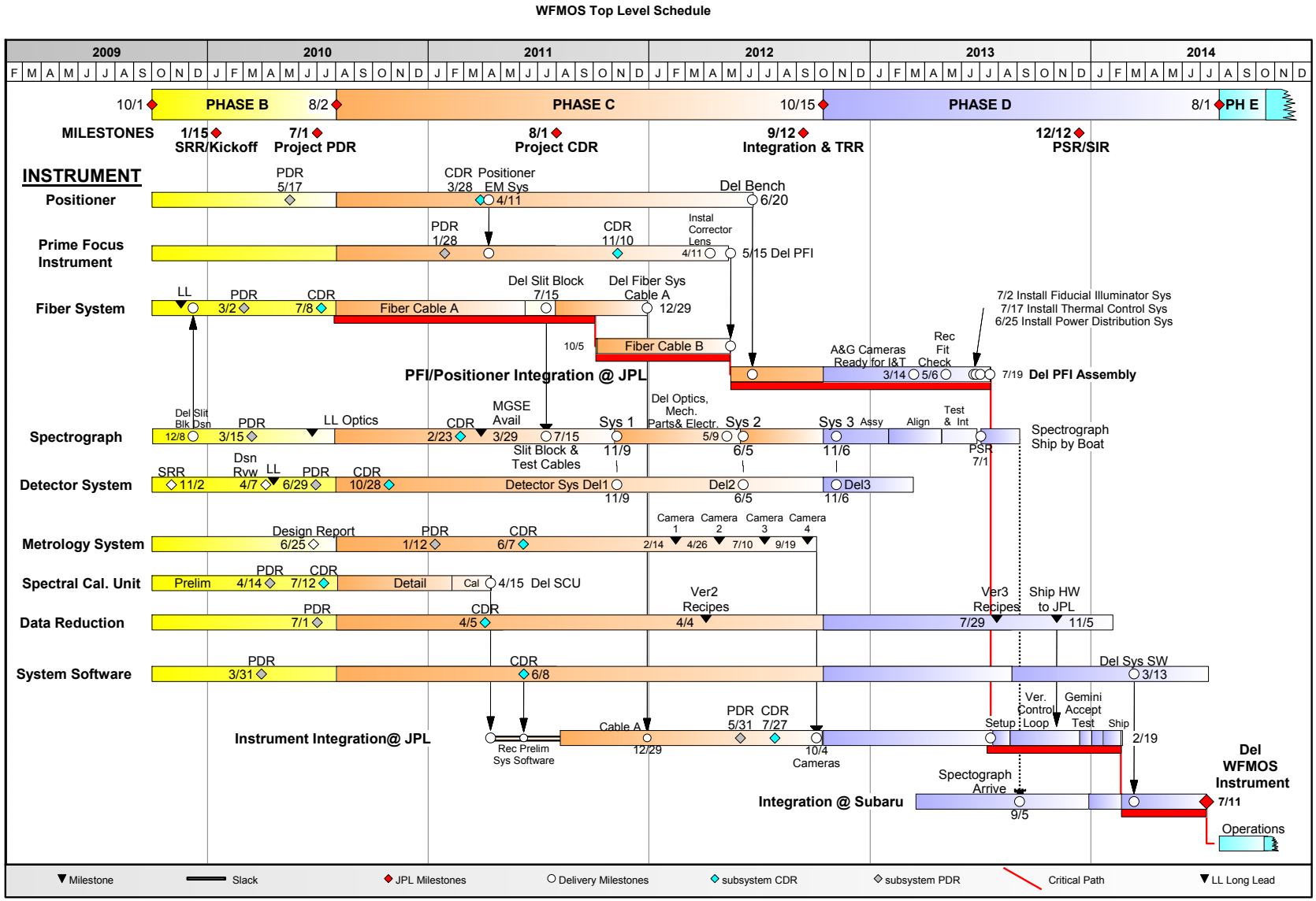

Figure 7.3-1: Top Level Schedule

7.4 Risk Management

Risk Management is used to balance the project risk position across all project resource areas (instrument success, technical reserves, schedule and cost reserves), controlling the distribution and magnitude of the identified risks against the cost constraints while obtaining the best possible confidence in achieving high science return. Accurate assessment of the risks and taking action in a timely manner is critical to managing the technical delivery and cost of this instrument.

The risk management strategy consists of risk identification, risk assessment, and risk mitigation. Risk identification defines the risk, likelihood of occurrence, and impact of the occurrence and is captured in a standard format as shown in Figure 7.4-1. All elements of the project, including reviewers, are involved in risk identification, and the risk list is managed by the system engineer. The risks and their ranking shown here represent the knowledge at this stage of the design. Risk items are reviewed monthly to track change in status as the instrument development proceeds and to identify whether any mitigation strategies need to be exercised. The top high-level risks for the WFMOS instrument are shown on this chart.

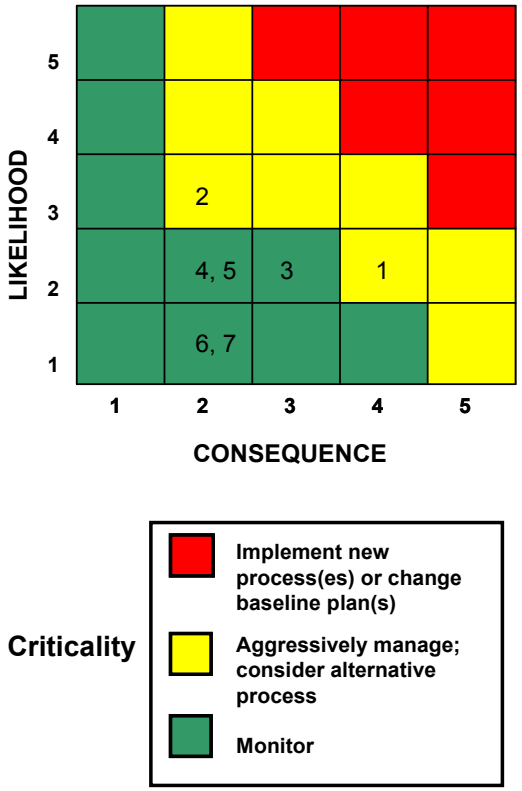

Risk Assessment Criteria for Consequence and Likelihood

Risk Type (either or both may apply to each risk)
Operational Risk
Implementation Risk

Consequence of Occurrence

Level	Implementation Risk Level Definition
5	Cannot complete with current budget and resources
4	Consume all contingency, budget or schedule, >90%
3	Significant reduction in contingency or schedule slack, >50%
2	Small reduction in contingency or schedule slack, >10%
1	Minimal reduction in contingency or schedule slack, >1%

Likelihood of Occurrence

Level	Likelihood	Level Definition (*)
5	Very High	almost certain > 70%
4	High	More likely than not > 50%
3	Moderate	Significant likelihood >30%
2	Low	Unlikely > 1%
1	Very Low	Very unlikely <1%

Figure 7.4-1: Summary of Risk Assessment and Management.

Table 7.4-1: Summary of Risk Assessment and Management

ID	Item	Likeli-hood	Conse-quence	Mitigation
1	Custom detectors don't meet performance requirement	2	4	Change to a 6k×4k format from Hamamatsu with 15µm pixels
2	schedule risk on the spectrograph gratings	3	2	Start testing w/ one grating or early low-spec grating. Consider Kaiser Optics as a second supplier
3	The square wave drive approach does not adequately drive the positioner motors.	2	3	Work w/ NST to modify motor design. Return to the sine wave drive and switching network - size growth could exceed envelope
4	Positioner resolution too high or velocity versus position and/or step size too erratic.	2	2	Enhanced positioner learning algortihm, Design modifications after EM characterization
5	Telescope environment not as expected and affects instrument performance	2	2	Early (design phase) test and/or characterization of telescope environment and interfaces
6	Positioner contractor unable to perform	1	2	JPL support to New Scale w/ engineering, facilities, other resources.
7	Spectrograph Aspherics difficult to manufacture	1	2	consider multiple vendors, manage aggressively, block off out of spec areas

Table 7.4-1 presents the current risks. The probability of occurrence is indicated by the likelihood rating. A short description of the risk and the mitigation plan is provided below.

1. The square wave drive approach does not adequately drive the positioner motors. Proper packaging design and techniques are necessary to make the 2.5-volt signals from the FPGA compatible with the 120-volt square wave out of the drivers. Testing will be performed to ensure noise and crosstalk issues are addressed. An electronics design that utilizes sine wave drive signals, increases isolation, and increases packaging volume of the electronics. If the noise and crosstalk cannot be minimized, the existing motor electronics design from NST may be repackaged as a third option.
2. Positioner Resolution too high or velocity vs. position and/or step size erratic. The current time allocation for repositioning fibers to a new target within 5 µm is 80 s. The completed positioner bench test indicates reposition can actually be done in 40 sec; however, the unknown of the consistency among positioners as well as any unpredicted errors when integrating the full system prevents retiring this risk completely. The current risk assessment represents growth in timeline. Modest design modifications and/or enhanced positioner software algorithms will be employed if needed after early testing with the positioner module EM.
3. Custom detectors do not meet performance requirement. The baseline design has custom detectors from LBL with custom coatings from JPL. The CCD and coating designs are not risky since they will be assembled from proven components and processes, however, this is dependent on a single resource at LBL. An alternate supplier (Hamamatsu) has been identified in case LBL withdraws for any reason. The penalty will be higher cost and lower sensitivity in the blue and extreme red.
4. Telescope environment not as expected and affects instrument performance. Additional information on the thermal and dynamic environment of the telescope may reveal the stability of the coupled system of the telescope and instrument does not meet performance requirements. Mitigation is early acquisition of additional data on the

telescope environment and interfaces in critical locations and/or simple measurements to characterize the local environments.

5. Some spectrograph gratings do not meet the delivery date. This schedule assumes delivery of all gratings is in time for integration and test. Sufficient testing and early integration can be done with a low-spec grating and/or a single accepted grating.
6. Positioner Contractor unable to Perform. This acknowledges a single source for a critical deliverable. Mitigate with close monitoring and supplement with JPL resources if needed. This approach has been used often in the past with good success.
7. Spectrograph aspherics difficult to manufacture. This risk is listed because only verbal quotes have been obtained from the vendors. It is expected to be addressed quickly by seeking alternate vendors as well as active involvement and management of the selected vendor.

Risk decisions are supported by analyses and recommendations from the project team, but are ultimately made by the Project Manager in the same manner that all cost, schedule and performance impact decisions are made. If the scope of any change impacts Level 1 or 2 requirements, the management team, the advisory board, and Gemini are part of the decision process.

The descope list provides the leverage for accepting reasonable risk and maintaining confidence that a meaningful instrument can be developed within the fixed budget even if many of the identified risks are actualized. The plan identifies functional or performance capabilities, which may be dropped at some later point of the project, allowing cost savings to be applied to the area where risks happened. It also describes where risks may be added (through dropping a test, or other activity with resulting cost avoidance) acceptably in order to cover unplanned costs in other areas. As with the risk list, the descope list will evolve through the instrument development and needs to be continuously assessed and updated.

7.5 Reserves

The total project reserves required is estimated at 20%; this 20% excludes the $8M allocated for the Subaru provided elements and does not factor in the Gemini-held contingency. The reserves are established by assessing risks associated with each WBS element (Management and Cost Volume, section 5.2). Higher reserves are allocated to areas that: 1) require more development effort and therefore have more uncertainty in meeting performance cost and schedule, 2) show risk of cost growth on procurements, 3) have a higher level of complexity in design or schedule coordination, and 4) have two or more identified significant risks at the project start. The reserves do not explicitly include an allocation for exchange rate uncertainty and instead a conservative exchange rate has been used to absorb rate fluctuations.

Reserves above the partners' contract-required 15% are held at JPL and managed at the project level to provide maximum flexibility in risk management. Allocation of reserves is a process that references the specific risk item and balances resources according to the summary of risks, schedule, and remaining resources. The project risks and reserves are reviewed and updated monthly with the project team and Gemini and quarterly with the advisory board. A clear assessment and justification for the release of reserves is developed with the subsystem leads to assess the impact across the instrument system. The final decision is made by the PM with concurrence from the PI. The advisory board will be notified of the potential for significant changes as they arise. A minimum level of reserves for each project phase is defined and managed to ensure sufficient funding is available through delivery. This is discussed further in the Management and Cost Volume.

8.0 References

Goodsell, Stephen J.; Blanken, Maarten F.; Corradi, Romano; Dee, Kevin M.; and Jolley, P. D., "AutoFib2: small fibers," *Proc. SPIE* 4841, 1367–1375, 2003.

Guzzo, Luigi et al., *Nature* 451, 541–544, 2008.

Parry, Ian R.; Lewis, Ian J.; Sharples, Ray M.; Dodsworth, G. N.; Webster, J.; Gellatly, David W.; Jones, Lewis R.; and Watson, Frederick G., "Autofib--2: an automated fiber positioner for the prime focus of the William Herschel Telescope," *Proc. SPIE* 2198, 125–133, 1994.

White, M., Song, Y.-S., and Percival, W.J., 2008. arXiv:0810.1518.

9.0 Acronyms and Abbreviations

1D	One-Dimensional
2dF	The 2 Degree Field instrument
2dFDR	2dF Data Reduction
2dFGRS	The 2dF Galaxy Redshift Survey
3D	Three-Dimensional
A&G	Acquisition and Guiding
A/R	Antireflection
AAO	Anglo-Australian Observatory
AAT	Anglo-Australian Telescope
ACSIS	Auto-Correlation Spectrometer and Imaging System
ACTDP	Advanced Cryocooler Technology Development Programs
AD	Applicable Document
ADC	Atmospheric Dispersion Compensator
ADU	Analog-to-Digital Unit
AES	Auger Electron Spectroscopy
AF2	Auto-fib2
AG	Autoguider
AGC	Acquisition and Guidance Camera
AIV	Assembly, Integration, and Verification
ALMA	Atacama Large Millimeter Array
AMNH	American Museum of Natural History
ANA	Analysis workstation
AO	Adaptive Optics
APD	Astronomy and Physics Directorate (JPL)
APG	Annealed Pyrolytic Graphite
API	Application Programming Interface
APS	Alignment and Phasing System
AR	Antireflection
ARC	Astronomical Research Cameras
ARGOS	Abundance and Radial Velocity Galactic Origins and Structure Survey
ARL	Applied Research Laboratory
ARR	Acceptance Readiness Review
ATC	Astronomy Technology Centre
ATP	Acceptance Test Plan
AURA	Association of Universities for Research in Astronomy
BAO	Baryonic Acoustic Oscillations
BBAR	Broadband AR
bHROS	Bench-mounted High Resolution Optical Spectrograph (Gemini)
BIT	Built in Test
BOM	Bill of Material
BOSS	Baryon Oscillation Spectroscopic Survey
BRI	Standard photometric bands (Johnson)
CAD	Computer-Aided Design
Caltech	California Institute of Technology
CAS	Central Alarm System
CCB	Change Control Board
CCD	Charge-Coupled Device
CCW	Counter-Clockwise
CDD	Concept Design Documentation
CDR	Critical Design Review
CELT	California Extremely Large Telescope
CFHT	Canada-France-Hawaii Telescope

CGS4	Cooled Grating Spectrometer 4
CIB	Configuration Implementation Board
CIRPASS	Cambridge Infrared Panoramic Survey Spectrograph
CIT	California Institute of Technology
CL	Center Line; *also* confidence level
CLD	Center for Life Detection
CM	Configuration Management
CMB	Cosmic Microwave Background
CMII	Configuration Management II
CMM	Coordinate Measuring Machine
CMOS	Complementary Metal Oxide Semiconductor
CMP	Configuration Management Plan
CMS	Configuration Management System
CNC	Computer Numerical Control
COB	Chip on Board
CoDR	Concept Design Review
COO	Caltech Optical Observatories
CosmoMC	A Markov-Chain Monte-Carlo software package
COTS	Commercial-Off-the-Shelf
CPU	Central Processing Unit
CR	Change Request; *also* Cosmic Ray
CRB	Configuration Review Board
CSRP	Center for Space Research Programs
CTE	Charge Transfer Energy
CTIO	Cerro Tololo Inter-American Observatory
CTM	Contract Technical Manager
CV	Curriculum Vitae
CVD	Chemical Vapor Deposition
CW	Clockwise
DAQtk	Data Acquisition Toolkit
DAZLE	Dark Age Z Lyman-alpha Explorer
DBSP	Double Spectrograph at Hale 200" Cass focus
DC	Direct Current
DCS	Detector Control Software
DE	Dark Energy
DEC	Declination
DEHZ	Dark Energy, High z / High Redshift Dark Energy
DE-HZ	Dark Energy, High z / High Redshift Dark Energy
DEIMOS	Deep Imaging Multi-Object Spectrograph (Keck)
DELZ	Dark Energy, Low z / Low Redshift Dark Energy
DETF	Dark Energy Task Force
DHS	Data Handling System
DID	Data Item Description
DLD	Digital Logic Decoder
DMA	Direct Memory Access
DoD	Department of Defense
DOE	Department of Energy
DOF	Degrees of Freedom
DOORS	Dynamic Object Oriented Requirements System
DPM	Deputy Project Manager
DR	Data Reduction
DRR	Design Release Review
DS	Data Set
DSP	Digital Signal Processor

E2V	e2v Technologies PLC, Essex, England
ECN	Enterprise Change Notice; *also* Engineering Change Notice
ECoS	Eberly College of Science
EGSE	Electrical Ground Support Equipment
ELT	Extremely Large Telescope
EM	Engineering Model
EMC	Electromagnetic Compatibility
EMI	Electromagnetic Interference
ESA	European Space Agency
ESD	Electro-Static Discharge
ESO	European Southern Observatory
EU	European Union
FAR	Final Acceptance Review
FEA	Finite Element Analysis
FIS	Fiducial Illumination System
FITS	Flexible Image Transport System
FLAMES	Fiber Large Array Multi Element Spectrograph
FLCG	Field Lens Collimator Group
FMEA	Failure Modes Effects and Analysis
FMOS	Faint Multi-Object Spectrograph
FOCCOS	Fiber Optical Cable and Connector System
FOV	Field of View
FPC	Fiber Positioner Controller
FPGA	Field-Programmable Gate Array
FPRD	Functional Performance Requirements Document
FRD	Focal Ratio Degradation
FRS	Fiber Routing System
FS	Feasibility Study; *also* Frame Set
FSL	Frequency Standards Laboratory
FTE	Full-Time Equivalent
Fundep	Fundação de Desenvolvimento da Pesquisa
FWHM	Full Width at Half Maximum
GA	Galactic Archaeology
GAHR	Galactic Archaeology–High Resolution / High Resolution Galactic Archaeology
GA-HR	Galactic Archaeology–High Resolution / High Resolution Galactic Archaeology
Gaia	An ESA-led astrometry space mission
GALEX	Galaxy Evolution Explorer
GALR	Galactic Archaeology–Low Resolution / Low Resolution Galactic Archaeology
GA-LR	Galactic Archaeology–Low Resolution / Low Resolution Galactic Archaeology
GCal	Gemini Calibration Unit
Gen2	.Generation 2. (next generation Subaru Operations System Software (SOSS))
G-ICD	Gemini ICD
GMOS	Gemini Multi-Object Spectrograph
GOODS	Great Observatory Origins Deep Survey
GPI	Gemini Planet Imager
GPMC	Governing Program Management Council
GPol	Gemini Polarimeter
gri	Standard photometric bands (SDSS)
GRS	Galaxy Redshift Survey
GSA	Gemini Science Archive
GUI	Graphical User Interface
H/W	Hardware
HALT	Highly Accelerated Life Test

HASS	Highly Accelerated Stress Streening
HETDEX	Hobby Eberly Telescope Dark Energy Experiment
HOMER	High Altitude Ozone Monitoring Experimental Rocket
HR	High Resolution
HRNIRS	High Resolution Near Infrared Spectrograph
HSC	HyperSuprimeCam
HTTP	Hypertext Transfer Protocol
I&T	Integration and Test
ICD	Interface Control Document
ICM	Institute of Configuration Management
ICS	Instrument Control Software
IFS	Integral Field Spectrograph
IFU	Integral Field Unit
IoA	Institute of Astronomy (Cambridge)
IP	Internet Protocol
IPAC	Infrared Processing and Analysis Center
IR	Infrared
IRAF	a library of astronomical data reduction software
IRMOS	Infrared Multi-Object Spectrograph
IRR	Integration Readiness Review
IS	Investigation Scientist; *also* Information System
ISOCAM	Infrared Space Observatory Camera
ISW	Integrated Sachs-Wolfe
IT	Information Technology
ITL	Imaging Technology Laboratory, University of Arizona
ITO	Indium Tin Oxide
IVOA	International Virtual Observatory Alliance
JAC OT	Joint Astronomy Center Observing Tool
JCMT	James Clerk Maxwell Telescope
JFET	Junction Field Effect Transistor
JHU	Johns Hopkins University
JPL	Jet Propulsion Laboratory
JWST	James Webb Space Telescope
K.A.O.S.	Kilo-Aperture Optical Spectrograph
KIDS	Kilo-Degree Survey
KPP	Key Performance Parameter
KVM-o-IP	Keyboard, Video, Mouse over Internet Protocol
LARS	Laboratory for Reliable Software
LBL	Lawrence Berkeley Laboratory
LBNL	Lawrence Berkeley National Laboratories
LDB	Logic Decoding Board
LED	Light-Emitting Diode
LFC	The Palomar Large-Format Camera
LGS	Laser Guide Star
LISA	Laser Interferometer Space Antenna
LNA	Laboratório Nacional de Astrofisica
LOE	Level of Effort
LR	Low Resolution
LRIS	Low Resolution Imaging Spectrometer
LRU	Line Replaceable Unit
M1CS	M1 Control System
M^3	Moon Mineralogy Mapper
MATLAB	Programming language for technical computing from The MathWorks
MAXR	The maximum resolution spectrograph mode

MBE	Molecular Beam Epitaxy
MCT	Ministry of Science and Technology
MDD	Mechanical Design Description
MDL	Micro Devices Laboratory
ME	Mechanical Engineer
Michelle	Mid-Infrared Echelle Spectrograph
MIP	Material Inventory Plan
MIRI	Mid-Infrared Instrument
MLS	Microwave Limb Sounder
MMR	Monthly Management Review
MMT	Multiple Mirror Telescope
MNRAS	Monthly Notices of the Royal Astronomical Society
MOE	Measure of Effectiveness
MOP	Measure of Performance
MOS	Multi-Object Spectrograph
MOSFET	Metal Oxide Semiconductor Field Effect Transistor
MPO	Multi-Fiber Push-on (a type of fiber optic connector)
MPS	Movement Planning Software
MRO	Mars Reconnaissance Orbiter
MROI	Magdalena Ridge Optical Interferometer
MRR	Make Release Review; *also* Manufacture Readiness Review
MS	Mechanical Specification
MT	Media-termination (a type of connector)
MTBF	Mean Time Between Failures
MTHR	Moderate to High Resolution Spectrograph
MTO	Motor Toggle Order
MUSE	Multi-Object Spectroscopic Explorer (ESO VLT)
N&S	Nod and Shuffle
NA	Not Applicable; *also* Numerical Aperture
NAOJ	National Astronomical Observatory of Japan
NAS	Network Attached Storage
NASA	National Aeronautics and Space Administration
NDEAA	Nondestructive Evaluation and Advanced Actuators
NIR	Near-Infrared
NOAO	National Optical Astronomy Observatory
NSCAT	NASA Scatterometer
NSF	National Science Foundation
NST	New Scale Technologies
OBCP	Observation Control Processor
OBS	Operational Business Schedule
OCD	Operational Concept Design
OCDD	Operational Concept Design Document; *also* Operational Concepts Definition Document
OCS	Observatory Control System; *also* Observation Control Software
OD	Optical Designer; *also* Outer Diameter
OFHC	Oxygen Free High Conductivity
OFS	Fiber connector manufacturer
OG	Output Gate
OIO	Oliveira Instrumentos Opticos
OLDP	On-Line Data Processing
OPE	Observation Procedure Editor
ORB	Orbital Sciences
ORR	Operations Readiness Review
OSL	Optical Science Laboratory

OSM	Object Selection Mechanism
OWS	Observation Workstation
OzPoz	A fiber positioner unit for the Very Large Telescope (VLT)
P2PP	Phase 2 Proposal Preparation
PALM-LGS	Palomar Laser Guide Star
PanSTARRS	Panaromic Survey Telescope and Rapid Response System
PASP	Publications of the Astronomical Society of the Pacific
PBS	Product Breakdown Structure
PC	Personal Computer
PCA	Principal Component Analysis
PCB	Printed Circuit Board
PCD	Product Concept Design
PCI	A computer bus standard
PCO	Project Close Out
PDMS	Project Database Management System
PDR	Preliminary Design Review
PDS	Power Distribution System
PECVD	Plasma Enhanced CVD
PFC	Prime Focus Corrector
PFI	Prime Focus Instrument
PFU	Prime Focus Unit
PHSC	PFU from the HyperSuprimeCam
PI	Project Initiation; *also* Principal Investigator
PM	Project Manager
PMS	Project Master Schedule
POP	Program Operating Plan
POSM	Prismatic Object Selection Mechanism
PPARC	Particle Physics and Astronomy Research Council
PRA	Project Resource Analyst
PRS	Pipeline Reduction System
PS	Project Scientist
PSA	Project Schedule Analyst
PSE	Project System Engineer
PSF	Point Spread Function
PSR	Pre-Ship Review
PSU	Pennsylvania State University
PTFE	Polytetrafluoroetheylene – Teflon
PTI	Palomar Testbed Interferometer
QA	Quality Assurance
QC	Quality Control
QE	Quantum Efficiency
QH	Quartz Halogen; *also* Quiet Hour
QTH	Quartz Tungsten Halogen
RA	Right Ascension
RAVE	Radial Velocity Experiment
RD	Reset Drain; *also* Reference Document
Req	Requirement
RFP	Request for Proposal
RM	Risk Management
RMS	Root Mean Square
ROE	Royal Observatory Edinburgh
ROI	Region of Interest
ROM	Rough Order of Magnitude
ROMPS	Robotically Manipulated Plug-Plate System

RR	Requirements Review
RSD	Redshift Space Distortions
RSS	Root Sum Squared
RTD	Resistance Temperature Detector; *also* Real Time Display
S/N	Signal to Noise
S/W	Software
SAA	Space Act Agreement
SAMP	Simple Application Messaging Protocol
SAN	Storage Area Network
SARR	System Architecture and Requirements Review
SC	Subprime Cam
SCP	Service Connection Point
SCUBA	Submillimeter Common-User Bolometer Array
SCUBA2	Submillimeter Common-User Bolometer Array 2
SDSS	Sloan Digital Sky Survey
SE	Systems Engineering
SEGUE	Sloan Extension for Galactic Understanding and Exploration
SHARAD	Shallow Radar
SIA	Simple Image Access
S-ICD	Subaru ICD
SIM	Space Interferometry Mission
SimCam	(a working name for the next generation instrument interface)
SIR-C	Spaceborne Imaging Radar–C
SIRR	System Integration Readiness Review
SKA	Square Kilometer Array
SKADS	Square Kilometre Array Design Studies
SNAP	SuperNova Acceleration Probe
SNR	Signal-to-Noise Ratio
SOAR	Southern Astrophysical Research Telescope
SOSS	Subaru Operations System Software
SOW	Statement of Work
SPEC	Specification
SPIE	Society of Photo-Optical Instrumentation Engineers
SPIRE	Spectral and Photometric Imaging Receiver
SPLAT	Spectral Analysis Tool
SQR	Rotary Squiggle Motors
SRB	Strain Relief Box
SRE	Spectral Resolution Element
SRF	Sequence Request File
SRL	Significant Risk List
SRR	System Requirements Review
SRS	Software Requirements Specification
SSA	SuperCosmos Science Archive
ST7	Space Technology 7
STARS	Subaru Telescope Archive System
STCS	Subaru TCS
STELES	SOAR Telescope Echelle Spectrograph
STFC	Science and Technology Facilities Council
SUBARU	Subaru Telescope Archive System
SW	Software
SWIFT	Short Wavelength Integral Field Spectrograph
TBA	To Be Announced
TBC	To Be Confirmed
TBD	To Be Defined; *also* To Be Decided

TBR	To Be Reviewed
TCP	Transmission Control Protocol
TCS	Telescope Control System
TES	Top-End Structure
TFCALC	Software package used for designing thin films
ThAr	Thorium Argon
TIKI	Telescope Interface Kit
TIM	Technical Interchange Meeting
TMC	Technical and Management Committee
TMT	Thirty-Meter Telescope
TPF	Terrestrial Planet Finder
TPM	Technical Performance Measure
TUE	Top-End Unit Exchange
UARC	University Affiliated Research Center
UCL	University College London
UCLES	University College London Echelle Spectrograph
UK	United Kingdom
UK ATC	United Kingdom Astronomy Technology Centre
UKIRT	United Kingdom Infrared Telescope
USA	United States of America
USM	Ultrasonic Motor
UUV	Unmanned Undersea Vehicle
UV	Ultraviolet
UVES	UV-Visual Echelle Spectrograph
V	Volts
V&V	Verification and Validation
VCP	Verification and Commissioning Plan
VDD	Version Description Document
VIPERS	VIMOS Public Extragalactic Redshift Survey
VISTA	Visible and Infrared Survey Telescope for Astronomy
VISTAIR-CAM	VISTA Infrared Camera
VLT	Very Large Telescope
VME	Versa Module Europa
VNC	Virtual Network Computing
VO	Virtual Observatory
VPH	Volume Phased Hologram
VPHG	Volume Phase Holographic Grating
WBS	Work Breakdown Structure
WCS	WFMOS Control System
WCSE	WFMOS WCS Electronics
WFC	Wide Field Corrector
WFCAM	Wide-field camera (IR camera for UKIRT)
WFMOS	Wide Field Fiber-Fed Optical Multi-Object Spectrometer
WFS	Wavefront Sensor
WHT	William Herschel Telescope
WM	Work Month
WMAP	Wilkinson Microwave Anisotropy Probe
WWW	World Wide Web
WY	Work Year
WYFFOS	An intermediate dispersion spectrograph for the WHT
XML	Extensible Markup Language